Institute of Human Genetics
University Duisburg-Essen

Identification of downstream genes of the TRPS1 transcription factor

Inaugural Dissertation

to obtain the degree of
Dr. rer. nat.
Fachbereich Bio- und Geowissenschaften
at the
University Duisburg-Essen

by

Paola Brega

from Genf

June 2005

Die der vorliegenden Arbeit zugrundeliegenden Experimente wurden am Institut für Humangenetik der Universität-Duisburg-Essen durchgeführt.

1. Gutachter: Prof. Dr. B. Horsthemke

2. Gutachter: Prof. Dr. H. Esche

Vorsitzender des Prüfungsausschusses: Prof. Dr. R. Küppers

Tag der mündlichen Prüfung: 23. Juni 2005

PUBLICATION

Kaiser F.J., Brega P., Raff M.L., Byers P.H., Gallati S., Taylor Kay T., de Almeida S., Horsthemke B. and Lüdecke H.-J. (2004) Novel missense mutations in the TRPS1 transcription factor define the nuclear localization signal. Eur J Hum Gen **12**: 121-126

CONTENTS

1. INTRODUCTION 1

1.1 Skeletal defects in the tricho-rhino-phalangeal syndrome 1
1.2 Endochondral bone formation and chondrocyte differentiation 1
1.2.1 Extracellular matrix in skeletal development 3
1.3 Tricho-rhino-phalangeal syndromes and the *TRPS1* gene 4
1.4 The TRPS1 transcription factor 7
1.5 Correlation between Trps1 in development and disease 9
1.6 Deletion of the GATA-type zinc finger in Trps1 provides new insight into the TRPS bone disorders 10

1.7 Aims 11

2. MATERIALS AND METHODS 12

2.1 Materials 12

2.1.1 Chemicals 12
2.1.2 Standard solutions and mediums 12
2.1.3 DNA and proteins markers 12
2.1.4 Restriction enzymes 13
2.1.5 Bacterial plasmids 13
2.1.6 *Trps1* knockout mice 13

2.2 Methods 14

2.2.1 Nucleic acid purification 14
2.2.1.1 DNA isolation from cells 14
2.2.1.2 RNA isolation from animal cells and tissues 14
2.2.1.2.1 DNase treatment of the RNA 15
2.2.2 Polymerase Chain Reaction (PCR) 15
2.2.3 Reverse-Transcriptase Polymerase Chain Reaction (RT-PCR) 16
2.2.4 In vitro site-directed mutagenesis 16
2.2.5 Restriction analysis 17
2.2.6 Agarose gel electrophoresis 17
2.2.7 Purification of DNA fragments 17
2.2.7.1 Purification of PCR products 17
2.2.7.2 Purification of restriction products 18
2.2.7.3 Gel slice extraction 18
2.2.8 Ligation 18
2.2.9 Bacterial transformation 19
2.2.9.1 Bacteria strain 19
2.2.9.2 Transformation of competent bacteria 19
2.2.10 Plasmid DNA isolation 19
2.2.10.1 Small-scale analytic preparation of plasmid DNA 19
2.2.10.2 Large-scale preparation of plasmid DNA 20
2.2.11 Quantification of nucleic acids concentration 20
2.2.12 Sequencing 21
2.2.13 Microarray analysis 21
2.2.14 Real-time PCR 22

2.2.15	Mutation analysis of the *TRPS1* gene	22
2.2.16	Cell culture	23
2.2.16.1	Cell lines	23
2.2.16.2	Cell cultures medium	23
2.2.16.3	Growth and maintenance of live cell cultures	23
2.2.17	Luciferase reporter gene assay	24
2.2.18	Proteins	24
2.2.18.1	Total cell protein extract	24
2.2.18.2	Quantification of proteins in solution	25
2.2.18.3	Discontinous SDS polyacrylamide gel electrophoresis (SDS-PAGE)	25
2.2.18.4	Western-blot and protein detection	26
2.2.19	RNA interference	27
2.2.20	*TRPS1* transgenic mice	28
2.2.20.1	*In situ* hybridization	28
2.2.20.2	Safranin staining	29
2.2.20.3	Mouse skeletal preparation	30

3. RESULTS 31

3.1	Mutation analyses	31
3.2	RNA interference and microarray analysis	32
3.2.1	*Trps1* silencing in NIH3T3 cells	33
3.2.2	cDNA microarray analysis	34
3.3	Generation and characterization of *TRPS1* transgenic mice	38
3.3.1	Generation of transgenic mice	38
3.3.2	Assessment of transgene expression	41
3.3.3	Gross phenotype and skeletal morphology	42
3.3.4	*In situ* hybridization	44
3.4	cDNA microarray analysis of mouse embryonic tissues	48
3.4.1	cDNA microarray analysis of mouse embryonic limbs	48
3.4.1.1	The relative expression of several genes was confirmed by real-time PCR experiments	52
3.4.1.2	TRPS1 actively represses the *HSPG2* promoter activity	55
3.4.2	cDNA microarray analysis of mouse embryonic snouts	57
3.4.2.1	The relative expression of three genes was confirmed by real-time PCR experiments	64
3.4.2.2	TPRS1 actively represses the *LAPTM4b* promoter activity	66

4. DISCUSSION 68

4.1	TRPS1 carries a single functional NLS	68
4.2	The *TRPS1* transgenic mouse does not represent a model for TRPS III	68
4.3	Identification of the downstream genes of the TRPS1 transcription factor	70
4.3.1	The silencing of the Trps1 transcription factor in NIH3T3 might interfere with the control of cell cycle progression	70
4.3.2	Microarray analysis of GATA Znf-deleted Trps1 mouse embryonic tissues	73
4.3.2.1	Downstream genes of Trps1 in embryonic limbs	75
4.3.2.2	Downstream genes of Trps1 in embryonic snouts	78

4.3.2.3 *Laptm4b* is the only gene upregulated in both *Trps1*$^{+/\Delta GATA\text{-}Znf}$ and in *Trps1*$^{\Delta GATA\text{-}Znf/\Delta GATA\text{-}Znf}$ mice, in embryonic limbs and snouts 79
4.3.2.4 TRPS1 directly represses *HSPG2* promoter activity 81
4.3.2.5 Is *Hspg2* overexpression in the growth plate responsible for disturbed cell-matrix interaction in the chondrocytes of TRPS patients? 83
4.3.2.6 Does *HSPG2* overexpression contribute to the onset of osteoarthritis in TRPS patients? 84

5. ABSTRACT 85

6. APPENDIX 86

7. LITERATURE 88

Danksagung/Ringraziamenti 98

***CURRICULUM VITAE* 99**

IMPORTANT ABBREVIATIONS

aa	amino acid
BM	basement membrane
bp	base pairs
BSA	bovine serum albumine
cDNA	complementary DNA
Ci	Curies
CSEs	cone-shaped epiphyses
DNA	deoxyribonucleic acid
ECM	extracellular matrix
min	minutes
mRNA	messenger RNA
NLS	nuclear localization signal
nt	nucleotide
O/N	overnight
ORF	open reading frame
RNA	ribonucleic acid
RNAi	RNA interference
RT	room temperature
sec	seconds
siRNA	small interfering RNAs
TRPS	tricho-rhino-phalangeal syndrome
Znf	zinc finger

1 INTRODUCTION

1.1 Skeletal defects in the tricho-rhino-phalangeal syndrome

The tricho-rhino-phalangeal syndrome (TRPS) is an autosomal dominant inherited disease characterized by craniofacial and skeletal defects (Giedion, 1966). The skeletal defects, which include cone-shaped epiphyses of the phalanges, varying degrees of brachydactyly and short stature, are probably due to an impaired maturation of chondrocytes in the growth plate of many tubular bones (Lüdecke *et al*., 2001).

1.2 Endochondral bone formation and chondrocyte differentiation

Bone formation begins when mesenchymal cells form condensations, clusters of cells that adhere through the expression of adhesion molecules (review: Olsen *et al*., 2000). In a few areas, like the flat bones of the skull, the cells of these condensations differentiate directly into bone-forming osteoblasts in a process called intramembranous bone formation.

Most condensations of the axial and appendicular skeleton, for example in the limbs, where extensive growth is required for proximal-distal extension of the long bones, form a cartilage template, which is then replaced by bone in the process of endochondral bone formation. At the beginning of this process, the condensed cells become chondrocytes, the primary cell type of the cartilage. The cells at the border of condensations form a perichondrium. Chondrocytes have a characteristic shape and they secrete a matrix rich in type II collagen and the proteoglycan aggrecan. More generally, chondrocytes express a characteristic genetic program driven by different transcription factors, like SOX9, essential for converting cells of condensations into chondrocytes (Bi *et al*., 1999) and CBFA1/RUNX2, master regulator of osteoblast differentiation (Otto *et al*., 1997; Komori *et al*., 1997). Mutations in *SOX9* cause the rare and severe dwarfism campomelic dysplasia (CD) (Foster *et al*., 1994; Wagner *et al*., 1994) whereas haploinsufficiency of CBFA1/RUNX2 causes cleidocranial dysplasia (CCD)

(Mundlos *et al*., 1997). The cartilage enlarges through proliferation of chondrocytes and perichondrial cells, as well as through deposition of new matrix. At a certain stage, specific for each skeletal element, cells in the center undergo further maturation into hypertrophic chondrocytes by stopping proliferation, enlargement and secretion of a new matrix composed uniquely by type X collagen that becomes progressively calcified. Changes in the composition and properties of the cartilage matrix in the hypertrophic zone allow invasion by capillaries and secretion of angiogenic factors, accompanied by apoptosis of terminally differentiated chondrocytes and replacement of the calcified cartilage matrix by the trabecular bone matrix secreted by invading osteoblasts. This results in the formation of primary ossification centers. At the same time, osteoblasts in the perichondrium form a collar of compact bone around the middle portion (diaphysis) of the cartilage, so that the primary ossification center ends up being located inside a tube of bone. At one or both ends (epiphyses) of the cartilage, secondary ossification centers are formed, leaving a plate of cartilage, called growth plate between epiphysis and diaphysis. In the growth plate, a coordinated sequence of chondrocyte proliferation, hypertrophy, and apoptosis results in longitudinal growth of bones. At the same time, these processes are coordinated with growth of the epiphysis and radial growth of the diaphysis.

Several complex signaling pathways control bone growth (review: Kronenberg, 2003). One of this is the Ihh/PTHrP signaling (Vortkamp *et al*., 1996; Lanske *et al*., 1996).

Indian hedgehog (Ihh), expressed by post mitotic cells in the prehypertrophic zone of growth plate cartilage, has several roles in regulating longitudinal bone growth. By signaling through Patched/Smoothened, Ihh controls bone formation in the bone collar and proliferation of chondrocytes in the proliferative growth plate zone by mechanisms that are independent of parathyroid hormone related protein (PTHrP) and it maintains the pool of proliferative chondrocytes in the growth plate through stimulation of PTHrP synthesis in the periarticular perichondrium. Increased signaling through the PTHrP receptor causes delay of chondrocyte hypertrophy and associated expression of *Ihh*, collagen X and vascular endothelial growth factor (*VEGF*), and expansion of the pool of proliferating cells (Schipani *et al*., 1997);

decreased signaling has the opposite effect (reviews: Wallis, 1996; Olsen *et al*., 2000).

Other signaling pathways involve the fibroblast growth factors (FGFs) (review: Ornitz and Marie, 2002) and the bone morphogenetic proteins (BMPs) (Minina *et al*., 2002). These locally produced factors are joined by systemic factors such as growth hormone, thyroid hormone, estrogen, androgen, vitamin D, and glucocorticoids to control bone growth (review: Van der Eerden *et al*., 2003).

1.2.1 Extracellular matrix in skeletal development

The extracellular matrix (ECM), a complex structural entity surrounding and supporting cells, is found within mammalian tissues. ECM is composed of three major classes of biomolecules: (a) structural proteins like collagen and elastin, (b) specialized proteins like fibrillin, fibronectin, and laminin, (c) proteoglycans, which are composed of a protein core to which long chains of repeating disaccharide units termed of glycosaminoglycans (GAGs) are attached forming extremely complex high molecular weight components of the ECM. Extracellular matrix components of cartilage and bone have critical roles in skeletal development as demonstrated by the large number of skeletal dysplasia caused by mutations in matrix molecules.

Heterozygous mutations in *COL1A1* and *COL1A2*, the genes coding for the α1(I) and α2(I) chains of collagen type I, respectively, cause osteogenesis imperfecta (OI) (Kocher and Shapiro, 1998), which is a heterogeneous group of skeletal disorders characterized by brittle bones, hearing loss, blue sclerae, and dentinogenesis imperfecta.

Type II collagen, a homotrimer encoded by *COL2A1*, is the major structural collagen component of the cartilage, vitrous of the eye, the nucleus pulposus of intervertebral discs, and the tectorial membrane of the ear. Mutations in type II collagen cause a spectrum of diseases known as type II collagenopathies, whose severity ranges from lethality (achondrogenesis type II, hypochondrogenesis) to severe dwarfism (spondyloepiphyseal dysplasia congenita, Kniest dysplasia), as well as normal stature with early-onset osteoarthritis (Stickler syndrome and others) (Spranger *et al*., 1994).

Type X collagen, a member of the short chain collagen family, is a homotrimeric molecule expressed by hypertrophic chondrocytes during endochondral ossification. In humans, mutations in *COL10A1* have been shown to cause the autosomal dominant disorder Schmid metaphyseal chondrodysplasia, which is characterized by bowing of the legs, growth retardation of the lower extremities, and coxa vara (Warman *et al*., 1993).
The major proteoglycan in cartilage, aggrecan, contains a core protein that is modified by substitution of chondroitin and keratan sulfate chains and other oligosaccharides. Mice with the aggrecan frameshift mutation, called cartilage matrix deficiency (*cmd*), have short limbs, tails and snouts, cleft palate, and intervertebral disc abnormalities (Watanabe *et al*., 1997).
Loss-of-function mutations in the major heparane sulfate proteoglycan in cartilage, perlecan, cause the Schwartz-Jampel syndrome which is a unique combination of myotonia and chondrodysplasia (Nicole *et al*., 2000).

1.3 Tricho-rhino-phalangeal syndromes and the *TRPS1* gene

Giedion (1966) first described the autosomal dominantly inherited tricho-rhino-phalangeal syndrome (TRPS). Major features are sparse, slowly growing scalp hair, laterally sparse eyebrows, a bulbous tip of the nose, and protruding ears. Highly characteristic are the long flat philtrum and the thin upper vermillion border (Fig. 1A). The most typical radiographic findings in TRPS are cone-shaped epiphyses (CSEs) (Fig. 1B), predominantly at the middle phalanges. Often, they are not detectable before two years of age (Giedion, 1998). CSEs and premature closure of the growth plates can also be found at other tubular bones, however, with a much lower incidence (Giedion, 1968). The skeletal age always lags behind the chronological age until puberty and then typical accelerates. Hip malformations are present in >70% of patients.
Langer (1969) described a thoraco-pelvic-phalangeal dystrophy that shared several symptoms with the TRPS, but in addition, the patients also had mental retardation, microcephaly and multiple cartilaginous exostoses (EXT). This disorder was termed TRPS type II (MIM 150230), whereas the originally described was designated TRPS type I (MIM 190350). In 1980, Bühler *et al*.

described the first report of an 8q deletion in a TRPS II patient and four years later, thanks to a clinical and cytogenetic review of 17 patients, the shortest region of overlap of the 8q deletion in TRPS II patients was defined at band 8q24.1 (Bühler and Malik, 1984).

Sugio and Kajii (1984) and Niikawa and Kamei (1986) described mentally normal patients with the typical facial appearance of TRPS I but with more severe brachydactyly and growth retardation. None of the patients has multiple exostoses. Niikawa and Kamei (1986) proposed the diagnosis of TRPS III (MIM 190351) for these patients. Since then, a few more patients have been described (Nagai *et al*., 1994; Itin *et al*., 1996; Vilain *et al*., 1999; Lüdecke *et al*., 2001; Kobayashi *et al*., 2002; Hilton *et al*., 2002).
An apparently balanced chromosome (8;18) translocation involving 8q24.11 in a family with two sibs with TRPS type I (Marchau *et al*., 1993) facilitated the narrowing down of the *TRPS1* gene proximal to the *EXT1* gene (Lüdecke *et al*., 1995).

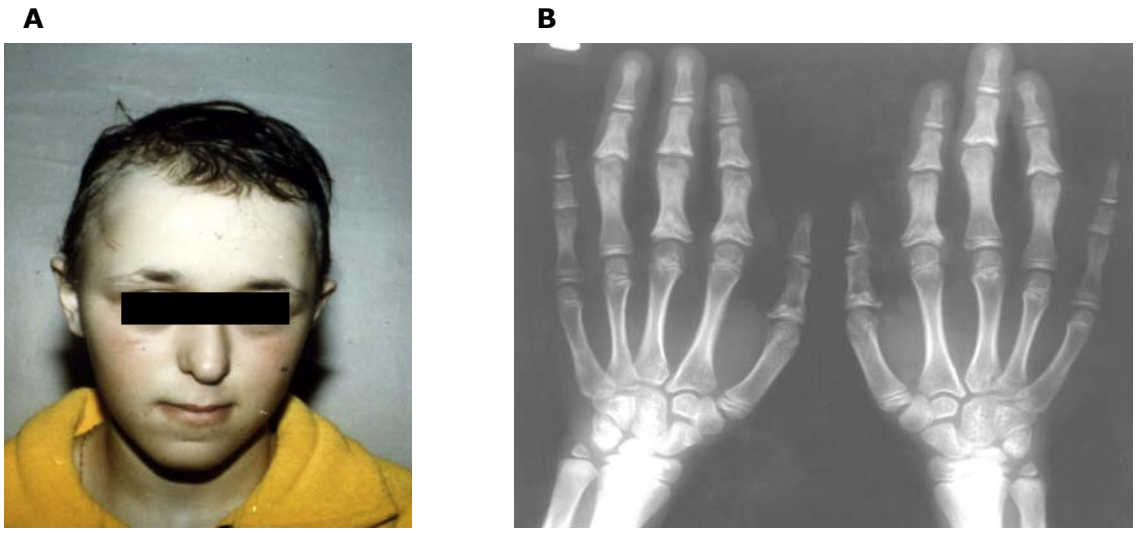

Fig. 1 A, Female patient who shows the typical craniofacial features of the TRPS type I. **B,** X-rays showing hands of a patient with TRPS type I. Note the characteristic cone-shaped epiphyses.

Recently the human *TRPS1* gene has been identified (MIM 604386, AF178030, AF183810) (Momeni *et al*., 2000) (Fig. 2A). It is composed of seven exons and spans 260500 bp of genomic DNA. The open reading frame

(ORF) is 3843 bp and starts at the third nucleotide of exon 3. The mouse *Trps1* gene has been also isolated and characterized (Momeni, 2001) (Fig. 2B). It is composed of six exons, because it has no equivalent to the non-coding human exon 2. The mouse *Trps1* ORF sequence shows 91.3% identity with the human *TRPS1* sequence. The two proteins display 93.1% identity in their amino acid sequences.

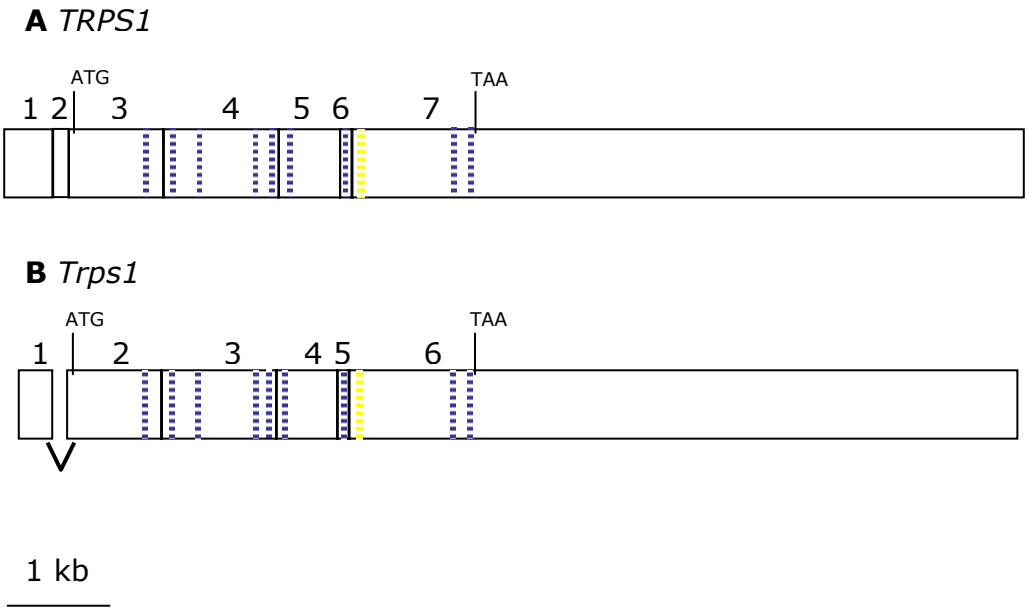

Fig.2 Comparison between the human *TRPS1* (**A**) and the mouse *Trps1* (**B**) gene. The open boxes represent the exons. The start and stop codons are indicated. The blue hatched boxes represent the zinc fingers motifs and the yellow hatched box represents the nuclear localization signal (NLS) (see section 1.4).

Point mutations, deletions of one complete *TRPS1* allele, translocations and inversions in the *TRPS1* gene are responsible for TRPS type I and type III (Hatamura *et al*., 2001; Lüdecke *et al*. 2001; Seitz *et al*., 2001; Hilton *et al*., 2002; Gentile *et al*., 2003; Kaiser *et al*, 2004). The deletion of both *TRPS1* and *EXT1* leads to TRPS II.

Independently, *TRPS1* was cloned and described by Chang *et al*. (2000), named as *GC79*, studying androgen-dependent LNCaP-FGC human prostate

cancer cells, where *TRPS1* is higher expressed when compared with androgen-independent LNCaP-LNO human prostate cancer cells.

1.4 The TRPS1 transcription factor

The *TRPS1* gene encodes the 1281 amino acids nuclear transcription factor TRPS1 (Fig. 3) with an unusual combination of nine zinc finger (Znf) motifs (Momeni *et al*., 2000). The function of the first six Znfs has not yet been determined. The seventh is a GATA-like Znf and it is able to bind to the GATA consensus sequence (Malik *et al.*, 2001). So far, six members of the GATA family of transcription factors have been identified in vertebrates and each of them contains a highly conserved DNA binding domain consisting of two Znfs. The C-terminal Znf domain is essential for recognition and binding to (A/T)GATA(A/G) motifs, whereas the N-terminal Znf domain contributes to this interaction by influencing the specificity and stability of the DNA binding (Molkentin, 2000; Trainor *et al*., 2000; Trainor *et al*., 1996). The presence of only a single GATA Znf, as in TRPS1, is only common in invertebrates like fungi, plants, nematodes and insects (Daniel-Vedele and Caboche, 1993). In vertebrates, only two other cases of single GATA Znf proteins are known. One protein is the so-called TSGA, which is a testis-specific putative transcription factor (Höög *et al*., 1991); the other protein is encoded by the hairless gene (Cachon-Gonzales *et al*., 1994).

The two most C-terminal Znfs (the eighth and the ninth) of TRPS1 exhibit a high similarity to the C-terminal double Znfs of the IKAROS family of lymphoid transcription factors, which are necessary for dimerization between IKAROS proteins and other family members (Sun *et al*., 1996; McCarthy *et al*., 2003). TRPS1 carries a single nuclear localization signal (NLS) (Kaiser *et al*., 2004). So far, TRPS1 is the only vertebrate and invertebrate recognized transcription factor that contains both GATA- and Ikaros-like Znfs.

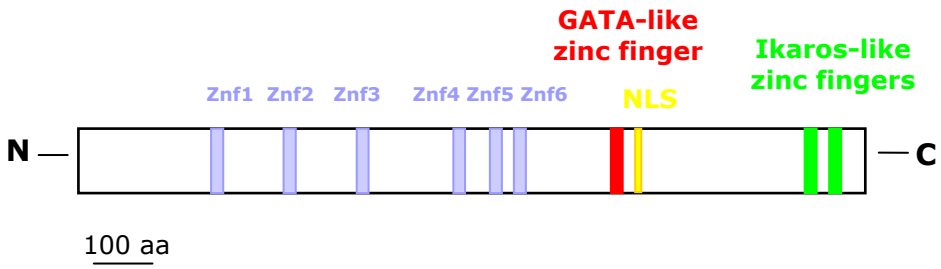

Fig. 3 Predicted structure of the TRPS1 protein. NLS: nuclear localization signal Znf: zinc finger

Genotype-phenotype correlation studies (Lüdecke *et al.*, 2001) indicated that missense mutations in the GATA zinc finger of *TRPS1* are associated with the severe TRPS type III phenotype. This is probably due to a dominant negative effect exerted by the mutant proteins with an altered GATA zinc finger, which have a decreased affinity to DNA but are still able to bind the co-factors of the involved protein complexes. In contrast, TRPS type I is correlated with nonsense mutations, deletions of one complete allele, and with the other two missense mutations, found in the NLS of *TRPS1* (Kaiser *et al.*, 2004). In this case, the disease is probably due to a reduction of the TRPS1 concentration in the nucleus, a phenomenon called haploinsufficiency (Seidman and Seidman, 2002).

Several functional analyses of this interesting and unusual transcription factor have been carried out in the last years.
Chang *et al*. (2000) observed that physiological levels of androgens repressed the expression of *TRPS1*/*GC79* mRNA in LNCaP-FGC (androgen-dependent human prostate cancer cells). Castration-induced androgen withdrawal in rat ventral prostate, used to induce apoptosis in the prostate, increased the expression of GC79 mRNA leading to the hypothesis that TRPS1/GC79 can be implicated in the process of apoptotic cell death in the rat ventrale prostate.
Malik *et al*. (2001) have shown that TRPS1 represses GATA-mediated gene activation and that its transcription repressional function is dependent on the presence of both the GATA- and the Ikaros-like Znfs.
Recently, two binding partners of the TRPS1 transcription factor have been identified. Kaiser *et al*. (2003a) reported that the nuclear interaction of the dynein light chain LC8a with TRPS1 suppressed the transcriptional repression

activity of TRPS1. The interaction of the RING finger protein RNF4 with TRPS1 was able to inhibit the repressional function of TRPS1 (Kaiser *et al*., 2003b).

Target genes of TRPS1 have not yet been identified. Thus, the signaling pathways in which TRPS1 acts, for example during endochondral ossification, are still unknown.

1.5 Correlation between Trps1 in development and disease

In order to get insight into the important function of Trps1 during mouse embryonic development, Kunath *et al*. (2002) performed whole-mount *in situ* hybridization of embryonic stage 10.5 (E10.5)-E14.5 mouse embryos with a *Trps1* antisense probe (Fig. 4). They showed that strong *Trps1* expression is found in the cartilage condensations, the hair follicles and in the developing snout, strongly suggesting that the main features of TRPS probably are the consequences of defects already occurring during embryonic stages.

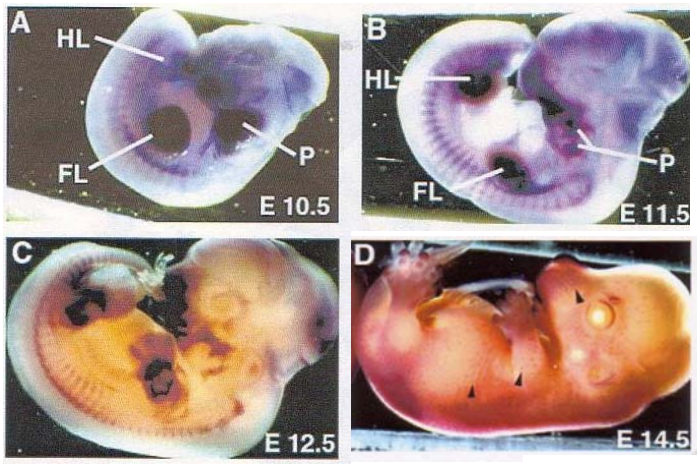

Kunath *et al*., 2002

Fig. 4 Whole-mount *in situ* hybridization (performed by Kunath *et al*., 2002) of E10.5 (A), E11.5 (B), E12.5 (C) and E14.5 (D) mouse embryos with a *Trps1* antisense probe. FL: forelimbs. HL: hindlimbs. P: pharyngeal arches. Arrowheads demarcate hair follicles.

By *in situ* hybridization performed on tissue sections, Kunath *et al*. (2002) showed that, in the developing skeletal elements of E14.5 limbs, *Trps1* is expressed in the joint regions, in the periarticular and in the prehypertrophic chondrocytes (data not shown).

1.6 Deletion of the GATA-type zinc finger in Trps1 provides new insight into the TRPS bone disorders

Lüdecke *et al*. (2001) described a mutation (IVS6+1G>T) in the splice-donor site of intron 6 of the *TRPS1* resulting in frame skipping of exon 6 and thus in the deletion of the entire GATA-Znf coding domain. This mutation led to a TRPS I phenotype in a female patient.

Malik *et al*. (2002) generated *Trps1* knockout mice, which lacks the mouse exon 5 (equivalent to human exon 6) and thus resembling the state present in the patient with the site splice mutation. The mutant allele, which does not contain the GATA-Znf coding domain (ΔGATA-Znf), is expressed in both *Trps1*$^{+/\Delta GATA\text{-}Znf}$ and *Trps1*$^{\Delta GATA\text{-}Znf/\Delta GATA\text{-}Znf}$ mice. The authors reported that *Trps1*$^{+/\Delta GATA\text{-}Znf}$ mice with deletions of the TRPS1 GATA Znf domain displayed facial anomalies that overlapped with findings for TRPS (a small recessed chin, abnormally arched palate) whereas *Trps1*$^{\Delta GATA\text{-}Znf/\Delta GATA\text{-}Znf}$ mice additionally showed a complete absence of vibrissae, the specialized sensory hairs found normally along the upper jaw. Unexpectedly, *Trps1*$^{\Delta GATA\text{-}Znf/\Delta GATA\text{-}Znf}$ mice died of neonatal respiratory failure due to abnormalities of the thoracic spine and ribs. *Trps1*$^{+/\Delta GATA\text{-}Znf}$ mice also developed thoracic kyphoscoliosis with age and had structural deficits in cortical and trabecular bones. The findings directly implicated the importance of the GATA-type Znf of TRPS1 in regulation of bone and hair development and suggested that skeletal abnormalities highlighted in descriptions of TRPS are only the extreme manifestations of a generalized bone dysplasia.

1.7 Aims

This PhD work aimed at understanding the pathogenesis of the TRPS and identifying the potential target genes of the TRPS1 transcription factor by means of several projects.

(I) Identification of novel mutations in patients with TRPS type I followed by functional analysis of the missense mutations.

(II) Combination of RNA interference-mediated *Trps1* silencing and cDNA microarray analysis to identify potential downstream genes of Trps1 in embryonic mouse fibroblasts.

(III) Generation of a *TRPS1* transgenic mouse model.

(IV) cDNA microarray analysis of different mouse embryonic tissues derived from wild type, *Trps1*$^{+/\Delta GATA\text{-}Znf}$ and *Trps1*$^{\Delta GATA\text{-}Znf/\Delta GATA\text{-}Znf}$ mice for identification of potential downstream genes of Trps1.

2. MATERIALS AND METHODS

2.1 Materials

2.1.1 Chemicals

The chemicals, if not otherwise indicated, were provided from Merck (Darmstadt), Sigma (Heidelberg) and GibcoBRL (Eggenstein).

2.1.2 Standard solutions and mediums

Standard solutions.

10X loading buffer:	15% Ficoll, 0.25% Bromphenolblue 10 mM EDTA
TAE buffer:	1 mM EDTA, 40 mM Tris-Acetate
TE:	1 mM EDTA, 10 mM Tris-HCl

Standard mediums (for bacterial culture)

LB medium:	1% NaCl, 1% Trypton, 0.5% Yeast extract (Difco)
LB plates:	LB medium, 1.2% Bacto-Agar (Biosciences Clontech)
LB X-Gal plates:	LB medium, 1.2% Bacto-Agar, 16 µg/µl X-Gal

2.1.3 DNA and proteins markers

DNA-markers:	1 kb DNA ladder, Invitrogen pUC19 MspI digested, MBI Fermentas λ-DNA HindIII digested, Roche

Protein-marker: prestained protein marker, Broad range, New England Biolabs

2.1.4 Restriction enzymes

The restriction enzymes used for this work were provided by Roche.

2.1.5 Bacterial plasmids

pBSGC79 pBluescript II Ks vector that carries the entire human TRPS1 cDNA (received from G. Chang)

pNASSßCol2a1 pNASSß vector that contains promoter and enhancer of the mouse Col2a1 gene (received from Toshihisa Komori)

pColTRPS1 pNASSß vector that carries the entire human TRPS1 cDNA under the control of the mouse *Col2a1* promoter and enhancer (used to generate TRPS1 transgenic mice)

HPG2-SV40 pGL3-control vector (Invitrogen) that carries a ~1.7 kb promoter region of *HPG2* (used as reporter plasmid in the luciferase reporter assay)

LAPTM4B-pGL3b pGL3-basic vector (Invitrogen) that carries a ~1.5 kb promoter region of *LAPTM4B* (used as reporter plasmid in the luciferase reporter assay)

2.1.6 *Trps1* knockout mice

The *Trps1* knockout mice (Malik *et al*., 2001) were generously provided by Dr. Ramesh A. Shivdasani from the Department of Medical Oncology, Dana-Farber Cancer Institute, Harvard Medical School, Boston, Massachusetts.

Genotype of the mice was assessed by RT-PCR (2.2.3), using primers chosen flanking the deleted mouse exon 5 (Appendix).

2.2 Methods

2.2.1 Nucleic acid purification

2.2.1.1 DNA isolation from cells

To isolate DNA from animal cells, for example from mouse fibroblasts, the cells were first detached from the dishes by using trypsin. The cell solution was then incubated O/N with 100 ng proteinase K (Roche), in 500 µl 75 mM NaCl/24mM EDTA and 10% SDS at 37 °C. After phenol/chloroform extraction the DNA was precipitated with 1 ml 100% ethanol and 50 µl NaOAc 3M. The DNA was fished with a glass pipette and washed with 70% ethanol and solved in TE.

2.2.1.2 RNA isolation from animal cells and tissues

RNA was extracted from the NIH3T3 cells and from mouse embryonic limbs and snouts according to the RNeasy Mini Handbook (QIAGEN). Frozen tissue samples or cell pellets were disrupted in buffer containing guanidine isothiocyanate (buffer RLT) and homogenized. For homogenization of cell lysates, QIAshredder spin columns were used. To disrupt and simultaneously homogenize animal tissues, the samples were applied within the Lysing Matrix D (Qbiogene) were agitated in the rotor-stator homogenizer FastPrep FP120 (Qbiogene, Carlsbad, CA) at 6.5 m/s for 45 sec with and then twice centrifuged (5 min/13000 rpm), before adding 70% ethanol and following the standard protocol. To obtain a better RNA quality for hybridization of the Affymetrix microarrays, after the QIAGEN protocol, the RNA was precipitated with 2.5 volumes 100% ethanol, 0.1 volumes NaOAc 3M and 1 µl Glycogen 5mg/ml. After centrifugation 20 min at 13000 rpm at 4 °C the RNA pellet

was washed 2x with 75% ethanol and then dissolved in H_2O to obtain a 1.5 µg/µl concentration.

2.2.1.2.1 DNase treatment of the RNA

To avoid DNA contamination in the RNA samples two different DNase treatments were used. One option was offered by the RNase-Free DNase Set (QIAGEN) to use during the preparation. Shortly, according to the RNeasy Mini Handbook after the centrifugation with 70% ethanol, 350 µl buffer RW1 were pipetted into the RNeasy mini column and centrifuged (15 sec, 10.000 rpm) to wash. 10 µl DNase I frozen solution (3U/µl) were added to 70 µl reaction buffer, gently mixed and the mix directly placed onto the RNeasy silica-gel membrane to incubate at least 15 min RT.
The other treatment was performed by using 3 Units DNase I (Roche) 5 mM $MgCL_2$, 0.1 mM EDTA, 25 mM Tris-HCL, und 1 Unit RNase Inhibitor for 5 µg RNA.

2.2.2 Polymerase Chain Reaction (PCR)

The polymerase chain reaction have been used to amplify specific DNA fragments by using the Perkin Elmer "PCR 9700 System" machines. Each PCR reaction was prepared in 50 µl of total volume combining the DNA template (1-10 ng of plasmid DNA or ~150 ng of genomic DNA), 2.5 Units AmpliTaq-Polymerase, 0.8-1.6 µM primers mix (forward and reverse), 800 nM dNTP-Mix and reaction buffer (50 mM KCl, 10 mM Tris-HCl pH 8,3, 1,5 mM $MgCl_2$, 0,001 % Gelatine). After 5 min at 94 °C the following thermal cycling parameters were used for the amplification:

15 s	DNA denaturation	94 °C
15 s	primer annealing	50-68 °C
30 s	primer extension	72 °C

with a variable number of cycles between 25 and 35.
To amplify PCR products longer than 1.5 kb the Platinum Taq DNA polymerase High Fidelity Kit (Invitrogen) was used following the

manufacturer protocol. To obtain genomic GC-rich PCR products region the BD Advantage™-GC 2 PCR Kit (BD Biosciences) was used following the manufacturer's protocol.

2.2.3 Reverse-Transcriptase Polymerase Chain Reaction (RT-PCR)

The RNA extracted from mammalian cells and/or tissues of different origins was reverse-transcribed in cDNA by using the GeneAmp RNA PCR Kit (ABI). The cDNA was then amplified by means of specific primer pairs. The 20 µl end volume of the reverse-transcription reaction contained: 100-500 ng RNA, 5 mM $MgCl_2$, 1 mM each dNTP, 2.5 Units MuLV (Murine Leukemia Virus) Reverse Transcriptase, 1 U RNase Inhibitor, 2.5 µM random hexamers and 2 µl 10X PCR buffer.

The following thermal cycle parameters were required for the reverse transcription:

10 min	room temperature
15 min	42 °C
5 min	99 °C
5 min	5 °C

2.2.4 In vitro site-directed mutagenesis

To introduce specific point mutations into an insert of interest ligated to a double-stranded DNA vector, the QuikChange Site-Directed Mutagenesis Kit (Stratagene) was used. Two primers between 25 and 45 bases in length containing the desired mutation were designed for the required PCR protocol. After the Dpn I digestion of the methylated, non-mutated parental DNA template, the PCR product was transformed into competent bacteria.

2.2.5 Restriction analysis

Plasmid DNA was digested for analytic and preparative purposes using 10-20 units restriction enzyme for each microgram DNA at 37 °C (or at the temperature indicated by the manufacturer, if different) for 2-20 h, in the suitable digestion buffer. For O/N digestion 1X BSA was included in the reaction

2.2.6 Agarose gel electrophoresis

DNA fragments were separated in relation to their size by means of 1-2 % agarose gel electrophoresis. The powdered agarose was melt in 1 X TAE buffer, cooled to about 60 °C and supplemented with a final concentration of 0.5 µg/ml Ethidium bromide (EtBr). The DNA samples were mixed with the gel-loading buffer and a voltage of 1-5 V/cm (measured as the distance between the electrodes) was applied to let the DNA migrate. The presence of EtBr allows the gel to be examined by ultraviolet illumination at any stage during electrophoresis.

2.2.7 Purification of DNA fragments

2.2.7.1 Purification of PCR products

The PCR products were purified by using the Microcon columns (Amicon). First the PCR reaction was filled up to 500 µl with H_20 and applied to the column. After centrifugation (15 min, 2300 rpm) the column was once again filled up to 500 µl with H_20, centrifuged again (15 min, 2300 rpm) and 15-30 µl H_20 were then pipetted into the column. The column was finally placed inverted in a new reaction tube and centrifuged (4 min, 2300 rpm).

2.2.7.2 Purification of restriction products

To purify double-stranded DNA fragments ranging from 70 bp to 4 kb from enzymatic reactions the MinElute Reaction Cleanup Kit (QIAGEN) was used following the manufacturer's protocol.

2.2.7.3 Gel slice extraction

To extract DNA fragments from agarose gels, the QIAquick gel extraction kit (QIAGEN) was used. According to the protocol, the gel slice containing the DNA fragment of interest was excised from the agarose gel with a scalpel, transferred in one reaction tube with 3 volumes buffer QG and incubated 10 min at 50 °C. The solution was then applied to the QIAquick column. After centrifugation (1 min, 10000 rpm) the sample was washed with PE buffer and finally eluted in 30-50 µl H_20.

2.2.8 Ligation

The ligation reaction was set up in 10 µl total volume containing 10-20 ng of vector DNA and insert DNA in a molar ratio 3:1 insert DNA: vector DNA. The reaction was incubated 2-3 h RT in the presence of 1 µl (5 units) of T4-DNA-Ligase (Roche) and 1 µl of 10X ligation buffer (Roche). To clone PCR products, the pGEM-T easy vector system I Kit (PROMEGA) and the pCR 2.1-TOPO cloning kit (Invitrogen) were used following the manufacturer's protocol.

2.2.9 Bacterial transformation

2.2.9.1 Bacteria strain

E.coli DH5α F', endA1, hdR17, ($r_K^- m_K^+$), supE44, thi-1, recA1, gyrA, (Nal^r), relA1, D(lacIZYA-argF), U169, deoR,

(Φ80dlacD(lacZ)M15)

2.2.9.2 Transformation of competent bacteria (heat-shock method)

The preparation of competent bacteria (bacterial cells that can take up DNA) was made by Stefanie Groß.
5 µl of the ligation reaction or 1-10 ng plasmids DNA were added to 50 µl of competent cells and the mix was stored on ice for 30 min. The tube was then transferred in a water bath at 42 °C for 2 min. After rapid transfer on ice, 450 µl of LB medium were added and the mix was then transferred to a shaking incubator set at 37 °C for 1 h. Next, the transformed cells were gently spread over the surface of the agar plate and at 37 °C O/N incubated.

2.2.10 Plasmid DNA isolation

2.2.10.1 Small-scale analytic preparation of plasmid DNA

A single bacterial colony was cultured at 37 °C O/N in LB medium (plus 100 µg/µl ampicillin as final concentration). After centrifugation of the culture (4 min/5000 rpm), the bacterial pellet was resuspended in 300 µl of P1 buffer and lysed by adding 300 µl of P2 buffer. 300 µl P3 buffer was then added to precipitate the SDS-protein complex. The mix was centrifuged (15 min/10.000 rpm) and the supernatant transferred in a new reaction tube in

the presence of 100 % ethanol to precipitate the DNA. After centrifugation (25 min/13.000 rpm) the DNA pellet was washed once with 70% ethanol, dried and dissolved in 20-50 µl H_20.

buffer P1:	10 mM	EDTA
	50 mM	Tris-HCl, pH 8,0
	100 µg/ml	RNaseA
buffer P2	0,2 M	NaOH
	1 %	SDS
buffer P3:	3 M	potassium acetate
	acetic acid up to pH	

2.2.10.2 Large-scale preparation of plasmid DNA

To prepare a large amount of plasmid DNA, 250 ml O/N bacterial culture was centrifuged and DNA was purified from bacterial pellet in accordance with a modified alkaline lysis procedure, followed by binding of plasmid DNA to QIAGEN Anion-Exchange Resin under appropriate low-salt and pH conditions (QIAGEN-System).

2.2.11 Quantification of nucleic acids concentration

The exact concentration of DNA and RNA was determined by measuring the absorbance at wavelength of 260 nm in the Ultrospec III (Pharmacia). An absorbance of 1 unit at 260 nm corresponds to 50 µg of DNA and 40 µg of RNA per ml in water.
The ratio of the readings at 260 nm and 280 nm (A_{260}/A_{280}) provides an estimate of the purity of the nucleic acid solution with respect to proteins, for example. Pure DNA and pure RNA have an A_{260}/A_{280} ratio of 1.8-1.9 and 1.9-2.0, respectively.

2.2.12 Sequencing

The sequencing reactions were performed by using the PrismTM BigdyeTM TerminatorCycle ReadyReactionKit (ABI). For a single reaction in 10 µl total volume were used 4 µl of the fluorescent labelled terminators (Bigdye) supplied in the Kit , 300-500 ng plasmid DNA or 200-400 ng PCR products and 5 pmol of the respective primer. The following thermal cycling parameters were used for 25 cycles:

10 sec	96 °C
5 sec	45-60 °C
4 min	60 °C

The sequencing products were then precipitated with 100% ethanol, washed with 70% ethanol, and resuspended in 20 µl HiDi FORMAMIDE (ABI). The sequencing of plasmid inserts and PCR products has been carried out by means of the 3100 Genetic Analyzer (ABI PRISM), which is an automatized capillary electrophoresis system that can separate, detect and analyze up to 16 capillaries of fluorescently labelled DNA fragments in one run.

2.2.13 Microarray analysis

Total RNA was extracted from NIH3T3 cells transfected with specific oligonucleotides (see 2.2.19) and from mouse tissues (whole limbs and snouts) removed from Trps1 knockout embryos (see 2.1.6) to hybridize Affymetrix U74Av2 and MOE430A oligonucleotides arrays, respectively. Hybridization, washing and scanning were performed by Dr. Ludger Klein-Hitpass (Institut für Zellbiologie, Uniklinikum Essen) following standard Affymetrix protocols (Technical Manual).

2.2.14 Real-time PCR

To obtain relative expression data of several genes in wild type and mutant mice real-time quantitative PCR was used. Real-time PCR was performed in triplicate, starting from 100-200 ng RNA (always the same amount of RNA is required for the same set of experiments) for the 20 µl finale volume reverse-transcriptase reaction (2.2.3) on ABI Prism 7000 (ABI) using glyceraldehyde-3-phosphate dehydrogenase (Gapdh) as endogenous control (all the assays, called Assay-On-Demand AOD, were supplied by ABI). Calculation was performed using values of delta Δ cycle threshold (ΔCt) using wild type mice as calibrator. For each experimental sample, the Ct of the target, normalized to the endogenous control and relative to the calibrator, is given by: $2^{-\Delta\Delta Ct}$ (Livak and Schmittgen, 2001).
Following the manufacturer protocol, each reaction in a 96-well Optical reaction Plate (ABI PRISM) was set up as follows: 1 µl from the RT reaction, 1 µl AOD, 10 µl TaqMan Universal PCR master Mix and H_20 up to 20 µl. The following thermal cycling parameters were used:

one cycle	50 °C	2 min
one cycle	95 °C	10 min
40 cycles	95 °C	15 sec
	60 °C	1 min

2.2.15 Mutation analysis of the *TRPS1* gene

DNA of patients and control individuals was prepared from peripheral blood lymphocytes from Stefanie Groß. Genomic PCRs were performed in reactions (50 µl total volume) containing 150 ng genomic DNA under standard conditions (2.2.2). Both strands were sequenced (2.2.12) using the same primers as for the amplification and analysed by means of the program Sequencher. The primer sequences were published by Momeni et *al*. (2000).

2.2.16 Cell culture

2.2.16.1 Cell lines

NIH3T3	mouse embryonic fibroblasts, adherent (ATCC CRL 1658)
COS-7	monkey kidney fibroblasts, SV40 transformed, adherent (ATCC CRL 1651)
HeLa	human cervix adenocarcinoma epithelial cells, adherent (ATCC CCL-2)

2.2.16.2 Cell cultures medium

DMEM (Gibco)	Dulbecco's Modified Eagle's Medium with 4500 mg/l Glucose + L-Glutamine + Pyruvate
Fetal calf serum, FCS (PAA)	10% final concentration
Antibioticum/Antimicoticum 100 x (PAA)	1% final concentration
Gentamycin	1% final concentration

2.2.16.3 Growth and maintenance of live cell cultures

The cells were grown in DMEM supplemented with FCS, Antibioticum/Antimicoticum and gentamycin at 37 ^{0}C under a 5% CO_2 atmosphere. Cells were disaggregated and detached routinely with 2-3 ml Trypsin EDTA 1x (Gibco) and replated at a split ratio of 1:10-1:5.

2.2.17 Luciferase reporter gene assay

To assess the capability of TRPS1 to influence the expression of some of its potential downstream genes, reporter gene experiments were performed. Transient transfection assays were carried out using FuGENE 6 (Roche). The day before the transfection the cells (HeLa and COS-7 cells) were trypsinized and transferred in a 6-well plate to have about $2X10^5$ cells/well in two ml DMEM medium supplemented with 10% FCS but without antibioticum and antimicoticum. FuGENE was used in a ratio 2:1 volume FuGENE (µl): mass DNA (µg). 0.5 µg of the reporter plasmid, 1 µg of the TRPS1 expression plasmid and 1 µg of the XGATA4 expression plasmid were used. The individual DNA mixtures were adjusted with respective amounts of empty plasmids. After 48 h the transfected cells were lysed with 100 µl of 1x lysis buffer provided from the Luciferase Reporter Gene Assay High Sensitivity Kit (Roche), scraped off the plate using a rubber policeman. The solubilized cells were transferred in reaction tubes and to remove cellular debris the lysates were spinned for few sec at 13000 rpm. Twenty µl of the cell extracts were transferred into an appropriate luminometer counter device and the reactions were started by injecting 100 µl of the luciferase assay reagent (Roche). The measurement of light emission by luminometry (LUMAT LB9507) was started within 0.5 –10 s after adding luciferase assay reagent for a period of 1– 5 s.

2.2.18 Proteins

2.2.18.1 Total cell protein extract

To extract their total protein content, the cells were detached from the Petri dish by using trypsin and then washed with PBS. After centrifugation (5 min, 1000 rpm) the pellet was resuspended in Flag-Lysis Buffer.

Flag-Lysis-Puffer:	25 mM	Tris-HCl, pH 7,4
	150 mM	NaCl
	1 mM	$CaCl_2$
	1 %	Triton-X-100
	1:1000	DTT (1M)

Proteinase-Inhibitors:	100 mg/ml	Phenylmethylsulfonyl Fluoride (PMSF)
	1 mg/ml	Pepstatin
	1 mg/ml	Bestain
	in 80 % Methanol und 20 % DMSO	
	1 mg/ml	Aprotenin
	1 mg/ml	E64
	1 M	NA_3VO_4
	1 M	Na_2MnO_4
	in bidest H_20	

2.2.18.2 Quantification of proteins in solution

The Bradford assay (Bradford, 1976) works by the action of Coomassie brilliant blue G-250 dye (CBBG) contained in the Bradford reagent, which binds specific amino acid residues exposed on the surface of the protein undergoing quantification. Two µl of the protein solution were added to 798 µl H_20 and to 200 µl Bradford reagent and 5 min RT incubated. It is monitored at 595 nm in a spectrophotometer by measuring the CBBG complex with the protein.

Bradford reagent:	100 mg	CBBG
	50 ml	ethanol
	100 ml	phosphoric acid
	up to 200 ml H_20	

2.2.18.3 Discontinous SDS polyacrylamide gel electrophoresis (SDS-PAGE)

To separate protein samples by size, a discontinuous SDS gel electrophoresis (SDS-PAGE) was used. Two different polyacrylamide gels, a collecting and a separating gel (7.5-10 % in relation to the size of the protein to analyse) were prepared. The collecting gel was layered on the top of the separating gel in a gel cassette supplied by the Mini-PROTEAN 3 Cell Kit (BIO RAD). The gel cassette was then placed into the inner chamber containing the electrode assembly. 10-20 µg from cell protein extract were denaturated at 95 °C for

10 min in a 4 X SDS-Probe buffer, loaded onto the gel and let migrate in 1 X Running buffer at 20-30 mA for 2-3 h.

Separating gel buffer:	1.5 M	Tris-HCl, pH 8,8
	0.4 %	SDS
Collecting gel buffer:	0.5 M	Tris-HCl, pH 6,8
	0.4 %	SDS
10x SDS-running buffer:	1.25 M	Tris-Base
	2 M	Glycin
	1 %	SDS
4x SDS-Probe buffer:	62 mM	Tris-HCl, pH 6,8
	2 %	SDS
	10 %	Glycerin
	5 %	DTT
	5 %	ß-Mercaptoethanol
	0,025 %	Bromphenolblue

2.2.18.4 Western-blot and protein detection

To transfer proteins from the SDS polyacrylamide gel to a nitrocellulose membrane the TRANS-BLOT semi dry transfer cell kit (BIORAD) was used. The transfer cassette was assembled as follows from the bottom to the top: five layers of Whatman 3MM paper, the Hybond C Membrane (Amersham), the polyacrylamide gel and on the top five layers of Whatman 3MM paper. Each component was previously soaked with transfer buffer. The negative charge was on the side of the gel and the positive charge on the side of the membrane. The transfer was accomplished in 1.5 till 2 h at 1.5 mA/cm^2. All sites on the membrane which did not contain blotted protein from the gel were "blocked" with blocking solution to prevent unspecific binding of the antibody to the membrane. To detect one specific protein the nitrocellulose membrane was incubated with a primary antibody (a rabbit polyclonal anti-TRPS1 antibody SN653 [Chang *et al*., 2002] for the detection of the human TRPS1 and the mouse Trps1) at 4 °C O/N, usually diluted 1:1000 in blocking solution. The membrane was washed with PBS for 1 h. In order to detect the antibodies which have bound, a second antibody conjugated with Horseradish peroxidase (HRP) was added (1:5000 in blocking solution). Excess of second antibody was washed free of the blot with PBS. 800-1000 µl of the

SuperSignal West Dura Kit (Pierce) were applied on the membrane immediately before placing the Film Super RX (Fuji Medical X-Ray Film). After 2-3 minutes the film was developed with the developer G153A and G153B (AGFA) and the fixer G354 (AGFA).

Transfer-Puffer:	5,82 g/l	Tris-Base
	2,93 g/l	Glycin
	3,75 ml	10 % SDS
	200 ml	Methanol
	ad 1000 ml	bidest H_20,
Blocking solution:	2 % in PBS	powdered milk

2.2.19 RNA interference

To achieve the post-transcriptional silencing of *Trps1* gene in mouse fibroblasts, 21-nucleotide small interfering RNAs (siRNA) were transfected in NIH3T3 by using the Oligofectamine™ Reagent (Invitrogen).
24 h before transfection the cells were trypsinized and transferred into a 12-well plate to have about $1X10^5$ cells/well in two ml DMEM medium supplemented with 10% FCS but without antibioticum and antimicoticum. Three µl of Oligofectamine were diluted in 12 µl DMEM and incubated 5 to 10 min RT. Ten µl of the siRNA (100nM final concentration) were diluted into 50 µl DMEM medium (without anything) and then added to the diluted Oligofectamine. The mix was carefully mixed and incubated at RT for 15-20 min. The mixture was then dropwise added to the cells. The day after the transfection the medium was changed with full medium and the cells harvested 48 h after transfection. The total protein cell extract was then prepared and afterward the proteins were separated in a SDS-PAGE. The Western-blot was first incubated with the specific primary antibody, then with the second antibody and after exposure the film was developed. Immunoblot with antibody against lamin A was used as loading control.

Trps1 sequences homologous to the oligonucleotides:

Mouse Trps A	AACAGCTACAGAGAGCAAGGT
Mouse Trps B	AAAGGCCACTGAGGAAACAGG

Mouse Trps C AACATTATGGCAAGCAGCACG
(provided by Dr. Matthias Truss, Charité University, Berlin)

2.2.20 *TRPS1* transgenic mice

The transgene includes the entire coding region of the human *TRPS*1 gene carrying a missense mutation at position 2701 (introduced by using the Mutagenesis Kit) (see Appendix for primer sequences). The mutated human *TRPS1* cDNA was cut out of the pBSGC79 vector by using *EcoRI* and *BamHI* sites. The pNASSßCol2a1 was digested with *NotI* and the linear plasmid was ligated with specific linkers containing a *EcoRI* and a *BglII* sites (see Appendix), which were used to clone the human *TRPS1* cDNA into the pNASSßCol2a1. The purified transgene, which was linearized with *AatII* and *BspLU11I* and was about 7.3 kb in length, was microinjected into the male pronucleus of fertilized single-cell eggs. These eggs were then surgically implanted into the oviduct of pseudo pregnant recipient female mice. The work required for the generation and preservation of the mice colonies was performed by Wojciech Wegrzyn and Ralph Waldschütz (Institut für Zellbiologie, Uniklinikum Essen), respectively. The southern blot analysis for the identification of transgenic animals was made by Christian Kosan (Institut für Zellbiologie, Uniklinikum Essen).

2.2.20.1 *In situ* hybridisation

In collaboration with the group of Andrea Vortkamp (Institut für Molekulargenetik, Max-Planck-Institut, Berlin) *in situ* hybridisation studies were performed in TRPS1 transgenic embryos to look for abnormal expression patterns of genes involved in bone development. Mouse limb explants from E14.5, E16.5 and E18.5 embryos were fixed in 4% paraformaldehyde at 4 ^{o}C and embedded in paraffin. The paraffin tissue sections were deparaffinized in xylenes and dehydrated through a graded series of EtOH (100%, 95%, 85%, 70%, 50% and 30 %). The sections were then digested with proteinase K (20 µg/ml) in PBS for 5 min and acetylated (0.1M Triethanolamine, 0.25% acetic anhydride) for 10 min.

For labelling the antisense riboprobes, a transcription reaction was set up with 1 µl (about 300 ng) of linearized DNA vector containing the desired insert and a T3 or T7 promoter, 2 µl of 10x transcription buffer, 2 µl of 5mM dNTPs mix, 1 µl of 40 U/µl RNAsin (inhibitor of RNAse), 2 µl of 20 U/µl T3 or T7 polymerase (according to the vector), 4 µl UTP^{33} (80 µCi) and 8 µl H_20. After incubation for 1 h 30 min at 37 ^{0}C, 20 U DNAse (Roche) were added for 20 min at 37 ^{0}C and then the RNA was precipitated with EtOH 100%. The pellet was washed with 80% EtOH and dissolved in 50 µl H_20. 1 ml of the melt hybridisation buffer was added to the 50 µl antisense riboprobe and carefully mixed. The probes can be stored maximum one week at -20 ^{0}C. Before use they were heated up for 5 min at 95 ^{0}C.

Tissue sections were hybridized O/N (50 µl hybridization buffer on every slide) in 50% formamide and 5% SSC. Following hybridisation, the sections were washed in 2x SSC and digested with 20 µg/ml RNase A in 1xSSC. After the RNase digestion, the slides were washed at 55 ^{o}C in 2x SSC with 50% formamide and in 2x SSC. The sections were dehydrated through a graded series of EtOH, air-dried and autoradiographed in NTB-2 (Kodak) emulsion. Section were developed in D-19 developer (Kodak) for 5 min at 15 ^{o}C, stopped in water for 15 sec and fixed to Kodak fixer for 15 min. After washing, the slides were counterstained with toluidine blue (Sigma).

Probes for in situ hybridisation were as follows: rat *ColII* (type II collagen), mouse *ColX* (type X collagen), mouse *Ihh* (Indian hedgehog), mouse *PTHrP* (parathyroid hormone-like peptide), mouse *Ptch* (Patched), mouse *Mmp13* (Matrix metalloproteinase 13) and mouse *Trps1.*

2.2.20.2 Safranin staining

In collaboration with the group of Andrea Vortkamp (Institut für Molekulargenetik, Max-Planck-Institut, Berlin) this method was used for the detection of cartilage in paraffin-embedded tissue sections. The sections were deparaffinized, hydrated to distilled water and then stained with Weigert's iron hematoxylin working solution for 2-3 min. Afterward the sections were washed in running tap water, stained with fast green solution for 2 min, rinsed quickly with 1% acetic acid and finally stained in 0.1% Safranin O

(Aldrich Chemical Co) for 5 min. Next the sections were dehydrated and cleared with 95% EtOH, 100% EtOH and xylene, using two changes each, 2 min each.

2.2.20.3 Mouse skeletal preparation

For staining and visualisation of whole-mount cartilage and ossified skeletal elements, E16.5 embryos and adult mice were dissected and stained with alizarin red (Sigma-Aldrich) and/or alcian blue 8GX (Sigma-Aldrich). Skin and internal organs were first removed from the specimens, if adults. For embryos this step was not necessary. The samples were fixed 2-3 days in 95% EtOH RT and then placed in acetone to remove fat for 2 days followed by staining with 0.03% alcian blue in 4:1 95% EtOH:glacial acetic acid at 37 °C (4 days for the embryos and 5-7 days for the adults). The samples were washed in 95% ethanol for 1 day RT (the ethanol was periodically changed) and then immersed in 2% KOH (about 1 h for the embryos, 12-48 h for the adults). As soon as the skeleton was clearly visible trough the surrounding tissue the samples were stained in 0.01% alizarin red in 1% KOH O/N at RT.
The samples were then processed through a graded series of glycerin (Merck) in KOH solutions:

20% 1 volume glycerin / 4 volumes 1% KOH
50% 1 volume glycerin / 1 volume 1% KOH
80% 4 volumes glycerin / 1 volume 1% KOH

and stored in 100% glycerol.
The blue tissues represented the cartilage and the red tissues represented the bone.

3 RESULTS

3.1 Mutation analyses

Mutation analyses on the *TRPS1* gene were performed in the attempt to augment the spectrum of *TRPS1* mutations and to identify functional domains of the TRPS1 transcription factor.

Ten novel mutations were identified: seven nonsense mutations (patients cases 17689, 16851, 17601, 17688, 16698, 17680 and 16687), two missense mutations (patients cases 18712 and 16908) and one splice site mutation (patient case 18058) (Table 1). To exclude a further mutation, the entire coding region as well as the noncoding exon 2 was sequenced in all cases, but no additional mutation was found (for the primer sequences: Momeni *et al*., 2000).

Table 1 Ten novel *TRPS1* mutations in patients with TRPS type I.

Case	Familial	Mutation[a]	Location	Amino acid change[b]
17689	yes	-36-+72del	exon 3	deletes translation start codon
16851	no	1650T>A	exon 4	Y550X
17601	yes	2718-2719delCT	exon 6	novel stop codon 936
17688	yes	2722C>T	exon 6	R908X
16698	yes	2745T>A	exon 6	Y915X
17680	no	2770C>T	exon 6	Q924X
18058	yes	IVS6+2G>T	IVS6	in frame skipping of exon 6
18712	yes	2854C>T	exon 7	R952C
16687	yes	3436-3472del	exon 7	novel stop codon 1152
16908	yes	3649T>C	exon 7	C1217R

[a] Nucleotide numbers refer to the TRPS1 cDNA sequence [b] Amino acid numbers refer to the deduced peptide sequence

The 2854C>T transition leads to the exchange of arginine to cysteine at position 952 situated in the predicted NLS (946-952 aa) in the TRPS1 protein. This was one of the first two missense mutations in the *TRPS1* gene that did not affect the GATA zinc-finger domain and that lead to TRPS type I. A functional study (Kaiser *et al.*, 2004) using, among other, this missense mutation, showed that the predicted NLS was indispensable for translocation of TRPS1 into the nucleus and that a single amino acid exchange was sufficient to prevent nuclear localization.
The 3649T>C transition leads to the exchange of cysteine to arginine at position 1217 situated in the first C-terminus Ikaros-like zinc finger. Ongoing functional studies investigate whether this mutation in the TRPS1 protein might interfere with the repressional function of the TRPS1 transcription factor (Kaiser, pers. communication).

3.2 RNA interference and microarray analysis

RNA interference (RNAi) is the process of sequence-specific, post-transcriptional gene silencing in animals and plants, initiated by double-stranded RNA that is homologous in sequence to the silenced gene (McManus and Sharp, 2002; Hammond *et al*., 2001). The mediators of sequence-specific messenger RNA degradation are 21- and 22-nucleotide small interfering RNAs (siRNAs) (Elbashir *et al*., 2001).
RNA interference experiments were performed to silence *Trps1* in NIH3T3 cells. To identify potential downstream genes of Trps1, the expression profile of cells where *Trps1* was silenced was compared with that of control cells. This procedure made possible the detection of either genes upregulated in the treated cells, whose expression is normally repressed by Trps1 or genes downregulated in the treated cells, whose expression is normally activated by Trps1.

3.2.1 *Trps1* silencing in NIH3T3 cells

By using short double-stranded RNAs (or small interfering RNAs, siRNAs), homologous in sequence to the *Trps1* gene, the expression of the *Trps1* genes was silenced in NIH3T3 cells. Three siRNAs were available: Mouse Trps A, Mouse Trps B, and Mouse Trps C (see Materials and methods 2.2.19). They were chosen following important criteria: (1) they were composed of 21-nucleotides sense and 21-nucleotides antisense strands, paired in a manner to have a 2-nucleotides 3' overhang, which contributes to the specificity of target recognition; (2) they were selected from the *Trps1* cDNA sequence beginning about 60 nucleotides downstream of the start codon; (3) they contain about 50% G/C nucleotides; (4) they are *Trps1* specific. The most significant decrease of the Trps1 protein expression in comparison with the control (NIH3T3 cells treated only with the transfection reagent Oligofectamine, without siRNA) was obtained transfecting the cells with the Mouse Trps A siRNA as proved by Western blot analysis (Fig. 5). As loading control, the *lamin A* expression was used.

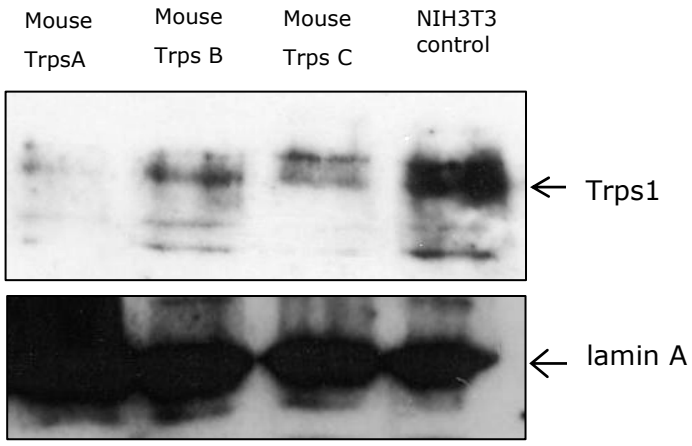

Fig.5 Western-blot analysis of Trps1 after transfection of NIH3T3 cells with 100 nM of siRNA Mouse Trps A, Mouse Trps B and Mouse Trps C. A rabbit polyclonal anti-TRPS1 antibody SN653 (Chang *et al*., 2002) was used for the protein detection. As loading control the *lamin A* expression was detected with a specific lamin A antibody (Santa Cruz Biotechnology).

3.2.2 cDNA microarray analysis

Three independent transfections of NIH3T3 cells with siRNA Mouse Trps A were performed. In experiments 1 and 2 it was still possible to detect a slight expression of *Trps1* after siRNA transfection, whereas in experiment 3 *Trps1* was totally silenced (Fig. 6). RNA was isolated from the three control NIH3T3 samples and from the three treated NIH3T3 samples to hybridize six Affymetrix U74Av2 arrays.

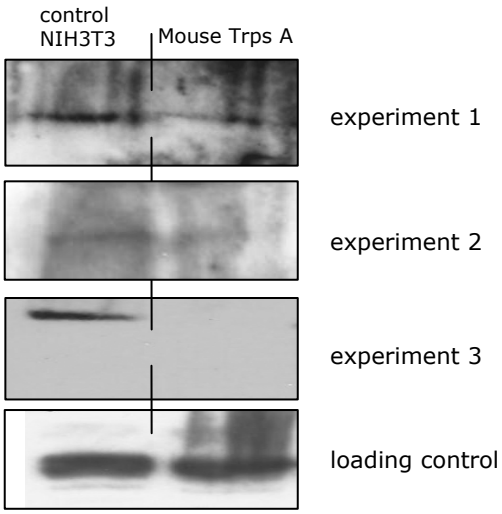

Fig. 6 Western-blot analysis of Trps1 after three independent NIH3T3 transfections with 100 nM of siRNA Mouse Trps. As loading control the *lamin A* expression was detected with a lamin A antibody.

The expression profiles of the three independent treated samples were compared with those of the controls. Genes were considered as differentially expressed when showing at least a 1.5-fold difference in the mean expression level between treated and untreated samples with a standard deviation of less than 25% between individual samples from one group. Moreover, genes were considered differentially expressed when scored as "absent" in at least two of the three cell cultures of one group and the calls in the other group were scored as „present" in all three cell cultures. In this case, the fold change was defined as >1.5 for the upregulated genes and <-1.5 for the downregulated genes. Following these parameters 59 genes were found to be abnormally expressed in the treated

cells, 30 downregulated (Table 2) and 29 upregulated (Table 3). The highest fold change in the mean expression values (2.1) was found for the *Hoxa4* (homeo box A4), which was upregulated in the treated cells. Most of the differentially expressed genes encoded for proteins involved in transcription regulation, signal transduction and in intracellular transport (Fig. 7). For 50% of the genes found to be downregulated in the treated cells the putative function of their gene products was unknown.

.

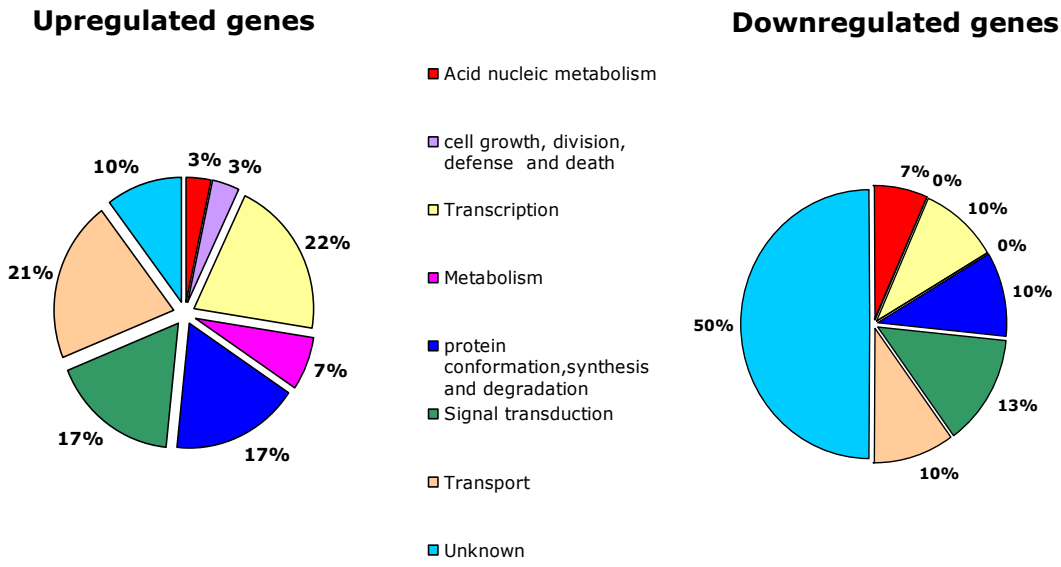

Fig. 7 Functional classification of the abnormally expressed genes in the treated NIH3T3. Most of the genes encode proteins involved in transcription, transport and signal transduction.

Table 2 Classified list of the genes downregulated in the treated NIH3T3

GenBank accession number	Affymetrix ID	Fold change	Description	Gene Symbol
Acid nucleic metabolism				
AA863742	104456_at	<-1.5	methyltransferase-like 3	*Mettl3*
Transcription				
X60136	100032_at	-1.5	trans-acting transcription factor 1	*Sp1*
X56690	96775_at	-2.0	chromobox homolog 1 (Drosophila HP1 beta)	*Cbx1*
AI847650	94945_at	<-1.5	hypertension-related, calcium regulated gene	*Hcarg-pending*
L12147	92535_at	<-1.5	early B-cell factor 1	*Ebf1*
Signal transduction				
AA919832	104742_at	-1.5	microsomal glutathione S-transferase 2	*Mgst2*
AF047704	102043_at	<-1.5	tuftelin 1	*Tuft1*
AF040094	94398_s_at	<-1.5	inositol polyphosphate-5-phosphatase B	*Inpp5b*
AF051367	94171_at	<-1.5	integrin beta 2-like	*Itgb2l*
Transport				
AA683883	99112_at	<-1.5	solute carrier family 25 (mitochondrial carrier; dicarboxylate transporter), member 10	*Slc25a10*
AI844369	102320_at	<-1.5	sorting nexin 12	*Snx12*
M59446	94140_at	<-1.5	macrophage scavenger receptor 1	*Msr1*
Protein conformation synthesis and degradation				
U79523	100496_at	<-1.5	peptidylglycine alpha-amidating monooxygenase	*Pam*
AI845578	99647_at	<-1.5	ribulose-5-phosphate-3-epimerase	*Rpe*
AW120756	96848_at	<-1.5	inositol polyphosphate-5-phosphatase E	*Inpp5e*
Unknown				
AW122812	103738_at	<-1.5	hypothetical protein MGC47434	
AI605538	104442_at	<-1.5	RIKEN cDNA A830021G03 gene	
AI152789	93411_at	<-1.5	RIKEN cDNA 2900057C09 gene	
AW048989	99360_at	<-1.5	serine active site containing 1	
C88243	102130_f_at	<-1.5	Mus musculus transcribed sequence	
AW050290	103375_at	<-1.5	RIKEN cDNA 2810406K24 gene	
AW124941	93776_at	<-1.5	RIKEN cDNA 1500001L15 gene	
U79962	103101_at	<-1.5	TAR (HIV) RNA binding protein 2	*Tarbp2*
AI852257	100904_at	<-1.5	DNA segment, Chr 14, ERATO Doi 209, expressed	
AW045230	100987_f_at	<-1.5	hsp70-interacting protein	*Hspbp1-pending*
AW123795	104035_at	<-1.5	RIKEN cDNA A930019L04 gene	
AI844196	93143_at	<-1.5	RIKEN cDNA 1190005I06 gene	
AA675006	103767_f_at	<-1.5	cDNA, clone:B930086G17	
AI642262	92245_at	<-1.5	RIKEN clone:6720481A07	
AV361953	162168_r_at	<-1.5	Mus musculus transcribed sequence	
AW122812	103738_at	<-1.5	hypothetical protein MGC47434	

Table 3 Classified list of the genes upregulated in the treated NIH3T3

GenBank accession number	Affymetrix ID	Fold change	Description	Gene Symbol
Acid nucleic metabolism				
X92410	92410_at	1.5	RAD23a homolog (S. cerevisiae)	*Rad23a*
Cell growth, division, defense and death				
AB005654	99036_s_at	>1.5	mitogen activated protein kinase kinase 7	*Map2k7* or *Mkk7*
Metabolism				
AI846600	97511_at	>1.5	monoglyceride lipase	*Mgll*
AV295044	161524_r_at	>1.5	glucose phosphate isomerase 1	*Gpi1*
Transcription				
AV279579	162402_r_at	2.1	homeo box A4	*Hoxa4*
AB010152	103810_at	1.8	transformation related protein 63	*Trp63* or *p63*
X73572	98367_at	1.5	homeo box D3	*Hoxd3*
X83971	103546_at	1.5	fos-like antigen 2	*Fosl2* or *Fra2*
J03750	101980_at	>1.5	RNA polymerase II transcriptional coactivator	*Rpo2tc1*
M58564	93944_r_at	>1.5	zinc finger protein 36, C3H type-like 2	*Zfp36l2*
Signal transduction				
AI852332	99497_at	1.6	ADP-ribosylation factor interacting protein 2	*Arfip2*
X02891	92783_at	1.5	growth hormone	*Gh*
AF063229	103809_r_at	1.5	dynein, cytoplasmic, intermediate chain 1	*Dncic1*
AF092050	98291_at	1.5	UDP-GlcNAc:betaGal beta-1,3-N-acetylglucosaminyltransferase 1	*B3gnt1*
U10094	97761_f_at	>1.5	killer cell lectin-like receptor, subfamily A, member 7	*Klra7*
Transport				
M21530	93895_s_at	1.8	inositol 1,4,5-triphosphate receptor 1	*Itpr1*
L20343	100757_at	1.6	calcium channel, voltage-dependent, beta 2 subunit	*Cacnb2*
AI843327	96276_r_at	1.5	SM-11044 binding protein	*Smbp-pending*
AV210775	161684_r_at	>1.5	lipocalin 2	*Lcn2*
AV362816	161784_f_at	>1.5	steroidogenic acute regulatory protein	*Star*
Protein conformation synthesis and degradation				
AI840454	101513_at	1.6	prefoldin 5	*Pfdn5*
AW049679	97331_at	1.5	calpain 10	*Capn10*
AV374357	162205_f_at	>1.5	RIKEN cDNA 2010001P08 gene	
Unknown				
AV356223	161471_f_at	1.7	hypothetical protein 5730409O11	
AW046757	102036_at	1.6	RIKEN cDNA 1810004B07 gene	
AV210958	161519_f_at	1.5	RIKEN cDNA 1700037H04 gene	
AA833293	104415_at	1.5	RIKEN cDNA 3110052D19 gene	
AA636966	103992_f_at	>1.5	Nur77 downstream protein 1	
AV346841	161462_r_at	>1.5	RIKEN cDNA 6720476A01 gene	

So far, no further analyses of the differentially expressed genes were performed, because of the opportunity to analyze different tissues from the Trps1 knockout mice (Malik *et al*., 2002), provided by Dr. Shivdasani (see 2.1.6), which were considered better material for the identification of Trps1 target genes.

3.3 Generation and characterization of *TRPS1* transgenic mice

3.3.1 Generation of transgenic mice

To study the dominant negative effect hypothesized to be exerted by TRPS1 proteins with missense mutations in the GATA zinc finger, transgenic mice were generated. The transgene contained the entire coding region of the human *TRPS1* gene and carried a missense mutation at position 2701 that leads to the amino acid substitution threonin (T) to proline (P) at position 901 in the GATA zinc finger (Fig. 8A). The human *TRPS1* cDNA was preferred to the mouse *Trps1* cDNA for the generation of the transgene, because the few differences with the mouse ORF sequence (~9%) allowed the discrimination and the estimation of the transgene expression rate by sequencing analysis. The A2701C mutation was found in a patient with TRPS type III (Vilain *et al*., 1999). The transgene was cloned into the pNASSßCol2a1 that contains the promoter and enhancer of the mouse *Col2a1* gene able to drive the expression only in chondrocytes (Ueta *et al*., 2001). Germline transmission was documented in four of the founder animals by Southern blot analysis digesting the genomic DNA with *BamHI* (probe shown in Fig. 8A; blot of the founder of line 2, Fig. 8B) and by their propagation four transgenic mice lines were established. The band pattern obtained by Southern blot analysis for the founder of line 2 showed a single integration site with the formation of a head-to-tail array given by two, maximum three copies of the transgene. In fact *BamHI* cuts once in each of the transgene constructs and yields a band of the same length as the injected fragment and a "junction fragment" containing genomic sequence.

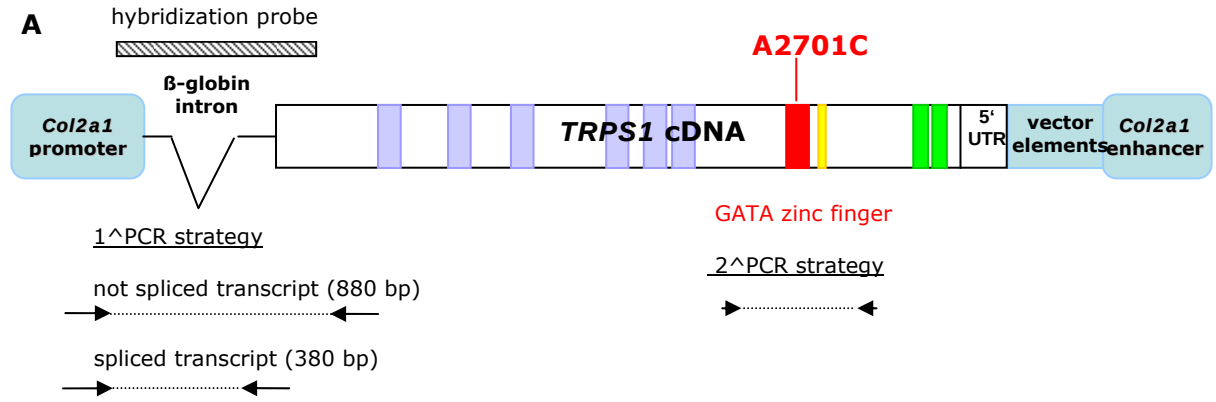
A
hybridization probe
ß-globin intron
A2701C
Col2a1 promoter
TRPS1 cDNA
5' UTR
vector elements
Col2a1 enhancer
GATA zinc finger
1^PCR strategy
2^PCR strategy
not spliced transcript (880 bp)
spliced transcript (380 bp)

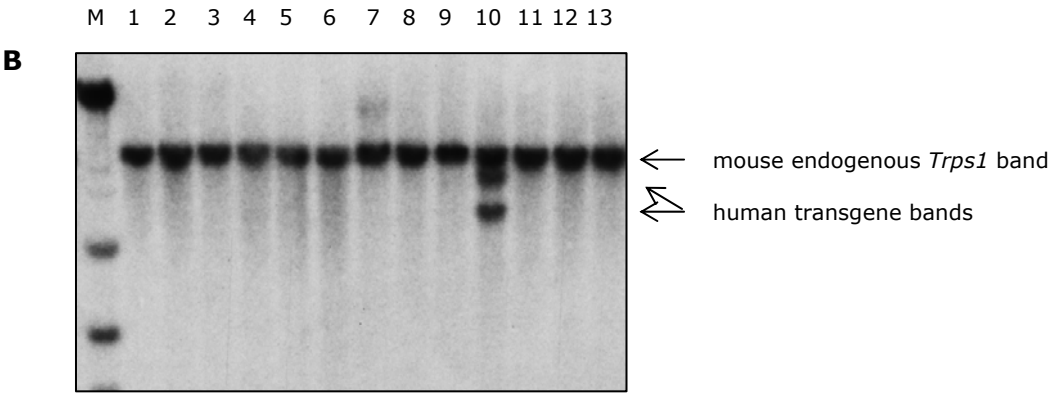
M 1 2 3 4 5 6 7 8 9 10 11 12 13
B
mouse endogenous Trps1 band
human transgene bands

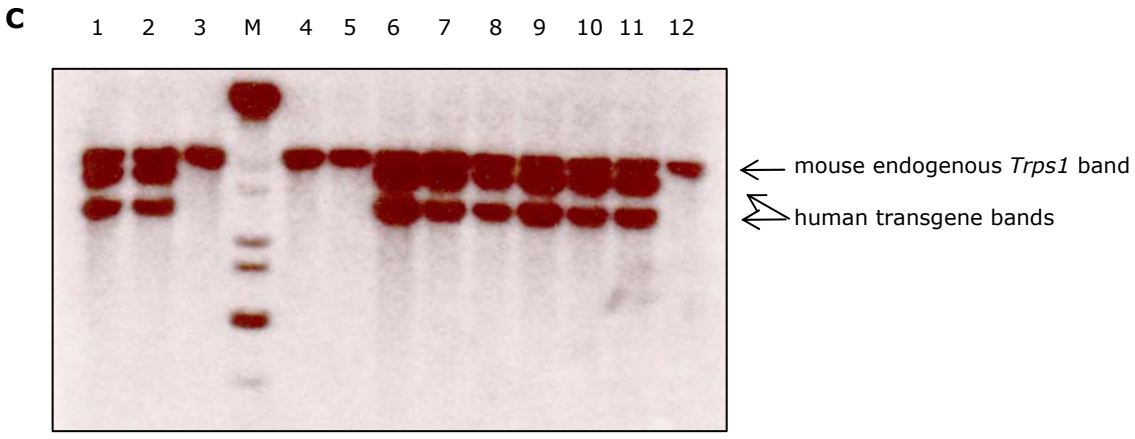
C
1 2 3 M 4 5 6 7 8 9 10 11 12
mouse endogenous Trps1 band
human transgene bands

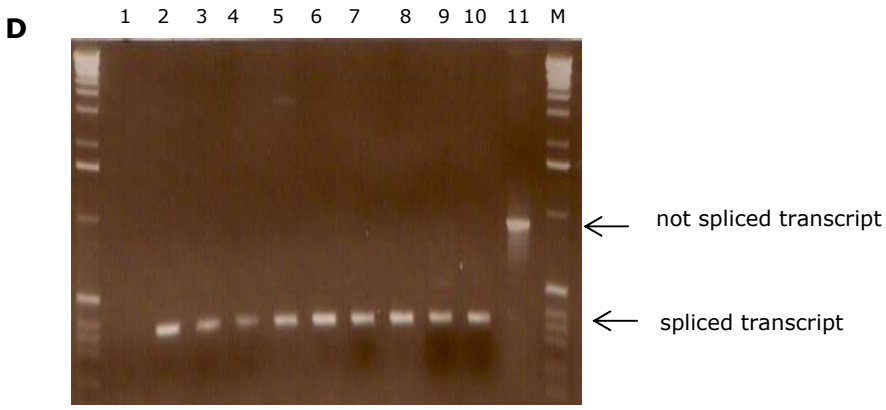
D
1 2 3 4 5 6 7 8 9 10 11 M
not spliced transcript
spliced transcript

E

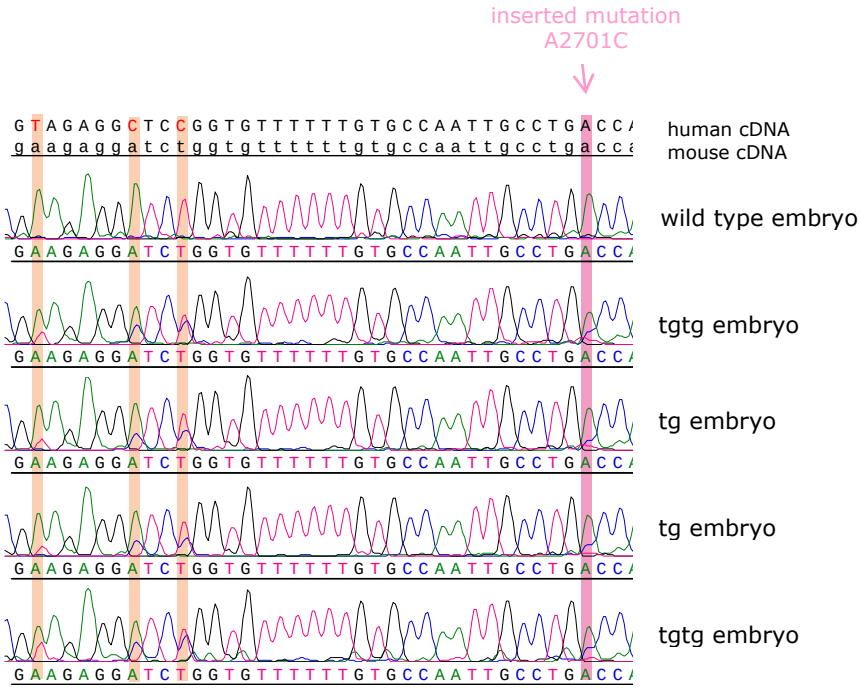

Fig. 8 Generation of *TRPS1* transgenic mice and verification of the transgene expression. **A**, Organization of the transgene and location of the primers used for the PCR strategies performed to analyze the transgene expression. The location of the hybridization probe used for the Southern blot experiments is also shown. **B**, Southern blot analysis performed to detect the founder of line 2 (lane 10), by digesting the genomic DNA with *BamHI*. **C**, Southern blot analysis of genomic DNA. Fragments corresponding to the mouse endogenous *Trps1* and to the human transgene are shown. Lanes 3,4,5,12 represent wt mice; lanes 2,7,8,10 represent tg mice and lanes 1,6,9,11 represent tgtg mice. **D**, 1^ PCR strategy for the assessment of the transgene expression. In lanes 2-10 it is possible to detect the properly processed human mutant *TRPS1* mRNA (tg embryos). Lane 1 represents a wt mouse and lane 11 corresponds to the construct used for the injection. **E**, Sequences obtained after the 2^ PCR strategy. The differences between the mouse *Trps1* and the human *TRPS1* sequences are highlighted by colored bars. In the wild type embryo only the mouse *Trps1* mRNA is detectable. In the tg and tgtg embryos are visible both the endogenous mouse *Trps1* mRNA and the mutant human *TRPS1* mRNA. Note the variation in transgene's expression between tg and tgtg embryos. M: DNA marker

3.3.2 Assessment of transgene expression

The expression of the transgene was proved for the four mouse lines by RT-PCR using RNA extracted from the limbs of 12.5 days old embryos (E12.5), because *Trps1* is high expressed at this stage of limb development (Kunath *et al*., 2002). The expression of *Col2a1* at this stage was proved as well (data not shown). After the reverse transcription, two different PCR strategies were chosen to detect the transgene expression (Fig 8A). By using primers flanking the ß-globin intron present in the transgene (the forward primer annealed in the *Col2a1* promoter and the reverse primer in *TRPS1* exon 3), it was possible to amplify only the transgene sequence and in transgene-expressing embryos its proper spliced products (1^PCR strategy, fig. 8D). In all the embryos identified as transgenic by Southern blot, the properly processed human mutant *TRPS1* mRNA was detected by PCR.

The human *TRPS1* and the mouse *Trps1* ORF sequences show a 91,3% identity. The nucleotide differences are spread over the entire sequences (excluding the zinc finger domain sequences, which are conserved between human and mouse). The 2^PCR strategy used primers chosen in a region identical between human and mouse sequence and they amplified the region containing the GATA domain with the missense mutation. The PCR products were sequenced and the few variations present between mouse and human allowed the simultaneous detection of both the endogenous mouse *Trps1* mRNA and the mutant human *TRPS1* mRNA (Fig. 8E).

The four lines of transgenic mice present different degrees of transgene expression and the transgenic mice from line 2 were those with the highest rate of expression. To increase the expression of the human transgene mice homozygous for the transgene (tgtg animals) were generated by breeding two transgenic mice from line 2. Fig. 8C shows a Southern blot of genomic DNA of wt, tg and tgtg animals. In Fig. 8E an example of sequences, which were obtained after RT-PCR performed on RNA extracted from E12.5 limbs of wild type, tg and tgtg embryos is shown. Although sequencing is not a precise quantitative method, looking at several sequences of tgtg embryos, it was possible to detect a slight but certain increase of the transgene expression in comparison to the tg embryos.

3.3.3 Gross phenotype and skeletal morphology

Neither the heterozygous nor the homozygous transgenic mice showed visible differences in their phenotype when compared with the wild type animals. To visualize and consequently better analyze the skeletal morphology of the transgenic mice, the whole skeletons of E16.5 embryos and 4-week old mice were stained with alcian-blue and alizarin red. No visible deformations in the skeleton of transgenic mice compared with that of wild type animals were detected (Fig. 9).

A wt 1 tgtg 1 **B** wt 2 tgtg 2

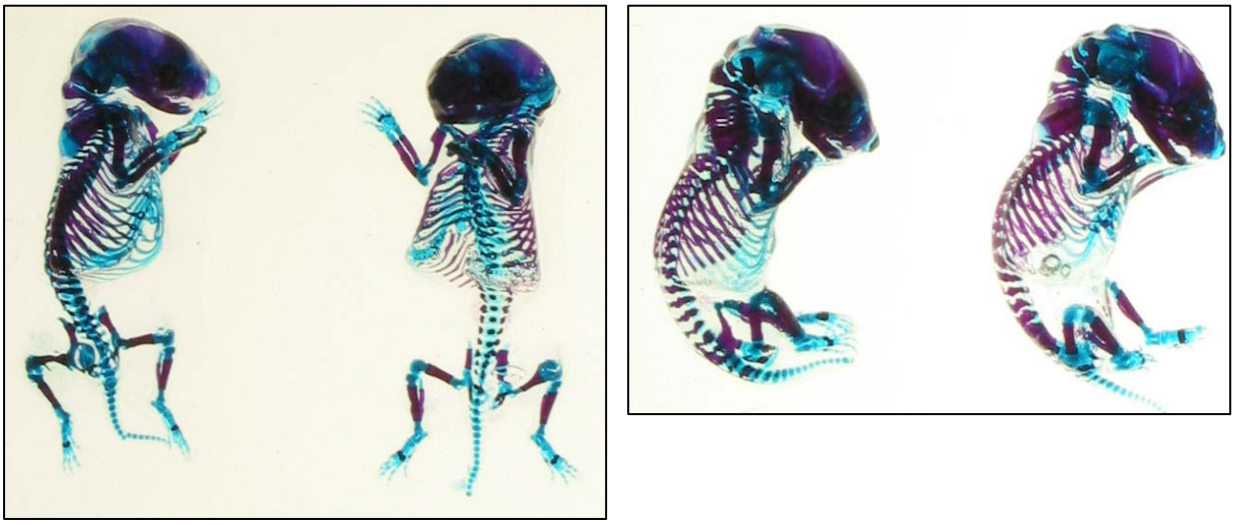

C wt 2 tgtg **2**

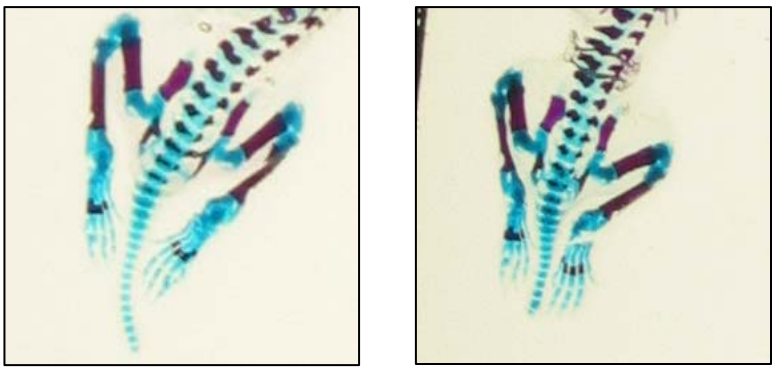

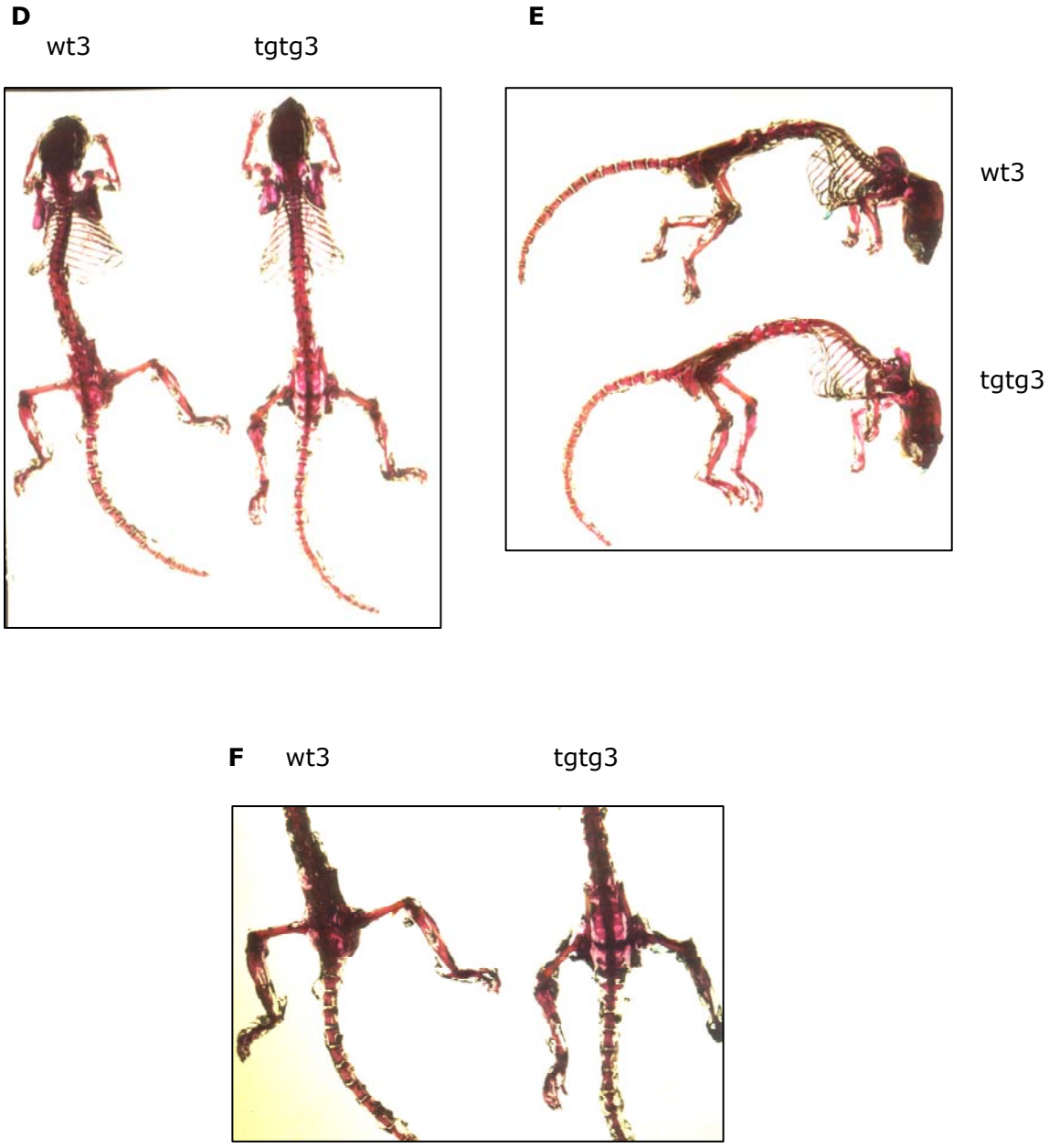

Fig. 9 Alizarin red- and alcian-blue-stained skeletal preparation of four sib E16.5 mouse embryos, wt1, wt2, tgtg1 and tgtg2, and two sib 4-week old mice, wt3 and tgtg3. **A,** Ventral view of wt1 and tgtg1. **B**, Lateral view of wt2 and tgtg2. **C**, Spinal column and hindlimbs view of wt2 and tgtg2. **D**, Dorsal view of wt3 and tgtg3. **E**, Lateral view of wt3 and tgtg3. **F**, Spinal column and hindlimbs of wt3 and tgtg3. Red staining represents the bone and blue staining represents the cartilage.

3.3.4 *In situ* hybridization

To examine possible defects in the differentiation process of the cartilage in the transgenic animals, *in situ* hybridization analyses were performed in collaboration with the group of Andrea Vortkamp (Institut für Molekulargenetik, Max-Planck-Institut, Berlin). Additionally, the forelimbs of wild type and transgenic animals (tg and tgtg) were stained with Safranin which allowed to detect the chondrocytes organization in the limb's growth plates (Fig. 10). The expression pattern of several genes known to be involved in limb development were analyzed, like *Ihh* (Indian hedgehog), *PTHrP* (Parathyroid hormone-like peptide), *ColII* (type II collagen), *ColX*, (type X collagen), *Mmp13* (Matrix metalloproteinase 13) and *Ptch* (Patched) (Table 4) in forelimbs of E14.5, E16.5 and E18.5 wild type embryos (wt), transgenic embryos (tg) and embryos homozygous for the transgene (tgtg). The results obtained for *Ihh*, *ColX* and *Trps1* are shown in Fig. 11.

Table 4 Expression pattern of the genes used for the *in situ* hybridization in cartilage and skeletal elements of mouse limbs

gene	expression pattern in cartilage and skeletal elements of mouse limbs
ColII	proliferating chondrocytes
ColX	hypertrophic chondrocytes
Ihh	prehypertrophic chondrocytes
PTHrP	joint regions, periarticular chondrocytes
Ptch	between proliferating and prehypertrophic chondrocytes
Mmp13	late hypertrophic chondrocytes
Trps1	joint regions, periarticular chondrocytes, prehypertrophic chondrocytes

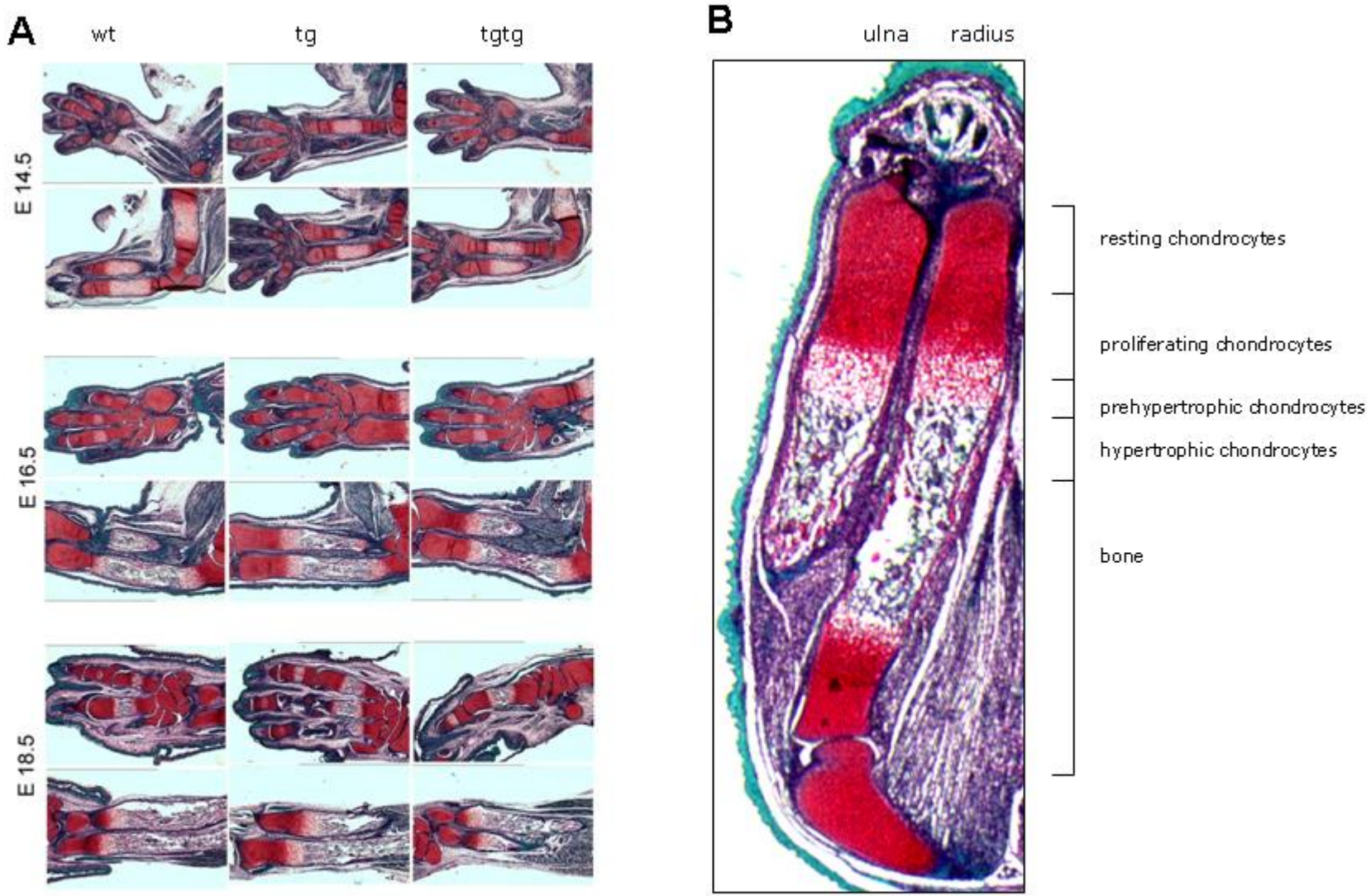

Fig. 10 A. Paraffin-embedded limbs sections stained with Safranin to visualize cartilaginous tissues (in red).

B. Chondrocytes organization in a Safranin-stained radio of a tg E16.5 forelimb.

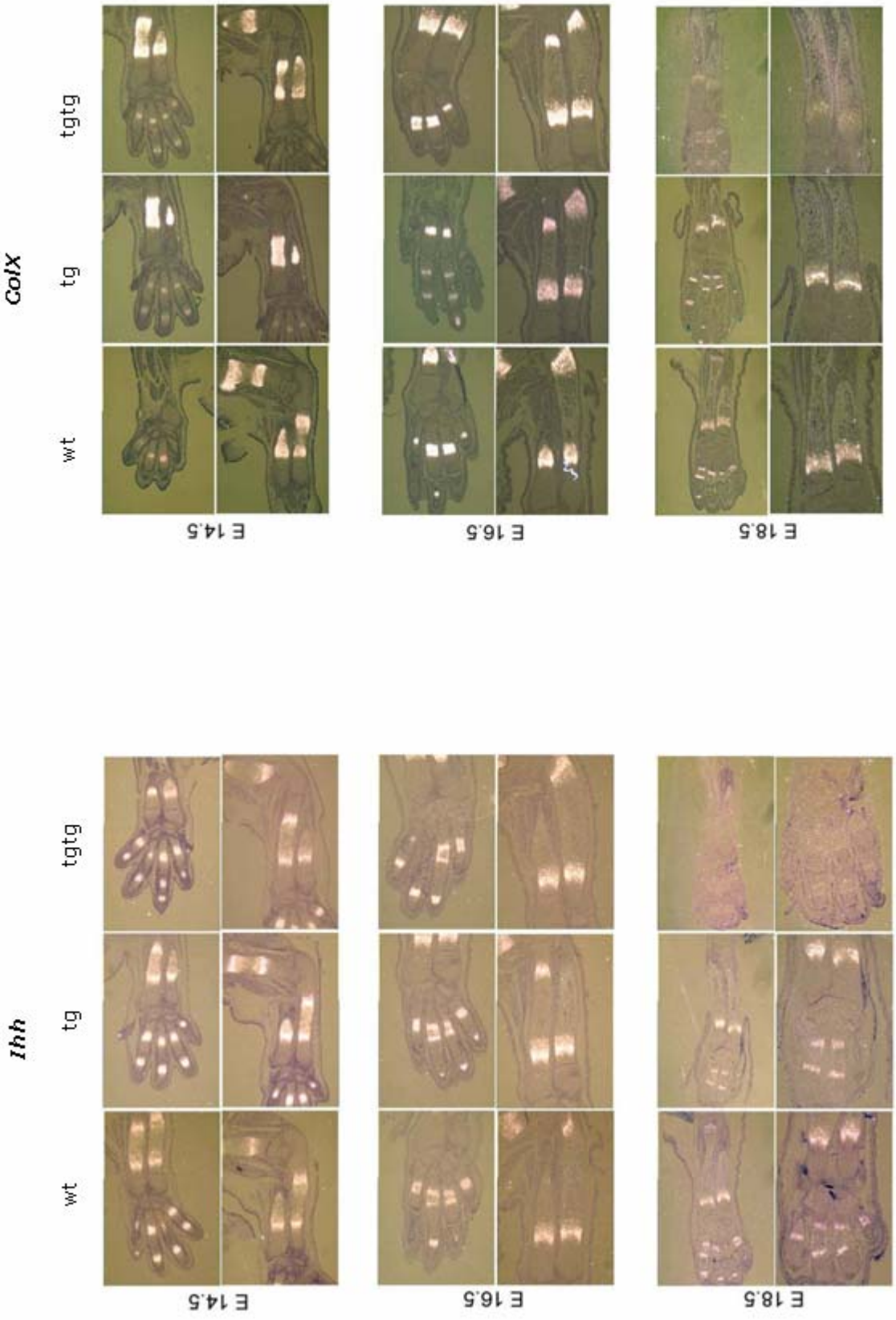

Fig. 11 *In situ* hybridization studies in the TRPS1 transgenic mice.

Fig. 11-continued

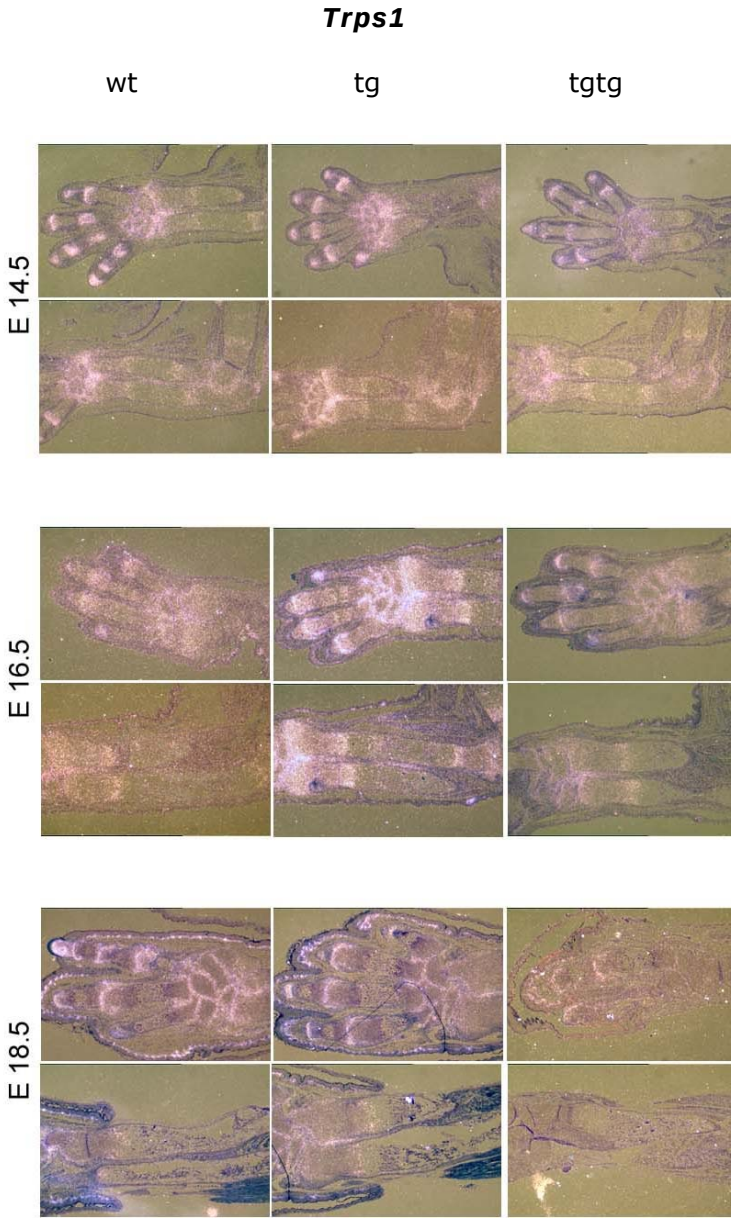

Several mice from different litters were analyzed but at these stages of limbs development (E14.5, E16.5 and E18.5) reliable variations in the expression patterns of the genes used for the *in situ* hybridization were not detected.

3.4 cDNA microarray analysis of mouse embryonic tissues

In order to identify potential targets of Trps1, expression profiles of the limbs and snouts of *Trps1*$^{\Delta GATA\text{-}Znf/\Delta GATA\text{-}Znf}$ and *Trps1*$^{+/\Delta GATA\text{-}Znf}$ mouse embryos (Malik *et al*., 2002) were compared with those of wild type embryos. Affymetrix MOE430A oligonucleotide arrays, containing about 22000 probe sets, were used to this purpose. Genes were defined as up- or downregulated, respectively, when their expression levels were at least 1.5 fold increased or decreased in the mutant mice with a standard deviation among the replicates of less than 25%. Moreover, genes were considered differentially expressed when in the replicates of one genotype at least two were scored as „absent" and the calls in the other genotype were scored as „present" in all samples. In this case, we defined the fold change as >1.5 for the upregulated genes and <-1.5 for the downregulated genes.
Some of the analyzed genes were represented by several sets on the array chip. Only the sets with the highest fold change were considered.

3.4.1 cDNA microarray analysis of mouse embryonic limbs

Expression profiles of the limbs of three wild type mouse embryos were compared with those of the limbs of two *Trps1*$^{+/\Delta GATA\text{-}Znf}$ and three *Trps1*$^{\Delta GATA\text{-}Znf/\Delta GATA\text{-}Znf}$ mouse embryos from the same litter at E11.5. Five hundred forty-nine genes fulfilled all criteria, listed above, and they were considered as abnormally expressed in the mutants (Table 5).
The highest fold change in the mean expression values was found comparing the expression profiles of the heterozygotes with those of the wild type. The genes *Extl2* (exotoses multiple-like 2) and *Matn2* (matrilin 2) were 2.1-fold upregulated in the heterozygotes and the gene *Shoc2* (soc-2, suppressor of clear homolog) was 2.1-fold downregulated in the heterozygotes.

Table 5 Number of differentially expressed genes in the expression profiles of the limbs of mutant embryos in comparison with those of the limbs of wild type embryos. -/-: *Trps1*$^{\Delta GATA\text{-}Znf/\Delta GATA\text{-}Znf}$ mice. +/-: *Trps1*$^{+/\Delta GATA\text{-}Znf}$ mice.

UPREGULATED		DOWNREGULATED	
-/-	+/-	-/-	+/-
86	237	115	111
total 323		total 226	

Fig. 12 shows a functional classification of the genes found to be upregulated and downregulated, respectively. Most of the differentially expressed genes were involved in signal transduction, in cell growth and in transcription.

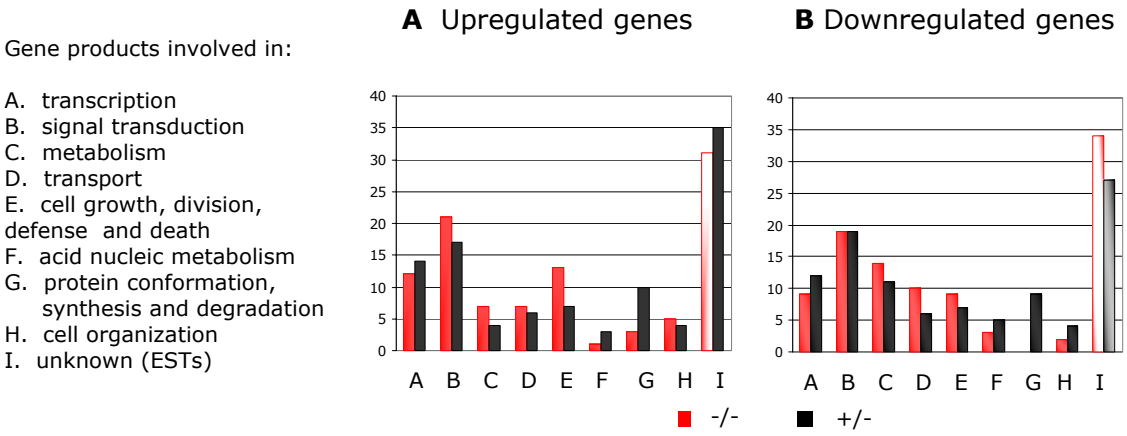

Fig. 12 Functional classification of the genes differentially expressed in the limbs of mutant mice. The Y-axis represents the percentage of genes. -/-: *Trps1*$^{\Delta GATA\text{-}Znf/\Delta GATA\text{-}Znf}$ mice. +/-: *Trps1*$^{+/\Delta GATA\text{-}Znf}$ mice.

Thirty-six genes showed the same tendency of regulation in both wild type-homozygous and wild type-heterozygous comparisons. They are listed and shortly described in Tables 6 (upregulated) and Table 7 (downregulated).

Table 6 Genes upregulated in limbs of both *Trps1*$^{\Delta GATA\text{-}Znf/\Delta GATA\text{-}Znf}$ and *Trps1*$^{+/\Delta GATA\text{-}Znf}$, when compared to the wild type.

-/-: *Trps1*$^{\Delta GATA\text{-}Znf/\Delta GATA\text{-}Znf}$ mice. +/-: *Trps1*$^{+/\Delta GATA\text{-}Znf}$ mice.

Gene GenBank accession number	Gene upregulated		(hypothetical) function
	-/- Fold change	+/- Fold change	
Arf3 ADP-ribosylation factor 3 NM_007478	1.5	1.5	Transport
Laptm4b lysosomal-associated protein transmembrane 4B NM_033521	1.8	1.5	Cell growth, division, defense and death
Arntl aryl hydrocarbon receptor nuclear translocator-like NM_007489	1.5	1.8	Transcription
Extl2 Mus musculus exotoses (multiple)-like 2 NM_021388	1.5	2.1	Cell organization
B4galt6 UDP-Gal:betaGlcNAc beta 1,4-galactosyltransferase, polypeptide 6 NM_019737	>1.5	>1.5	Metabolism
Setdb1 SET domain, bifurcated 1 C77070	>1.5	>1.5	Unknown
Cstf1 cleavage stimulation factor, 3' pre-RNA, subunit 1 NM_024199	>1.5	>1.5	Acid nucleic metabolism
Akt3 human protein kinase Bgamma NM_011785	>1.5	>1.5	Signal transduction
Exosc1 exosome component 1 NM_011785	>1.5	>1.5	Protein conformation, synthesis and degradation
Rnf-37 ring finger protein 37NM_080562	>1.5	>1.5	Transcription
expressed sequence AI428936 NM_153577	>1.5	>1.5	Unknown
expressed sequence NM_175127	>1.5	>1.5	Unknown
Sod2 superoxide dismutase 2, mitochondrial NM_013671	>1.5	>1.5	Metabolism
Dab1 disabled homolog 1 NM_010014	>1.5	>1.5	Signal transduction
cDNA clone BG965874	1.9	2.0	Unknown
Cyp4f16 cytochrome P450, family 4, subfamily f, polypept.16 NM_024442	1.7	1.8	Signal transduction
DC6 protein NM_175009	1.7	1.6	Unknown
cDNA cone BE628832	1.6	1.5	Unknown
cDNA clone NM_028242	1.9	1.6	Unknown

Table 7 Genes downregulated in limbs of both *Trps1*$^{\Delta GATA\text{-}Znf/\Delta GATA\text{-}Znf}$ and *Trps1*$^{+/\Delta GATA\text{-}Znf}$ mice, when compared to the wild type mice. -/-: *Trps1*$^{\Delta GATA\text{-}Znf/\Delta GATA\text{-}Znf}$ mice. +/-: *Trps1*$^{+/\Delta GATA\text{-}Znf}$ mice.

Gene GenBank accession number	Gene downregulated		(hypothetical) function
	-/- Fold change	+/- Fold change	
Ywhaz tyrosine 3-monooxygenase/tryptophan 5-monooxygenase activation protein, zeta polypeptide NM_011740	-1.8	-1.6	Cell growth, division, defense and death
Emp3 epithelial membrane protein 3 NM_010129	-1.8	-1.6	Cell growth, division, defense and death
Mt1a metallothionein-I activator NM_023127	-1.7	-1.8	Transcription
cDNA clone NM_026846	<-1.5	<-1.5	Unknown
Tm4sf7 transmembrane 4 superfamily member 7 NM_053082	<-1.5	<-1.5	Unknown
Ncf2 neutrophil cytosolic factor 2 NM_010877	<-1.5	<-1.5	Metabolism
Eng Endoglin NM_007932	<-1.5	<-1.5	Signal transduction
Pik3cg phosphoinositide-3-kinase, catalytic, gamma polypeptide NM_020272	<-1.5	<-1.5	Signal transduction
LynB Mouse lyn B protein tyrosine kinase NM_010747	<-1.5	<-1.5	Signal transduction
Gadd45g growth arrest and DNA-damage-inducible 45 gamma NM_011817	<-1.5	<-1.5	Cell growth, division, defense and death
Tsix X (inactive)-specific transcript AF138745.1	<-1.5	<-1.5	Unknown
cDNA clone BG069250	<-1.5	<-1.5	Unknown
cDNA clone BC022145.1	<-1.5	<-1.5	Unknown
cDNA clone BC025863.1	<-1.5	<-1.5	Unknown
F11r F11 receptor NM_172647	<-1.5	<-1.5	Signal transduction
Ptdss2 phosphatidylserine synthase 2 NM_013782	<-1.5	<-1.5	Metabolism
cDNA clone AA185884	<-1.5	<-1.5	Unknown

3.4.1.1 The relative expression of several genes was confirmed by real-time PCR experiments

The relative gene expression for a subset of differentially expressed genes was assessed using real-time PCR as an independent method for validating the microarray data. RNA was isolated from the limbs of sixteen E11.5 mouse embryos (two wild type, six *Trps1*$^{\Delta GATA\text{-}Znf/\Delta GATA\text{-}Znf}$ and eight *Trps1*$^{+/\Delta GATA\text{-}Znf}$ animals). They derived from four different litters, different from the ones used for the microarray hybridization. A short description of the 12 genes and their fold expression changes by microarray and real-time PCR are summarized in Table 8. The overall tendency of changes was confirmed for seven genes: *Emp3*, *Laptm4B*, *Hoxb8, Hspg2* and *Lamb1-1* and partially (only for the *Trps1*$^{\Delta GATA\text{-}Znf/\Delta GATA\text{-}Znf}$ mice) for *Gadd45g* and *Eng*. In Fig. 13 the detailed real-time PCR results for the confirmed differentially expressed genes are shown.

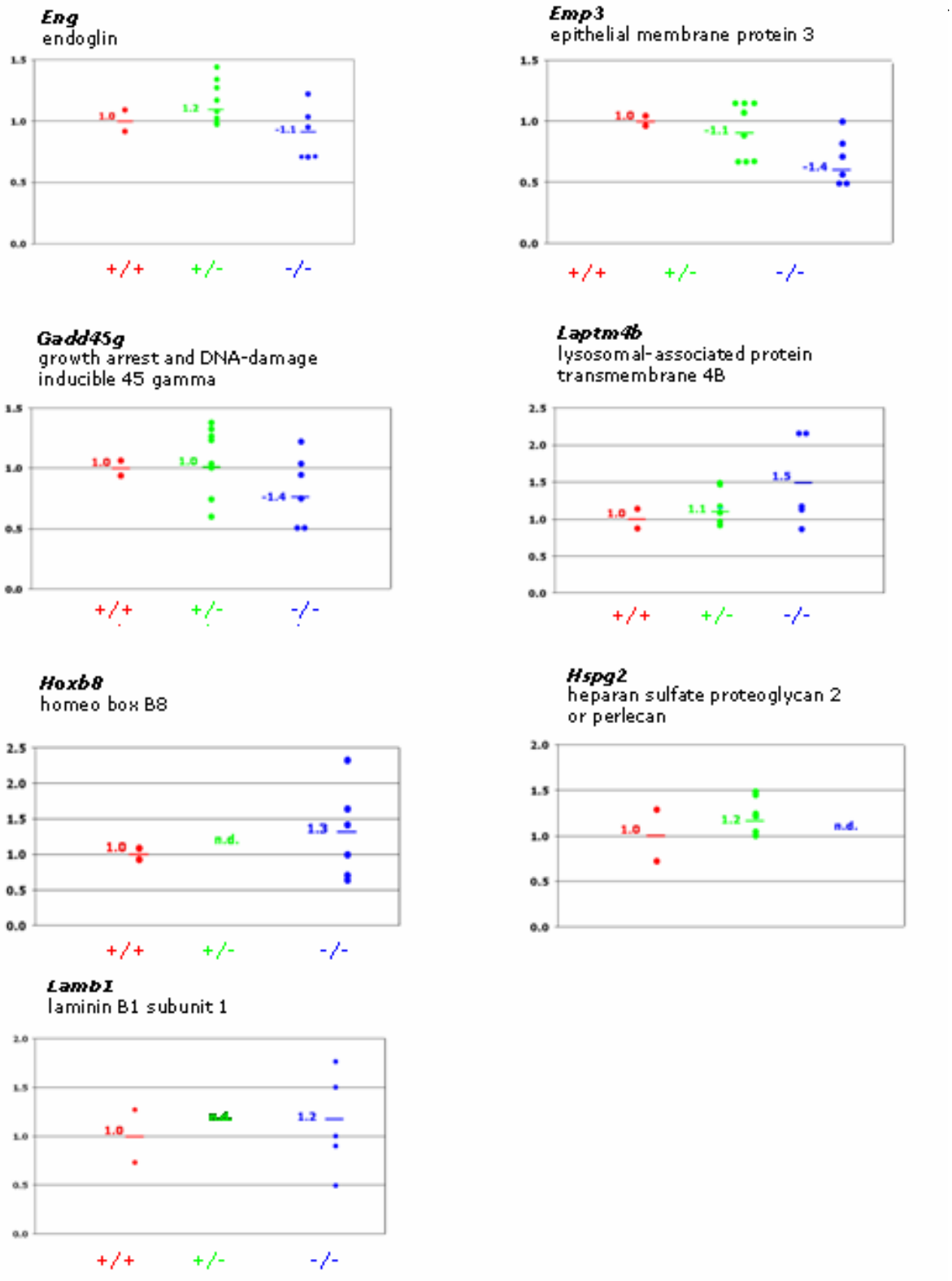

Fig. 13 Real-time PCR results for the seven genes whose relative expression changes confirmed the microarray data. Each point represents the values for a single embryo. The values are the averages of at least two independent experiments. +/+: wild type mice. -/-: *Trps1*$^{\Delta GATA\text{-}Znf/\Delta GATA\text{-}Znf}$ mice. +/-: *Trps1*$^{+/\Delta GATA\text{-}Znf}$ mice. n.d.: not done.

Table 8 Differentially expressed genes selected for the real-time PCR validation. The genes whose direction of the relative fold change is concordant with the microarray data are shown in red.
-/-: *Trps1*$^{\Delta GATA\text{-}Znf/\Delta GATA\text{-}Znf}$ mice; +/-: *Trps1*$^{+/\Delta GATA\text{-}Znf}$ mice; n.d.: not done.

gene	(hypothetical) function	reason for the real-time PCR validation	relative expression			
			microarray		real-time	
			+/-	-/-	+/-	-/-
Eng **endoglin**	**Signal transduction**	**downregulated in both +/- and -/-**	<-1.5	**<-1.5**	1.2	**-1.1**
Emp3 **epithelial membrane protein 3**	**Cell growth, division, defense and death**	**downregulated in both +/- and -/-**	**-1.6**	**-1.8**	**-1.1**	**-1.4**
Gadd45g **growth arrest and DNA-damage-inducible 45 gamma**	**Cell growth, division, defense and death**	**downregulated in both +/- and -/-**	<-1.5	**<-1.5**	1.0	**-1.4**
Laptm4B **lysosomal-associated protein transmembrane 4B**	**Cell growth, division, defense and death**	**upregulated in both +/- and -/-**	**1.5**	**1.8**	**1.1**	**1.5**
Extl2 exotoses (multiple)-like 2	Cell organization	upregulated in both +/- and -/-; involved in heparane sulfate biosynthesis	2.1	1.5	1.0	-1.4
Wnt5B wingless-related MMTV integration site 5B	Signal transduction	expressed in epiphysial growth plates; controls the pace of transitions between different chondrocyte zones	1.3	1.6	n.d.	-1.1
Madh4 'mothers against decapentaplegic' homolog 4 (Drosophila)	Transcription	expressed in epiphysial growth plates	1.3	1.5	n.d.	-1.2
Hoxb8 **homeo box B8**	**Transcription**	**expressed in epiphysial growth plates, role for proper pattern formation in higher vertebrates**	absent in +/-	**>1.5**	n.d.	**1.3**
Hspg2 **heparan sulfate proteoglycan 2**	**Cell organization**	**expressed in epiphysial growth plates; critical role in cartilage development**	**>1.5**	absent in -/-	**1.2**	n.d.
Traf6 receptor-associated factor 6 Traf6	Signal transduction	essential for development of normal bone formation and important role in the development of tooth number and shape	1.1	1.5	n.d.	1.0
Lamb1-1 **laminin B1 subunit 1**	**Cell organization**	**important role in the extracellular matrix**	-1.1	**1.6**	n.d.	**1.2**
Dlx3 distal-less homeobox 3	Transcription	expressed in epiphysial growth plates; mutations are associated with tricho-dento-osseous (TDO) syndrome, autosomal dominant disorder characterized by abnormal hair, teeth and bone	>1.5	absent in -/-	1.0	n.d.

3.4.1.2 TRPS1 actively represses the *HSPG2* promoter activity

Since TRPS1 is known to repress GATA-dependent gene activation, those genes, whose promoter regions were already characterized and contained GATA consensus sequences, were considered for further analyses. The functional activity of the human *HSPG2* promoter (~ 2.5 kb of the 5'-flanking region) was previously assessed in HeLa cells (Iozzo *et al*, 1997) and it contained nine GATA-1 motifs. To analyze whether TRPS1 could directly influence the *HSPG2* promoter activity, a luciferase reporter gene assay was set up. The 1711 bp from the *HSPG2* promoter region (see appendix for GenBank Accession number and for primer sequences) were amplified and inserted into the reporter plasmid containing the luciferase cDNA, upstream of the *SV40* promoter, to obtain *HSPG2*-SV40. The luciferase activity of HeLa cells transfected with *HSPG2*-SV40 was arbitrarily set as 1.0 fold activation (Fig. 14, *column 3*). Control transfections could exclude a significant increase of the SV40 reporter plasmid activity in the presence of the *HSPG2* promoter elements (Fig. 14, *columns 1* and *3*) and an effect of TRPS1 on the *SV40* promoter alone (Fig. 14, *column 2*). Co-transfection with TRPS1 led to a dosage-dependent reduction of the *HSPG2*-SV40 reporter plasmid activity up to 2 folds (Fig. 14, *columns 4* and *5*). On the contrary, only a slight repression of the reporter plasmid activity took place when the cells were transfected with T901P (Fig. 14, *column 6*), that is a mutated form of TRPS1 with a missense mutation in the GATA Znf-encoding region. The transcriptional repression of TRPS1 was not compromised by the co-transfection of the cells with GATA4 factor (Fig. 14, *column 7*), that, even alone, had no significant influence on the reporter plasmid *HSPG2*-SV40 (Fig. 14, *column 8*). These results could be confirmed also in COS7 cells (data not shown).

In summary, these findings indicated that TRPS1 was able to actively repress the transcription of *HSPG2*.

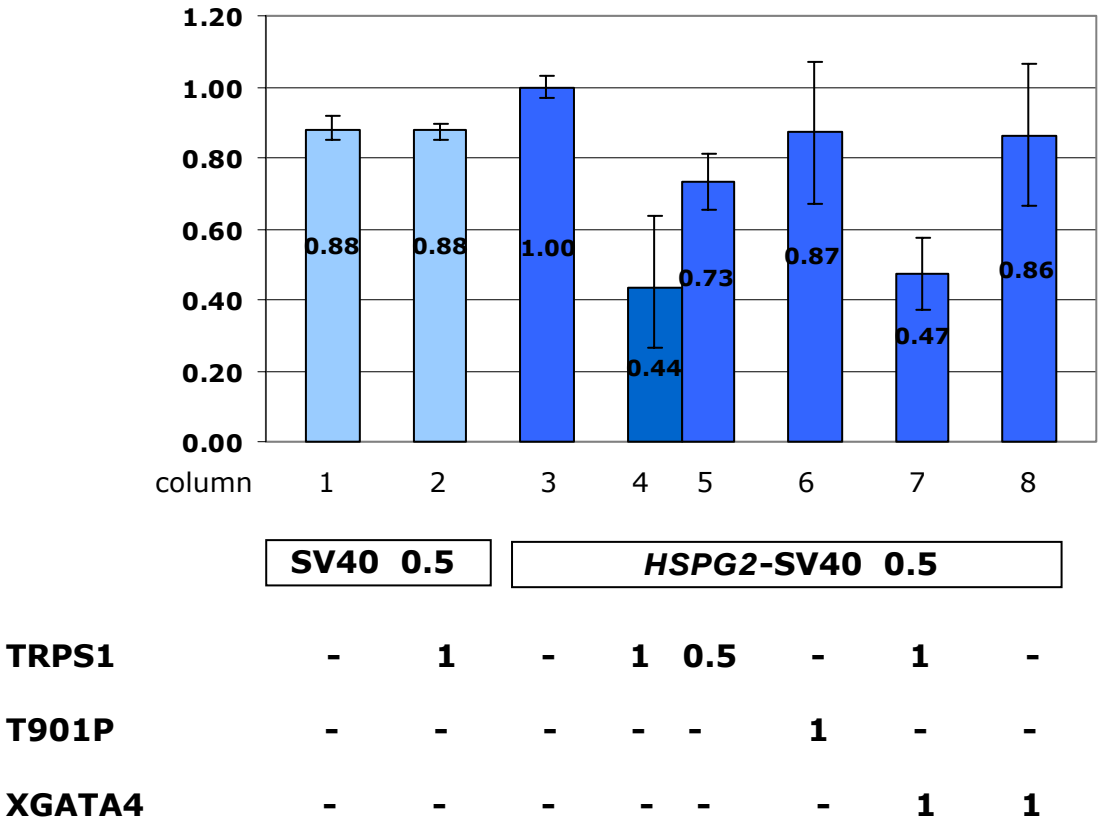

Fig. 14 Luciferase reporter gene assay in HeLa cells. HeLa cells were transiently transfected with plasmids encoding the *HSPG2*-SV40 reporter (0.5 µg), the SV40 plasmid (0.5 µg), the TRPS1 transcription factor (1 or 0.5 µg), the mutated form of TRPS1 transcription factor, T901P (1 µg) and the XGATA4 transcription factor (1 µg). The results are representative of at least two independent experiments.
The Y-axis represents the fold activation

3.4.2 cDNA microarray analysis of mouse embryonic snouts

Snout RNAs obtained from three wild type mouse embryos, three *Trps1*$^{\Delta GATA\text{-}Znf/\Delta GATA\text{-}Znf}$ and three *Trps1*$^{+/\Delta GATA\text{-}Znf}$ mouse embryos, from the same litter at E12.5, were hybridized to the Affymetrix MOE430A cDNA microarray. The expression profiles of the mutant animals were then compared with those of the wild type animals. According with the criteria pointed out in section 3.4, 715 differentially expressed genes were identified in the mutant embryos (Table 9). The highest fold change in the mean expression values was found comparing the expression profiles of the *Trps1*$^{\Delta GATA\text{-}Znf/\Delta GATA\text{-}Znf}$ mice with those of the wild type mice. The gene *Rnpc2* (RNA-binding region (RNP1, RRM) containing 2) was 2.6 fold upregulated in the *Trps1*$^{\Delta GATA\text{-}Znf/\Delta GATA\text{-}Znf}$.

Table 9 Number of differentially expressed genes in the expression profiles of the snouts of mutant embryos in comparison with those of the snouts of wild type embryos. -/-: *Trps1*$^{\Delta GATA\text{-}Znf/\Delta GATA\text{-}Znf}$ mice. +/-: *Trps1*$^{+/\Delta GATA\text{-}Znf}$ mice.

UPREGULATED		DOWNREGULATED	
-/-	+/-	-/-	+/-
212	128	128	247
total 340		total 375	

A functional classification of the abnormally expressed genes showed that many of these genes were involved in signal transduction and in transcription regulation (Fig. 15). Interestingly, among them, several genes whose loss-of-function mutations were already known to cause craniofacial defects in mice were identified (Wilkie *et al*., 2001) (Tables 10 and 11). The 61 genes that showed the same tendency of regulation in both wild type- *Trps1*$^{\Delta GATA\text{-}Znf/\Delta GATA\text{-}Znf}$ and wild type-*Trps1*$^{+/\Delta GATA\text{-}Znf}$ comparison are listed and shortly described in Tables 12 (downregulated) and Table 13 (upregulated).

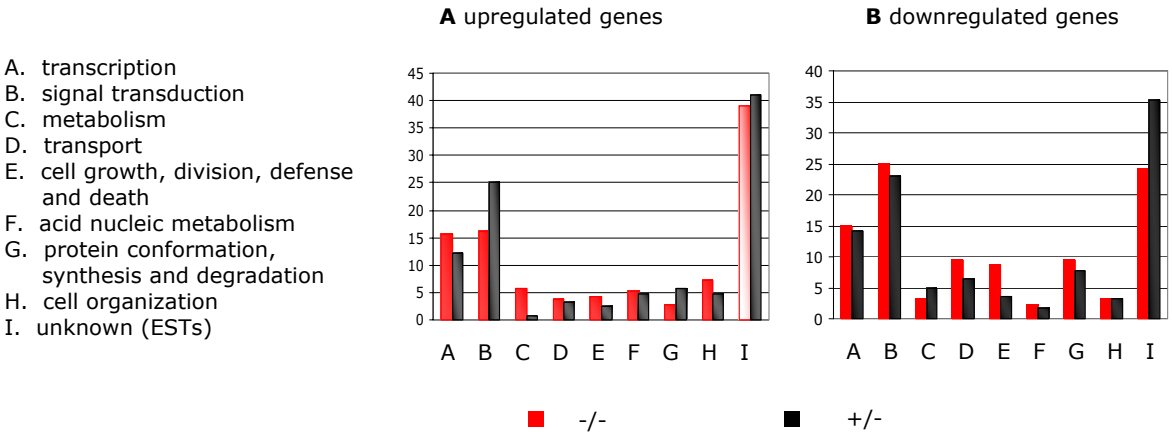

Fig. 15 Functional classification of the genes differentially expressed in the snouts of mutant mice. The Y-axis represents the percentage of genes. -/-: *Trps1*$^{\Delta GATA\text{-}Znf/\Delta GATA\text{-}Znf}$ mice. +/-:*Trps1*$^{+/\Delta GATA\text{-}Znf}$ mice.

Table 10 Genes upregulated in *Trps1*$^{\Delta GATA\text{-}Znf/\Delta GATA\text{-}Znf}$ mice whose loss-of-function mutations cause craniofacial defects in mice.
-/-: *Trps1*$^{\Delta GATA\text{-}Znf/\Delta GATA\text{-}Znf}$ mice. +/-:*Trps1*$^{+/\Delta GATA\text{-}Znf}$ mice.

Gene Protein	Major defects (time when defects first show)	Primary abnormality	fold change upregulation microarray	
			-/-	+/-
Dlx1 Distal-less homeobox 1	Abnormal ala temporalis, minor abnormalities of some other bones, small cleft palate in 10% of cases (-)	-	1.5	1.1
Pax6 Paired box 6	Homozygote:absent eyes and nasal cavities. Heterozygote: small eyes, iris hypoplasia (E10.5)	Aberrant lens and nasal placode formation, delayed closure of optic fissure	1.6	absent in +/-

Table 11 Genes downregulated in *Trps1* mutant mice whose loss-of-function mutations cause craniofacial defects in mice.
-/-: *Trps1*$^{\Delta GATA\text{-}Znf/\Delta GATA\text{-}Znf}$ mice. +/-:*Trps1*$^{+/\Delta GATA\text{-}Znf}$ mice.

Gene Protein	Major defects (time when defects first show)	Primary abnormality	fold change downregulation microarray	
			-/-	+/-
Col2a1 Procollagen, type II, α1	Bulging forehead, short snout, cleft palate (E13)	Defective endochondral bone formation	-1.6	-1.6
Dlx5 Distal-less homeobox 5	28% exencephaly, hypomineralized parietal/interparietal bones, abnormal nasal and otic capsules, branchial arches, 88% cleft palate, malformed teeth (E9.5)	-	-1.1	-1.6
Gli2 GLI-Kruppel family member 2	Deficient medial ossification of frontal and parietal bones, upper/lower incisors, cleft palate (64%) (E10.5)	Skeletal development	-1.2	-1.6
Hhex Hematopoietically expressed homeobox	Variable anterior truncations (E8.5)	Required for specification of axial mesendoderm	<-1.5	1.0
Pdgfra Platelet-derived growth factor receptor, α-poly-peptide	Cleft face, bleb over neural tube (E8)	Failure of subset of non-neural-crest cells to migrate	-1.3	-1.8
Prrx1 Paired-related homeobox 1	Cleft secondary palate, absent squamosal, zygomatic , tympanic ring, hypoplastic mandible (E13.5)	Defective growth of mandibular arch components	-1.7	-1.9
Trp53 transformation-related protein 53 (p53)	8-16% exencephaly	-	<-1.5	<-1.5

Table 12 Genes upregulated in snouts of both *Trps1*$^{\Delta GATA\text{-}Znf/\Delta GATA\text{-}Znf}$ and *Trps1*$^{+/\Delta GATA\text{-}Znf}$ mice, when compared with the wild type mice.
-/-: *Trps1*$^{\Delta GATA\text{-}Znf/\Delta GATA\text{-}Znf}$ mice. +/-:*Trps1*$^{+/\Delta GATA\text{-}Znf}$ mice.

Gene GenBank accession number	**Gene upregulated**		**(hypothetical) function**
	-/- Fold change	**+/- Fold change**	
cDNA clone AI645547	>1.5	>1.5	Unknown
Lactb lactamase, beta NM_030717.1	>1.5	>1.5	Signal transduction
cDNA clone BB536931	>1.5	>1.5	Unknown
Ppp1r14b protein phosphatase 1, regulatory (inhibitor) subunit 14B BM941586	>1.5	>1.5	Signal transduction
cDNA clone BC017633.1	>1.5	>1.5	Unknown
cDNA clone BM217857	>1.5	>1.5	Unknown
Pkp4 plakophilin 4 AW764208	>1.5	>1.5	Unknown
D16Wsu73e DNA segment, Chr 16, Wayne State University 73, expressed BB751546	>1.5	>1.5	Unknown
cDNA clone BE992311	>1.5	>1.5	Transcription
Zwint ZW10 interactor BC013559.1	>1.5	>1.5	Unknown
ESTs, Moderately similar to ubiquitin A-52 residue ribosomal protein fusion product 1 AU043470	>1.5	>1.5	Unknown
Sytl3 synaptotagmin-like 3 AB050743.1	>1.5	>1.5	Signal transduction

Table 12-continued

Gene GenBank accession number	Gene upregulated		(hypothetical) function
	Homozygotes Fold change	Heterozygotes Fold change	
Ywhaz tyrosine 3-monooxygenasetryptophan 5-monooxygenase activation protein, zeta polypeptide BF608615	2.3	1.9	Signal transduction
Laptm4b lysosomal-associated protein transmembrane 4B BB560429	1.8	1.9	Cell growth, division and death
Rpl41 ribosomal protein L41 BI694945	1.9	1.6	Protein conformation,synthesis, degradation
Hnrpa1 heterogeneous nuclear ribonucleoprotein A1 BE685966	1.9	1.8	Acid nucleic metabolism
cDNA clone BM235840	1.8	1.5	Unknown
Lap3 leucine aminopeptidase 3 AI875680	1.7	1.6	Protein conformation,synthesis, degradation
Snx6 sorting nexin 6 BC025911.1	1.6	1.6	Transport
D4Wsu53e DNA segment, Chr 4, Wayne State University 53, expressed NM_023665.1	1.6	1.5	Unknown
HnRNP A1 Heterogeneous nuclear ribonucleoprotein A1 BE685966	1.5	1.5	Acid nucleic metabolism
Nov nephroblastoma overexpressed X96585.1	1.5	1.9	Cell growth, division and death
Ankib ankyrin repeat and IBR domain containing 1 C80642	>1.5	>1.5	Transcription
similar to heterogeneous nuclear ribonucleoprotein A3 BB723867	>1.5	>1.5	Unknown
cDNA clone BC020137.1	>1.5	>1.5	Unknown
cDNA clone AV271161	>1.5	>1.5	Unknown
Calm3 calmodulin 3 AV047570	>1.5	>1.5	Cell growth, division and death

Table 13 Genes downregulated in snouts of both *Trps1*$^{\Delta GATA\text{-}Znf/\Delta GATA\text{-}Znf}$ and *Trps1*$^{+/\Delta GATA\text{-}Znf}$ mice, when compared with the wild type mice. -/-: *Trps1*$^{\Delta GATA\text{-}Znf/\Delta GATA\text{-}Znf}$ mice. +/-:*Trps1*$^{+/\Delta GATA\text{-}Znf}$ mice.

Gene GenBank accession number	Gene downregulated		(hypothetical) function
	-/- Fold change	+/- Fold change	
Golga3 golgi autoantigen, golgin subfamily a,3 BI693873	<-1.5	<-1.5	Signal transduction
Sema4a *s* semaphorin 4A NM_013658.1	<-1.5	<-1.5	Signal transduction
St7 suppression of tumorigenicity 7 NM_022332.1	<-1.5	<-1.5	Signal transduction
V1rc5 vomeronasal 1 receptor, C5 NM_053235.1	<-1.5	<-1.5	Signal transduction
Zfp36l2 zinc finger protein 36, C3H type-like 2 BG094962	<-1.5	<-1.5	Unknown
Aqp4 aquaporin 4 BB193413	<-1.5	<-1.5	Transport
Zfp261 zinc finger protein 261 AV370364	<-1.5	<-1.5	Unknown
Rusc1 RUN and SH3 domain containing1 BB806780	<-1.5	<-1.5	Unknown
Slc16a2 solute carrier family 16 (monocarboxylic acid transporters), member 2 AW105741	<-1.5	<-1.5	Transport
Mafb v-maf musculoaponeurotic fibrosarcoma oncogene family, protein B (avian) AW412521	<-1.5	<-1.5	Transcription
Cacng5 calcium channel, voltage-dependent, gamma subunit 5 AF458900.1	<-1.5	<-1.5	Transport
expressed sequence AW557946	<-1.5	<-1.5	Unknown
Matn4 matrilin 4 NM_013592.1	<-1.5	<-1.5	Cell organization
Trp53 transformation related protein 53 BB828014	<-1.5	<-1.5	Transcription
cDNA clone BB350484	<-1.5	-1.7	Unknown
cDNA clone AK014318.1	<-1.5	<-1.5	Unknown
Fzd6 frizzled homolog 6 NM_008056.1	<-1.5	<-1.5	Signal transduction
Tgfbr2 transforming growth factor, beta receptor II BG793483	<-1.5	<-1.5	Signal transduction

Table 13-continued

Gene GenBank accession number	Gene downregulated -/- Fold change	 +/- Fold change	(hypothetical) function
Ywhaz tyrosine 3-monooxygenasetryptophan 5-monooxygenase activation protein, zeta polypeptide NM_011740	-2.1	-1.9	Cell growth, division, defense and death
cDNA sequence BB770932	-1.8	-1.5	Unknown
Dnm dynamin L29457.1	-1.7	-1.6	Signal transduction
Prrx1 paired-related homeobox gene 1	-1.7	-1.9	Transcription
Col2a1 procollagen, type II, alpha NM_031163.1	-1.6	-1.6	Cell organization
Top2b topoisomerase (DNA) II beta BB166592	-1.6	-1.9	Acid nucleic metabolism
Col9a1 procollagen, type IX, alpha 1 AK004383.1	-1.5	-1.5	Cell organization
Pdlim4 PDZ and LIM domain 4 NM_019417.1	<-1.5	<-1.5	Signal transduction
Opn1sw opsin 1 (cone pigments), short-wave-sensitive (color blindness, tritan) BC026021.1	<-1.5	<-1.5	Signal transduction
Mint Msx2 interacting nuclear target protein NM_019763.1	<-1.5	<-1.5	Transcription
Oprk1 opioid receptor, kappa 1 L11065.1	<-1.5	<-1.5	Signal transduction
Ott ovary testis transcribed X96606.1	<-1.5	<-1.5	Unknown
Aqr aquarius AK020468.1	<-1.5	<-1.5	Unknown
Bcl2l11 BCL2-like 11 BB667581	<-1.5	<-1.5	Cell growth, division, defense and death
Similar to vesicle amine transport protein 1 BB559097	<-1.5	<-1.5	Unknown
Mid2 midline2 AF196480.1	<-1.5	<-1.5	Cell growth, division, defense and death
cDNA clone BB133120	<-1.5	<-1.5	Unknown

3.4.2.1 The relative expression of three genes was confirmed by real-time PCR experiments

Six abnormally expressed genes (*Laptm4*b, *Nov*, *Prrx1*, *Col2a1*, *Col9a1* and *Fzd6*) were chosen for validation by real-time PCR analysis. We used RNAs isolated from the snout of fifteen E12.5 mouse embryos (four wild type, five *Trps1*$^{\Delta GATA\text{-}Znf/\Delta GATA\text{-}Znf}$ and six *Trps1*$^{+/\Delta GATA\text{-}Znf}$ mice) originating from three litters, different from the ones used for the microarray hybridization. The differential expressions of mRNAs encoding *Laptm4b*, *Nov* and *Fzd6* (only for the homozygotes) were confirmed (Table 14).

Table 14 Differentially expressed genes selected for the real-time PCR validation. The genes whose direction of the relative fold change is concordant with the microarray data are shown in red. -/-: *Trps1*$^{\Delta GATA\text{-}Znf/\Delta GATA\text{-}Znf}$ mice. +/-:*Trps1*$^{+/\Delta GATA\text{-}Znf}$ mice. ECM: extracellular matrix

gene	(hypothetical) function	reason for real-time PCR validation	relative expression			
			microarray		real-time PCR	
			+/-	-/-	+/-	-/-
Laptm4b **lysosomal-associated protein transmembrane**	**Cell growth, division, defense and death**	**the only gene upregulated in the limb and snout knockout mice, in both +/- and -/-**	**1.5**	**2.3**	**1.4**	**1.6**
Nov **nephroblastom overexpressed gene**	**Cell growth, division, defense and death**	**the human gene is localized in 8q24.1; upregulated in both +/- and -/-**	**1.9**	**1.5**	**1.2**	**1.2**
Prrx1 paired-related homeobox gene 1	Transcription	the knockout mice show malformation of craniofacial, appendicular and axial structures; downregulated in both +/- and -/-	-1.9	-1.7	1.2	1.2
Col2a1 type II collagen, a1	Structural molecule activity	important component of the cartilage ECM; downregulated in both +/- and -/-	-1.6	-1.6	1.2	1.9
Col9a1 type IX collagen, a1	Structural molecule activity	downregulated in both +/- and -/-	-1.5	-1.5	1.1	1.5
Fzd6 **frizzled 6**	**Signal transduction**	**important role in hair follicle; downregulated in both +/- and -/-**	<-1.5	**<-1.5**	1.2	**-1.3**

In Fig. 16 the detailed real-time PCR results for the confirmed differentially expressed genes are shown.

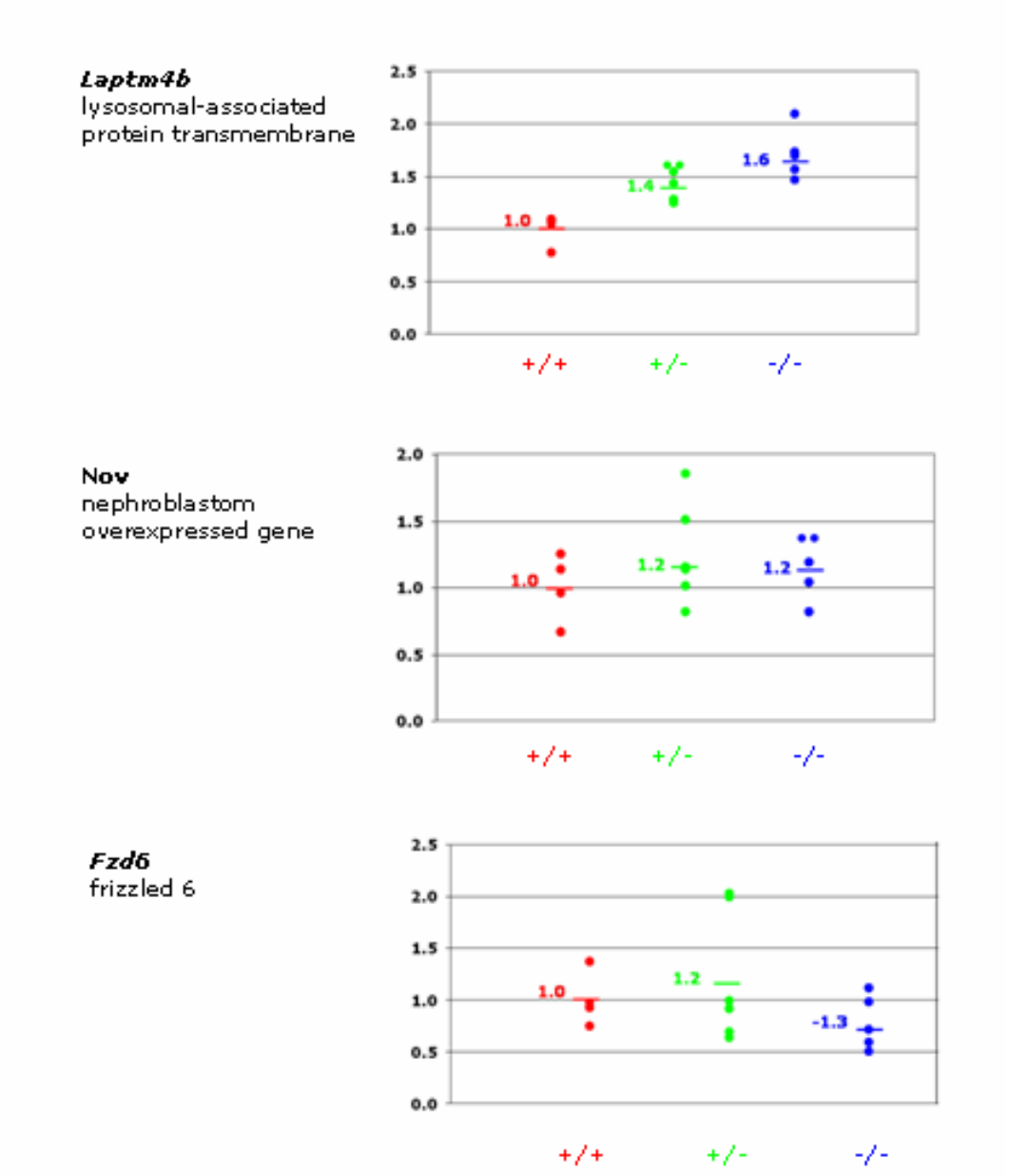

Fig. 16 Real-time PCR results for the three genes whose relative expression changes validate the microarray data. Each point represents the values for a single embryo. The values are the averages of at least two independent experiments. +/+: wild type mice. -/-: *Trps1*$^{\Delta GATA\text{-}Znf/\Delta GATA\text{-}Znf}$ mice. +/-: *Trps1*$^{+/\Delta GATA\text{-}Znf}$ mice.

3.4.2.2 TPRS1 actively represses the *LAPTM4b* promoter activity

Laptm4b was the only gene found to be upregulated in the microarray data of E11.5 limbs and of E12.5 snouts in both *Trps1*$^{+/\Delta GATA\text{-}Znf}$ and *Trps1*$^{\Delta GATA\text{-}Znf/\Delta GATA\text{-}Znf}$ mice. Moreover, its relative expression was confirmed by real time PCR experiments.

The functional activity of the *LAPTM4b* promoter region (~ 1.5 kb of the 5'-flanking region) was previously analyzed in hepatocellular carcinoma-related cell lines (Shao *et al*., 2003) and it contained two GATA-consensus motifs. To determine whether TRPS1 was able to directly affect the *LAPTM4b* promoter activity, a luciferase reporter gene assay was set up. Using specific primers, the *LAPTM4b* promoter was amplified and the 1532 bp PCR product (see appendix for GenBank Accession number and for primer sequences) was cloned into the pGL3b reporter plasmid (it does not contain any promoter) upstream to the luciferase cDNA, obtaining the *LAPTM4b*-pGL3b.

In HeLa cells, the *LAPTM4b* promoter did not show any activity.

Therefore, the reporter gene assays were carried out in COS7 cells, where the analyzed promoter was active and the luciferase activity of the cells transfected with the reporter plasmid *LAPTM4b*-pGL3b was set as 1.0 fold activation (Fig. 17, *column 2*). The pGL3b vector alone showed no activity (Fig. 17, *column 1*). When 1 µg of TRPS1-encoding plasmid was added the transcriptional activity of the reporter plasmid was repressed up to 50% (Fig. 17, *column 3*). Further analyses are required to analyze the effect of mutant TRPS1 proteins and of XGATA factors on the *LAPTM4b* promoter activity.

These findings demonstrated that *LAPTM4b* promoter activity can be directly repressed by TRPS1.

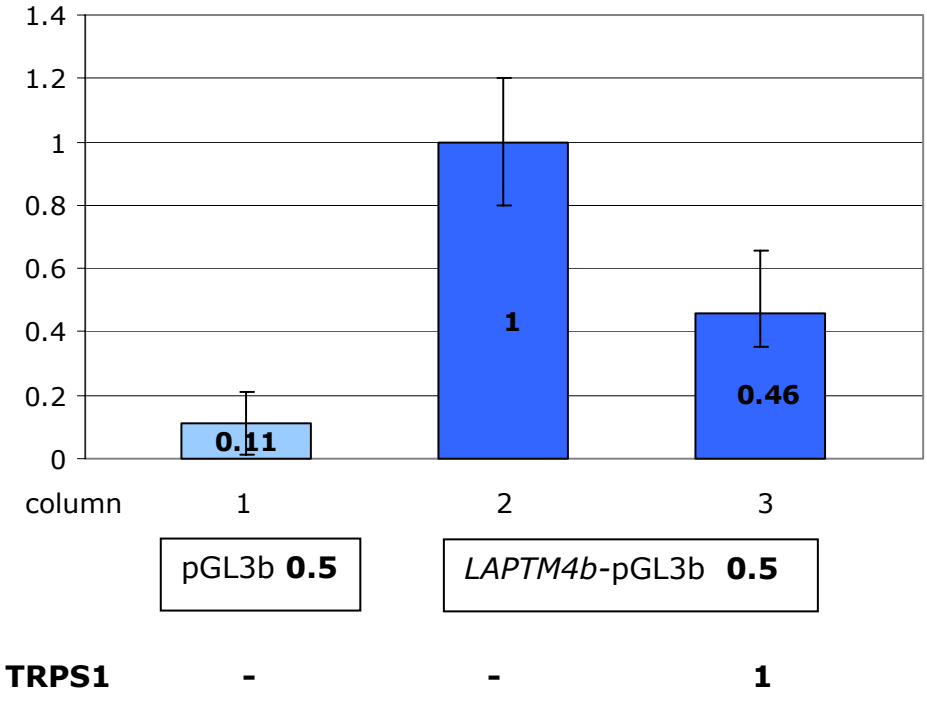

Fig. 17 Luciferase reporter gene assays in COS7 cells. The cells were transiently transfected with plasmids encoding the *LAPTM4b*-pGL3b reporter (0.5 µg) and the TRPS1 transcription factor (1 µg). As control the cells were transfected with the pGL3b alone (0.5 µg), which did not contain any promoter. The Y-axis represents the fold activation.

4. DISCUSSION

4.1 TRPS1 carries a single functional NLS

By mutation analysis of TRPS type I patients, the single base exchange 2854C>T was identified in the *TRPS1* (see Results 3.1), which affected the last arginine residue of one of the two predicted NLS (RRRTRKR at position 946-952 aa) of the TRPS1 transcription factor. Localization studies indicated that the single aa substitution R952C, prevents the TRPS1 from entering the nucleus (Kaiser *et al*., 2004).
These findings highlighted the importance of the mutation analysis in TRPS patients to detect functional domains of the TRPS1 transcription factor.

4.2 The *TRPS1* transgenic mouse does not represent a model for TRPS III

To study the pathogenesis of the severe TRPS type III, a transgene carrying the entire coding region of the human *TRPS1* with the T901P missense mutation inserted in the GATA Znf, under the control of *Col2a1* promoter, was used to generate a transgenic mouse model (see Results 3.3). This specific mutation was chosen, because the affected patient defines the severe end of the TRPS spectrum (Vilain *et al*., 1999; Lüdecke *et al*., 2001). Probably, the T901P mutation leads to the disruption of the ß-sheet structure of this portion of the zinc finger and to the alteration of the shape of the entire zinc finger. Furthermore, current functional studies show that the mutant TRPS1 protein is able to antagonize the function of the TRPS1 wild type protein, not only through the abrogation of the TRPS1 repressional function, but even upregulating the GATA-mediated gene activation (Kaiser, pers. communication). The *Col2a1* promoter and enhancer were selected to direct the expression of the transgene to chondrocytes in a developmental stage, in which the wild-type Trps1 is active (Ueta *et al*., 2001). This allows the analysis of the dominant negative effect exerted by the overexpression of a human mutated TRPS1 protein in the growth plates in the presence of two normal endogenous *Trps1* copies.

Patients with TRPS usually display a progressive degeneration of their typical abnormal phenotype beginning from their childhood. Unexpectedly, even the 4-week old transgenic mice did not show the TRPS typical brachydactyly or growth retardation (see Results 3.3.3).

There are several explanations to account for the apparently normal phenotype of the transgenic mice.

(I) By sequence analysis a surprisingly low transgene expression rate (~30%) was detected (see Results 3.3.2, Fig. 8E). If the amount of the mutant *TRPS1* transgene is not high enough, the quantity of co-regulators that it can recruit does not disturb the function of the endogenous Trps1, which carries on its normal regulatory functions. Ueta *et al*. (2001) used exactly the same *Col2a1* promoter/enhancer elements to overexpress *Cbfa1* or its dominant negative form in chondrocytes, causing severe skeletal malformations in the mice. The difference of transgene expression between *Cbfa1* and *TRPS1* can be attributed to several factors, including differences in the chromosome position of the transgene integration site and copy number. In particular, expression from a transgenic locus may be silenced when repeated transgene copies are arranged as a concatameric array. Furthermore, chromatin structure at the site of integration can affect transgene expression, not only in plants (van Leeuwen *et al*., 2001), but in mammals as well (Garrick *et al*., 1998).

(II) In the growth plates of the embryonic mouse limb, *Col2a1* is highly expressed in resting and in proliferating chondrocytes and is less expressed in hypertrophic chondrocytes (Ueta *et al*., 2001; Olsen *et al*., 2000; Zhou *et al*., 1995). Kunath *et al*. (2002) showed that *Trps1* is highly expressed in the joint regions of the skeletal elements of the limbs, in the periarticular chondrocytes and in prehypertrophic chondrocytes of the growth plates of the limbs, during mouse embryonic development. Since the endochondral ossification is a very tightly regulated process, a slight difference of temporal and spatial expression of *Col2a1* and *Trps1* in the growth plates could prevent a dominant negative effect of the mutated TRPS1 protein.

(III) The human mutated protein may not be recognized by the mouse protein complexes, which are involved in Trps1 regulatory activity and it is perhaps subject to the quality-surveillance mechanism and degraded (Clausen *et al*., 2002). This hypothesis, however, is not very likely, considering that the only seven percent differences between the mouse and the human protein

sequences do not reside in the zinc finger regions, which are involved in protein-protein interactions.

Highly sensitive studies like the *in situ* hybridization experiments (see Results 3.3.4), which have been performed in limbs of transgenic mice at stages E14.5, E16.5 and E18.5, did not show any reliable differences in the expression pattern of genes like *Ihh*, *PTHrP*, *ColII*, *ColX*, *MMP13* and *PTCH*.

In addition to the explanations mentioned above, it is also possible that TRPS1 does not interfere during endochondral ossification with the pathways in which those genes are involved. In fact, in the cDNA microarray analyses (see Results 3.4) performed later on tissues from the GATA-Znf deleted *Trps1* knockout mice, none of the genes used for the *in situ* hybridization, with the exception of *ColII*, was found to be differentially expressed in the mutant mice.

4.3 Identification of the downstream genes of the TRPS1 transcription factor

A growing list of human diseases can be attributed to mutations in the genes coding for transcription factors (Latchman, 1996; Villard, 2004) causing disruption of biological pathways, which can lead to malformation, or tumorigenesis.

Of great importance to disclose the physiological processes controlled by these transcription factors is the identification of their direct and indirect targets. Several methods can be used for this purpose. For example the combined use of siRNA-mediated gene silencing and cDNA microarray analysis can be useful to determine the effects of a gene knockdown in the cell (example *Rb1*, Semizarov *et al*., 2004).

However, tissues or organs obtained from *in vivo* models such as knockout mice offer the best material to compare gene expression of the affected organism to that of the normal one, by using cDNA microarray analyses (example *Pax6*, Chauhan et al., 2002).

4.3.1 The silencing of the Trps1 transcription factor in NIH3T3 might interfere with the control of cell cycle progression

Fifty-nine genes were found to be abnormally expressed in NIH3T3 cells (29 upregulated and 30 downregulated in treated cells) in which *Trps1* expression was silenced as effect of transfection of siRNAs, homologous in sequence to the *Trps1* gene (see Results 3.2.1). The NIH3T3 cell line was chosen for the RNA interference experiments for several reasons. First, *Trps1* is highly expressed in these cells. Second, NIH3T3 can easily be transfected with siRNAs (Elbashir *et al*., 2001; Harborth *et al*., 2001). Third, functional analyses of TRPS1 have already been performed in human fibroblasts (Kaiser *et al*., 2003a; Kaiser *et al*., 2003b).

Some of the genes upregulated upon reduction of endogenous Trps1 level by siRNA transfection, thus normally repressed by Trps1, are involved in control of cell cycle progression.

The Fos-like antigen 2, also called Fra2, is one of the four members of the Fos gene family. These genes encode leucine zipper proteins that can dimerize with proteins of the JUN family, thereby forming the transcription factor complex AP-1. As such, the FOS proteins have been implicated as regulators of cell proliferation, differentiation, and transformation (Review: Shaulian and Karin, 2001). In some cases, expression of the FOS gene has also been associated with apoptotic cell death (Ameyar *et al*., 2003).

Bakiri *et al*. (2002) studied the functions of specific AP-1 dimers. The authors showed that NIH3T3 cells transiently transfected with cJun~Fra2 dimers (the tilde indicates a tethered dimer) were able to progress through S and G_2/M phases of the cell cycle, while control cells stopped proliferating and accumulated in the G_o/G_1 compartments, in the presence of both increased cell density and serum withdrawal. This finding leads to the hypothesis that down regulation of c-Jun and Fra2 upon serum deprivation or cell-to-cell contact could therefore be a prerequisite for growth arrest (Lallemand *et al*., 1997).

On the other hand, upregulation of *FRA2* in chondrocytes due to a mutated TRPS1 could lead to an increased proliferation of normally resting chondrocytes and finally to premature closure of the growth plate.

Also the protein kinase, mitogen-activated, kinase 7 (named MKK7 or JNKK2) was found to be upregulated in the expression profiles of the treated NIH3T3 cells. MKK7 belongs to the mitogen-activated protein kinase kinase (MAPKK) proteins and is a specific activator of JNK1 and JNK2 (Wu *et al*., 1997), which control a spectrum of cellular processes, including cell growth, differentiation, transformation, and apoptosis. Wada and Penninger (2004) demonstrated that MKK7 links stress signaling, among other to G_2/M cell cycle progression and they discuss the importance of the MKK4 (another direct activator of JNK)/MKK7-JNK-c-Jun pathway linking stress and developmental signals to cell proliferation, cell cycle progression, cellular senescence, and apoptosis.

p63 was also found to be upregulated in treated NIH3T3 cells. Together with p73, p63 is high homolog to p53. Like p53, both p63 and p73 bind to the canonical p53-responsive element, transactivate p53 target gene expression, and induce apoptosis when overexpressed (Review: Yang and McKeon, 2000).

These findings suggest a role of Trps1 in the cell cycle control of mouse fibroblasts, in particular in the regulation of growth arrest and cell death, by means of transcriptional repression (direct or indirect) of transcription factors involved in important signaling pathways. The hypothesis that Trps1 may be implicated in apoptosis was raised by Chang *et al*. (2000;2002). The authors observed that physiological levels of androgens repressed the expression of GC79/*TRPS1* mRNA in LNCaP-FGC (androgen-dependent human prostate cancer cells). Castration-induced androgen withdrawal in rat ventral prostate, used to induce apoptosis in the prostate, increased the expression of GC79/*TRPS1* mRNA leading to the hypothesis that GC79/TRPS1 can be implicated in the process of apoptotic cell death in the rat ventral prostate.
Moreover, TRPS1 interacts with the dynein light chain LC8a, which is able to strongly reduce the transcriptional repression activity of TRPS1 (Kaiser *et al*., 2003a). LC8a interacts with Bim, a member of the Bcl-2 family, and is able to regulate its pro-apoptic activity (Puthalakath *et al*., 1999). Apoptosis is probably the mechanism responsible for the death of mature hypertrophic chondrocytes during endochondral bone formation and deletion of the gene encoding Bcl-2, which is a cell-death inhibitor, leads to accelerated maturation of chondrocytes and shortening of long bones (Amling *et al*., 1997).

Furthermore, Bcl-2 regulates hair follicle apoptosis as well (Müller-Röver *et al*., 1999).
These results obtained in NIH3T3 cells indicate that Trps1 may play an important role in the cell cycle control.

4.3.2 Microarray analysis of GATA Znf-deleted Trps1 mouse embryonic tissues

So far, no further analysis of the differentially expressed genes in NIH3T3 cells was performed, because the study of the different tissues from the GATA Znf-deleted Trps1 mice (Malik *et al*., 2002), provided by Dr. Ramesh Shivdasani (2.1.6) represented an enhanced model of study. In particular, the expression profiles of limbs and snouts of the *Trps1* knockout mice have been analyzed, as these are the tissues usually affected by mutations in the *TRPS1* gene in the human patients (see Results 3.4).

The mice generated by Malik *et al*. (2002) are not *Trps1*-null mice. Like the TRPS type I patient described by Lüdecke *et al*. (2001) who carries the splice site mutation IVS6+1G>T, only one domain of the Trps1, the GATA-like Znf domain, is deleted in the mutant mice. RT-PCR analyses demonstrated the presence of stable GATA Znf-deleted Trps1 mRNA in both *Trps1*$^{+/\Delta GATA\text{-}Znf}$ and *Trps1*$^{\Delta GATA\text{-}Znf/\Delta GATA\text{-}Znf}$ mice (data not shown). This could in part explain the low fold change (comprised between 1.5 and 2.6) in the expression values, detected comparing the expression profiles of limbs and snouts of wild type and mutant animals. So far, the only known function of TRPS1 is as repressor of GATA-mediated transcription. The *Trps1* GATA Znf-knockout does probably not abrogate completely the function of the transcription factor, because it still contains eight of its nine Znfs and its NLS domain. Only the GATA-mediated repressional activity may be affected. If, for example, the six N-terminal Znfs control a pathway different and independent from the GATA-mediated, these pathways should not be affected. Moreover, it is not yet known whether TRPS1 acts as repressor or as co-repressor. In the latter case, the reduced Trps1 repressional function in the GATA Znf-deleted *Trps1* knockout mice could be replaced by other still intact transcription factors.

Anyway, to discriminate between truly differentially expressed genes and false positives and to obtain a consistent confirmation of the microarray data, RNAs from limbs and snouts of additional wild type and mutant animals from several litters, at stage E11.5 (for the limbs) and E12.5 (for the snouts) of development, were analyzed by real-time PCR.
In this way, also the limitations due to normal physiological variance in gene expression (even found in members of the same litter) and due to the process of sacrificing the animals or to different RNA preparations (Pritchard *et al*., 2001) can be partially overridden. Therefore, the confirmation of the overall expression changes for about 50% of the 18 genes selected for the validation was a promising result for further experiments. Based on these considerations, it can be expected that of the total differentially expressed genes in the mutant mice, a similar percentage to that detected by real-time PCR will also be confirmed.

Only 7.5% of the abnormally expressed genes were found to follow the same direction of expression in both *Trps1*$^{+/\Delta GATA\text{-}Znf}$ and in *Trps1*$^{\Delta GATA\text{-}Znf/\Delta GATA\text{-}Znf}$ mice. This finding was not unexpected. In fact, haploinsufficiency in mice does not seem to be as critical as in humans for the onset of genetic diseases. In addition to the heterozygous GATA Znf-deleted *Trps1* mice, which have a milder phenotype than the TRPS patients, other examples of heterozygous mouse models for dominantly inherited diseases not affected as severely as the human patients are existing. The *Ext1*$^{+/-}$ embryos, for example, do not show the typical multiple exostoses of the long bones and deformities of legs, forearms and hands, usually present in patients with the autosomal dominant disorder human hereditary multiple exostosis type 1 (Lin *et al*., 2000). More, whereas the *Msx1*$^{-/-}$ mice show defective and thinner nail plates than those of the wild type littermates, the *Msx1*$^{+/-}$ mice are normal without the typical features of Witkop syndrome or TNS (tooth and nail syndrome), a dominant disorder characterized by nail dysplasia and missing teeth (Jumlongras *et al*., 2001). On the other hand, haploinsufficiency of *Sox9* (Bi *et al*., 2001) and *Cbfa1/Runx2* (Otto *et al*., 1997) in heterozygous mice display the typical features of campomelic dysplasia (CD) and cleidocranial dysplasia (CCD) respectively. In the case of Trps1, the pathways controlled by Trps1 appear not be as concentration sensitive as in humans.

Since cDNA microarray analyses allow the identification of both direct and indirect downstream genes of a transcription factor, the largest part of the genes found to be differentially expressed in Trps1 mutant mice is probably a result of secondary events mediated by the directly induced or repressed transcriptional repressors and activators respectively, or a result of pathological processes.

4.3.2.1 Downstream genes of Trps1 in embryonic limbs

Using the Affymetrix arrays MOE430A, which contain about 22000 probe sets, 323 and 226 differentially expressed gene were identified by comparing the expression profiles of wild type mouse embryonic limbs with those of *Trps1*$^{+/\Delta GATA\text{-}Znf}$ and *Trps1*$^{\Delta GATA\text{-}Znf/\Delta GATA\text{-}Znf}$ mouse embryonic limbs respectively (see Results 3.4.1). The very small range of fold change (between 1.5 and 2.1) in the expression values obtained for the abnormally expressed genes may partially be due to the dilution of the GATA Znf-deleted Trps1 effects in the growth plates, where it is expected to exert its main regulatory function by surrounding tissues (muscle, skin etc.). Anyway, this finding did not prevent the identification of direct downstream genes.

Different criteria were considered for the selection of twelve genes chosen for independent validation, since only few genes, which are known to act in the most important pathways involved in endochondral ossification, were present among the differentially expressed genes. *Eng*, *Emp3* and *Gadd45g* were selected because they were downregulated both in the *Trps1*$^{+/\Delta GATA\text{-}Znf}$ and in the *Trps1*$^{\Delta GATA\text{-}Znf/\Delta GATA\text{-}Znf}$ mice. Extl2 is involved in biosynthesis of heparan sulfate. *Hspg2* encodes the core protein of an important heparan sulfate proteoglycan, named perlecan, which is a major component of the basement membrane and has critical role in cartilage development. *Wnt5b*, *Madh4*, *Hoxb8* and *Dlx3* are expressed in epiphyseal growth plates and the gene products are involved in bone development. Traf6 plays an important role in the development of tooth number and shape [teeth anomalies such as malocclusion and supernumerary teeth have been reported for TRPS patients (Gorlin *et al*., 2001)]. Lamb1 is an important component of the basement

membrane. *Laptm4b* is the only gene to be upregulated in heterozygotes and homozygotes, in both examined tissues embryonic limbs and snouts.

The real time PCR experiments confirmed the overall tendency of *Hoxb8*, *Lamb1*, *Emp3, Laptm4b* and *Hspg2* values. The relative expression values of *Eng* and *Gadd45g* could be confirmed only in the *Trps1*$^{\Delta GATA\text{-}Znf/\Delta GATA\text{-}Znf}$ animals.

As already mentioned, Trps1 might be involved in the regulation of cell cycle arrest and apoptosis (see 4.3.1). Gadd45g (growth arrest and DNA-damage-inducible 45 gamma) is a member of a family of evolutionarily conserved, small, acidic, nuclear proteins, which have been implicated in terminal differentiation, growth suppression, and apoptosis. Gadd45 proteins are likely to cooperate in activation of S and G_2/M checkpoints following exposure of cells to UV irradiation (Vairapandi *et al*., 2002). There are no reports about expression of *Gadd45g* in chondrocytes, but Northern blot analysis showed expression in skeletal muscle (Takekawa and Saito, 1998), which is present in the whole limb used to isolate the RNA for the microarray analyses.

Taylor and Suter (1996) proposed that EMP3 is involved in cell proliferation and cell-cell interaction. Eng (endoglin) is a homodimeric membrane glycoprotein primarily associated with human vascular endothelium and it is a component of the transforming growth factor beta receptor complex. Endoglin is essential during angiogenesis (Li *et al*., 1999) and recent studies indicate that it promotes endothelial cell proliferation (Lebrin *et al*., 2004). It is not known whether they are expressed, for example, in chondrocytes or in hair follicles. Anyway, a disturbed chondrocyte proliferation in the growth plates is likely to be involved in TRPS skeletal pathogenesis, making these two genes interesting for further analyses.

Noteworthy is the overexpression of *Hoxb8* in the *Trps1*$^{\Delta GATA\text{-}Znf/\Delta GATA\text{-}Znf}$ mice. Hox proteins are transcription factors that control developmental pathways along the anteroposterior axis of vertebrates. This information is consistent with the high expression of Trps1 along the axial skeleton of E11.5-E12.5 mouse embryos (Kunath *et al*., 2002). Ectopic expression of *Hoxb8* was shown to cause, beside the duplication of the ZPA (zone of polarizing activity) in the forelimb, homeotic transformation of axial structures (Charité *et al*., 1994). Also the *Trps1*$^{\Delta GATA\text{-}Znf/\Delta GATA\text{-}Znf}$ mice display axial skeletal defects that are responsible for the lethal respiratory failure in newborns. Axial skeletal abnormalities, like kyphoscoliosis, have been described in *Trps1*$^{+/\Delta GATA\text{-}Znf}$ mice

and in some TRPS patients as well (Felman and Frias, 1977; Goodman *et al*., 1981; Howell *et al*., 1986; Cope *et al*., 1986).

The expression of two genes encoding widespread components of the basement membrane (BM), *Lamb1* (one of the four different laminin beta chains, components of some of the laminin molecules) and *Hspg2*, was upregulated in the *Trps1*$^{\Delta GATA\text{-}Znf/\Delta GATA\text{-}Znf}$ and in the *Trps1*$^{+/\Delta GATA\text{-}Znf}$ mice, respectively. BMs are thin sheets of specialized extracellular matrix at the epithelial/mesenchymal interface of most tissues, whose components are able to regulate biological activities such as cell growth, differentiation, and migration, and to influence tissue development and repair (review: Erickson and Couchman, 2000). Perlecan and laminin are also present in the matrices of hyaline cartilage in the nasal septum, the articular surface of the bone and the growth plate of the developing bone (SundarRaj *et al*., 1995).

Both proteins play crucial roles during early development events as demonstrated by loss-of-function mutations mouse models: Lamb1 is essential for BM integrity (Miner *et al*., 2004) and perlecan for cartilage and cephalic development (Arikawa-Hirasawa *et al*., 1999). These features make these genes interesting in correlation with TRPS. Moreover, the *HSPG2* promoter contains nine GATA-consensus sequences (Iozzo *et al*., 1997) and consequently was selected for further functional studies, which demonstrate that *HSPG2* is a direct target of the TRPS1 transcription factor (see 4.3.2.4 for comments). Similar studies were performed with *LAPTM4b* promoter region, which has two GATA-consensus sequences. TRPS1 was able to repress the promoter activity of this gene as well (see 4.3.2.3 for comments).

It is not yet known whether *Gadd45g*, *Emp3*, *Eng*, *Hoxb8* and *Lamb1* are direct targets of Trps1 or downstream genes, whose abnormal expression derive from regulation of secondary transcription factors. Furthermore, many other differentially expressed genes deserve to be deeply analyzed in further experiments. These investigations will be performed in the next future.

4.3.2.2 Downstream genes of Trps1 in embryonic snouts

Since rodents accurately reproduce human head development, gene targeting in mice has generated more than 90 loss-of-function mutants that show craniofacial malformations (review: Wilkie and Morris-Kay, 2001).
However, some features of TRPS, like the thin upper lip, the bulbous tip of the nose and the protruding ears are difficult to find in the related TRPS mouse model, if present at all. On the contrary, other defects detected in the mouse snouts, like the abnormally arched palate in heterozygotes and the recessed chin in homozygotes are also found in patients with TRPS. Thus, the high level of expression of Trps1 during embryonic development in mouse snouts and the hair follicle defects present in the patients, as well as in the mice, make the snout an interesting model of study to understand the TRPS pathology (see Results 3.4.2).

There are many genes worth more accurate investigations. For a start, six genes among the ~700 differentially expressed were selected for validation with real-time PCR, according to different criteria. *Col2a1*, whose product is a marker for the matrix of proliferating chondrocytes, is involved in many skeletal dysplasia known as type II collagenopathies (see introduction 1.1.1). *Col9a1*, if mutated, causes multiple epiphyseal dysplasia (see introduction 1.1.1). *Nov*, which maps to 8q24.1 telomeric to *TRPS1*, is expressed in prehypertrophic and early hypertrophic chondrocytes. *Fzd6* is involved in hair patterning. *Prrx1*, which is a homeobox gene, is required for early events of skeletogenesis in multiple lineages. *Laptm4b* is the only gene overexpressed in mouse limbs and snouts of both *Trps1*$^{+/\Delta GATA\text{-}Znf}$ and *Trps1*$^{\Delta GATA\text{-}Znf/\Delta GATA\text{-}Znf}$ mice. All genes followed the same trend of abnormal expression in both mutant genotypes.
During this PhD work the overall tendency of change was confirmed for the three genes *Nov*, *Fzd6* (only for the homozygotes) and *Laptm4b*.
Nov (nephroblastoma overexpressed) is a member of the CCN family of genes [Connective tissue growth factor (CTGF), Cystein rich protein (Cyr61) and Nephroblastoma overexpressed gene (NOV)], which are known to participate in fundamental biological processes such as cell proliferation, attachment, migration, differentiation and angiogenesis. Nov provided the first example of

a CCN protein with negative regulatory properties (review: Perbal, 2001). Nov is expressed in differentiating growth plate chondrocytes and is negatively regulated by PTHrP (Yu *et al*., 2003). Previous immunocytochemistry studies performed on paraffin embedded chicken wing bud sections demonstrated the association of NOV with the ECM (Perbal, 1994).
Fzd6 (frizzled6) is a member of a large family of integral membrane Wnt receptors. It is expressed in the skin and hair follicles and is important for cell polarity and controls hair polarity in mice (Guo *et al*., 2004).

4.3.2.3 *Laptm4b* is the only gene upregulated in both *Trps1*$^{+/\Delta GATA\text{-}Znf}$ and in *Trps1*$^{\Delta GATA\text{-}Znf/\Delta GATA\text{-}Znf}$ mice, in embryonic limbs and snouts

The *LAPTM4b* promoter region, which carries two GATA-consensus sequences, was used to drive the cDNA luciferase in a reporter gene assay, showing that TRPS1 was able to directly reduce its transcriptional activity (see Results 3.4.2.2).
LAPTM4b is a novel gene, which encodes two isoforms of proteins with molecular masses 35-kDa and 24-kDa, designated as LAPTM4b-35 and LAPTM4b-24, translated from the first and second ATG in ORF (Shao *et al*., 2003; Liu *et al*., 2004). Computer analyses showed that *LAPTM4b* is an integral membrane protein with four highly conserved hydrophobic transmembrane domains, forming two extracellular loops, a cytoplasmic loop and intracellular amino- and carboxyl tails. It is widely expressed in human tissues, mainly in heart, skeletal muscle, kidney and testis (Shao *et al*., 2003).
LAPTM4b is upregulated in hepatocellular carcinoma (HCC) when compared with paired non cancerous liver (PNL) or normal liver tissues (NL) of the same patient. Notably, the expression level of LAPTM4b-35 was significantly related to the differentiation status of HCC tissues, higher in poorly differentiated HCCs than in moderately and well-differentiated HCCs. In addition, the ratio of LAPTM4b-35 to LAPTM4b-24 was remarkably higher in HCC than in PNL and NL. The authors suggest that *LAPTM4b*-24 may play an antagonistic role in cell survival and proliferation, and the equilibrium of *LAPTM4b*-35 and *LAPTM4b*-24 in expression is involved in controlling cell survival/proliferation and

differentiation. Promoter activity studies in two HCC-related cell lines showed different levels of activity suggesting two different mechanisms regulating the expression of LAPTM4b in the two cell lines (Shao *et al*., 2003).
LAPTM4B was not detected in human cervical carcinoma cell line HeLa (Liu *et al*., 2004), and infact its promoter did not show any activity in these cells in the reporter gene assay performed during this PhD work (see Results 3.4.2.2).

Interestingly, the expression of LAPTM4B was also higher in highly metastatic cell lines including prostate carcinoma PC-3M androgen-independent cell line, and pulmonary giant cell carcinoma BE1 cell line (Liu *et al*., 2004). Since TRPS1 is higher expressed in androgen-dependent human prostate cancer cells (initial phase) than in androgen-independent human prostate cancer cells (next phase) (Chang *et al*., 2000), the reduction of the TRPS1 repressional activity on *LAPTM4b* could explain its overexpression in highly metastatic prostate carcinoma cells. Moreover, LAPTM4b was reported to be involved in increased cell growth and proliferation rates, when transfected in NIH3T3 cell (He *et al*., 2003).
These findings might indicate that the repressional activity of TRPS1 on *LAPTM4b* is important in the control of cell cycle.

The fact that *Laptm4b* is overexpressed in both *Trps1*$^{+/\Delta GATA\text{-}Znf}$ and *Trps1*$^{\Delta GATA\text{-}Znf/\Delta GATA\text{-}Znf}$ mice confirmed the hypothesis of Malik *et al*. (2001) that the repressional activity of TRPS1, exerted here on *LAPTM4b*, depends on an intact GATA-Znf. Additional functional analyses are required to understand the possible role of LAPTM4b in the pathogenesis of the TRP Syndromes. It would be interesting to know the exact expression pattern, for example in cartilage during endochondral ossification or in hair follicle and to identify putative binding partners. Anyway, *Laptm4b* overexpression in both embryonic limbs and snouts implicate that the signaling pathway where Laptm4b acts depends in part on Trps1.

4.3.2.4 TRPS1 directly represses *HSPG2* promoter activity

It was demonstrated that *HSPG2* is a direct target of TRPS1 (see Results 3.4.1.2).

HSPG2 maps to 1p36 and has 97 exons (Cohen *et al*., 1993). It encodes the core protein of a large heparan sulfate proteoglycan, called perlecan, which is present in all native BMs. The core protein consists of five distinct domains (Cohen *et al*., 1993) and is post-translationally modified by two or three heparan sulfate (HS) chains at the N-terminus (Paulsson *et al*., 1987) and one choindroitin sulfate or HS chain at the C-terminus (Tapanadechopone *et al*., 1999). The ~1.7 kb of the perlecan promoter analyzed with the reporter gene assay (see Results 3.4.1.2) have only a reduced transcriptional activity (Iozzo *et al*., 1997) and contain nine GATA motifs.

Perlecan exerts many functions. Among other, it stabilizes matrix organization and cell-matrix interaction by binding other BM molecules (laminin, collagen IV and nidogen/entactin) (Hopf *et al*., 1999), ECM molecules (fibulin, fibronectin) (Brown *et al*., 1997) and cell surface receptors (integrin ß1 and α-dystroglycan) (Brown *et al*., 1997; Talts *et al*., 1999). It binds and stores growth factors like FGF and platelet-derived growth factors (Knox *et al*., 2002; Mongiat *et al*., 2000; Gohring *et al*., 1998). It possesses angiogenic and growth-promoting attitudes by acting as a coreceptor for basic fibroblast growth factor, FGF2 (Aviezer *et al*., 1994).

The *HSPG2* gene is already expressed during the 2-4 cell stage of mouse development (Dziadek *et al*., 1985) and disruptions of both the *Drosophila* (*trol*) (Datta and Kankel, 1992) and *C. elegans* (*Unc-52*) (Rogalski *et al*., 1993; Rogalski *et al.,* 2001) orthologues result in severe developmental defects in eye and muscle respectively (Datta and Kankel, 1992; Rogalski *et al*., 1995).

Important to understand the correlation with TRPS pathogenesis, is the strong *Hspg2* expression, in addition to the BMs, in matrix of cartilage (especially in the pericellular matrix, surrounding the periphery of chondrocytes) undergoing endochondral ossification in the growth plate, mainly in the prehypertrophic and hypertrophic zones (Arikawa-Hirasawa *et al*., 1999). It is also expressed in adult hyaline cartilage, including the articular cartilage (SundarRaj *et al*.,

1995). Interestingly, French *et al*. (1999) probed frozen sections from mouse embryos with a specific mouse perlecan antibody and showed that at E12.5 perlecan protein was low in cartilage primordial (where *Trps1* is very high expressed), but it accumulated as development progressed through E13.5 and E14.5 (when *Trps1* expression is reduced). They also demonstrated that perlecan, in the presence of its constituent HS chains, maintained and strongly potentiated chondrogenic differentiation *in vitro*.

Two *Hspg*2-null mouse models (Arikawa-Hirasawa *et al*., 1999; Costell *et al*., 1999) and a HS chain-deficient perlecan mouse model have been generated (Rossi *et al*., 2003). Some of the perlecan-null embryos die during an early crisis (E10.5-E12.5) because of severe defects in cephalic or hearth development, probably due to altered basement membrane formation in the absence of perlecan. The remaining mutants survive to the perinatal period but develop severe brain and skeletal defects, like short long bones and craniofacial defects. The perlecan-null mice show severe defects in the growth plates (reduced chondrocytes proliferation and differentiation) during the endochondral ossification. No significant cartilage abnormalities were found prior to E13.5 (when the endochondral ossification starts) and afterward matrix disruption becomes evident and progressively severe. These findings suggest an essential role of perlecan for cartilage development, even if its precise role is not yet known. Mutant mice whose fibroblasts secrete perlecan that mainly carries chondroitin sulfate and only a small amount of HS are viable and fertile, but have defective eyes (like *Drosophila* perlecan-null mutants, see above). The lenses of the homozygous mice degenerate within three weeks after birth, because of an altered structure of the lens capsule, which is a specialized, very thick BM where perlecan is normally found. The fine structure of the cartilage in the affected mice has not been examined.

Similarities of the skeletal abnormalities of perlecan-null embryos led to the identification of a human disorder, Dyssegmental dysplasia, Silverman-Handmaker type, which is a lethal autosomal recessive skeletal dysplasia characterized by anisospondyly and micromelia. The fibroblasts of the three patients identified for perlecan mutations were not able to secrete the truncated perlecan proteins (Arikawa-Hirasawa *et al*., 2001). Mutations in

HSPG2 are also involved in the rare recessive disorder Schwartz-Jampel syndrome, which is a unique combination of myotonia and chondrodysplasia. In this case, different forms of perlecan are secreted to the ECM and are partially functional (Nicole *et al*., 2000; Arikawa-Hirasawa *et al*., 2002).

4.3.2.5 Is *Hspg2* overexpression in the growth plate responsible for disturbed cell-matrix interaction in the chondrocytes of TRPS patients?

According to the microarray data, *Hspg2* is upregulated only in the embryonic limbs of mutants but not in embryonic snouts, albeit it is expressed. This could implicate that the overexpression of *Hspg2* is involved only in the pathways which, if disturbed by mutated Trps1, lead to the skeletal defects but not the facial features present in TRPS patients.

The typical skeletal defects of the TRPS patients, like the short stature and the cone-shaped epiphysis are due to a premature closure of the growth plates.
In normal growth plates, perlecan binds many molecules and many growth factors, which are involved in cartilage development, stimulates angiogenesis and induces chondrocyte differentiation. The high level of *HSPG2* expression in the growth plates is likely to change the composition of the ECM in the growth plates. Regional differences in the cartilage matrix composition probably are functionally critical in hyaline cartilage of the growth plate. During endochondral ossification, the matrix is likely to influence the continuous behavioral and metabolic changes in the chondrocytes. So maybe the altered cell-matrix interactions due to a higher level of perlecan in the cartilage matrix could be responsible, at least in part, for the impaired differentiation of chondrocytes in the growth plates of TRPS patients. Moreover, perlecan may modulate signaling pathways regulating chondrocyte proliferation and hypertrophy by sequestering important ligands.
Further functional analyses are required to corroborate this hypothesis. For example, it would be important to know whether *HSPG*2 is really overexpressed in chondrocytes of TRPS patients. If this is the case, *Hspg2* overexpression studies in mice under the control of a chondrocyte specific

promoter would help to understand in detail the defects supposed to be caused by disturbed cell-matrix interactions in the growth plate.

4.3.2.6 Does *HSPG2* overexpression contribute to the onset of osteoarthritis in TRPS patients?

An important complication of TRPS is a progressive degenerative arthritis (Felman and Frias, 1977; Cope *et al*., 1986). Osteoarthritis (OA) is a disorder of the joints, characterized by progressive deterioration of the articular cartilage. Central point in the pathogenesis is a disturbed cell-matrix relationship. Recently, Tesche and Miosge (2004) found an increased level of perlecan protein in the area adjacent to the main cartilage defect in the knee joints of ten patients suffering from OA. In particular, more perlecan was produced by the elongated type 2 chondrocytes, mainly found in the deep zones of articular chondrocyte of the areas adjacent to the main defect, which are the cells principally responsible for the regeneration processes of cartilage matrix (Bock *et al*., 2001). In normal cartilage, perlecan interacts with other adhesive extracellular macromolecules to stabilize and produce the compressed matrix and to enable the adhesion of chondrocytes to their own substrate. Therefore, the authors suggested that the higher level of perlecan could be an attempt on the part of the cartilage tissue to stabilize and protect the remaining matrix of late-stage osteoarthritic cartilage from further destruction.

In contrast, the data obtained in this PhD work would suggest that the high level of perlecan present in the articular cartilage could be the cause for the onset of OA, at least in the TRPS patients, and not a way to protect the matrix. If *TRPS1* is mutated, the repression of *HSPG2* expression by TRPS1 may not normally take place and thus perlecan accumulates, among other, in the articular cartilage, causing disturbances in the cell-matrix interactions, which could contribute to the origin of OA.

5. ABSTRACT

Mutations in the *TRPS1* gene cause the tricho-rhino-phalangeal-syndrome (TRPS) type I and III, which are characterized by craniofacial and skeletal defects. The gene encodes a transcription factor that has a GATA-binding zinc finger and represses GATA-regulated gene expression.

Mutation analysis of TRPS type I patients helped to identify the nuclear localization signal of TRPS1.

To study the pathogenesis of TRPS, a *TRPS1* transgenic mouse model expressing a potentially dominant negative *TRPS1* allele in chondrocytes was generated. However, the mice expressed the transgene at a low rate only, and even adult mice did not show the typical brachydactyly or growth retardation.

For identifying genes that are directly and indirectly regulated by TRPS1 two different strategies were followed.

(I) A combination of RNA interference-mediated *Trps1* silencing and cDNA microarray analysis allowed the identification of putative downstream genes of Trps1 in mouse NIH3T3 cells. Several genes overexpressed in cells where *Trps1* was silenced are involved in the control of cell cycle progression or apoptosis.

(II) Expression profiles of normal mouse embryonic limbs and snouts were compared with embryonic limbs and snouts of mice carrying a targeted deletion of the Trps1 GATA zinc finger. Several downstream genes implicated in cell cycle control, signal transduction, cell organization and transcription regulation were identified, and their relative expression values were verified by real-time PCR. Luciferase reporter-gene assays allowed the identification of the first potential TRPS1 target genes, *LAPTM4b* and *HSPG2.* Both promoters contain GATA motifs and can be repressed by TRPS1. LAPTM4b (lysosomal-associated transmembrane protein 4b) is probably involved in cell cycle control. *HSPG2* codes for perlecan, the major heparan sulfate proteoglycan in the cartilage matrix.

These findings suggest a role for Trps1 in the regulation of cell cycle control and in the maintenance of cell-matrix interactions.

6. APPENDIX

TRPS1 TRANSGENIC MICE

primer sequences 5'-3'

(f):forward (r):reverse

- to insert the specific A2701C mutation in the human *TRPS1* cDNA by in vitro site-directed mutagenesis (in bold is indicated the location of the mutation)

GATA5 GCCTG**C**CCACAAAGACCTCTCTC

GATA3 GAGAGAGGTCTTTGTGG**G**CAGGC

- to insert the human TRPS1 cDNA in the pNASSßCol2a1 (underlined are the *EcoRI* site in linker 1 and the *BglII* site in linker 2)

linker 1 (f) GGCCGCATGAGATCTGCAGATATCAG

linker 2 (r) CGTACTCTAGACGTCTATAGTCGCCGG

- probe for Southern blot analysis

***Col2a1* promoter** (f) TCCTAGGGCCTCCTGCATGAGG

***TRPS1* exon 3** (r) TTGAAGCCAGCCTTCTCACT

- to asses the transgene expression

1^PCR strategy

***Col2a1* promoter** (f) TCCTAGGGCCTCCTGCATGAGG

***TRPS1* exon 3** (r) TTGAAGCCAGCCTTCTCACT

2^PCR strategy

exon 5 (f) TTGGAGAGGGGCAGACATCC

exon 7 (r) CCTGAGGACTTTTTATCTGAATGT

LUCIFERASE REPORTER-GENE ASSAYS

primer sequences 5'-3'

- to amplify the 1711 bp *HSPG2* promoter region (GenBank accession n. L81166), then inserted into the reporter plasmid (pGL3-Control) for the luciferase reporter-gene assay. The parentheses indicate the location into the promoter region.

***HSPG2*_forward**	CCTGGTGTACTCTCCCCTCA	(nt 125-144)
***HSPG2*_reverse**	GGACGCCTTTTCACATAG	(nt 1819-1836)

- to amplify the 1532 *LAPTM4b* promoter region (GenBank accession n. AY057051F), then inserted into the reporter plasmid (pGL3-basic) for the luciferase reporter-gene assay. The parentheses indicate the location into the promoter region.

***LAPTM4b*_forward**	GCTCCAGGTGGAAGAGTGTGC	(nt 1-21)
***LAPTM4b*_reverse**	GGACTTGGCCATGTGACCCG	(nt 1513-1532)

7. LITERATURE

Ameyar M., Wisniewska M. and Weitzman J.B. (2003) A role for AP-1 in apoptosis: the case for and against. Biochimie **85**: 747-752

Amling M., Neff L., Tanaka S., Inoue D., Kuida K., Weir E., Philbrick W.M., Broadus A.E. and Baron R. (1997) Bcl-2 lies downstream of parathyroid hormone–related peptide in a signaling pathway that regulates chondrocyte maturation during skeletal development. J Cell Biol **136**:205-213

Arikawa-Hirasawa E., Watanabe H., Takami H., Hassell J.R. and Yamada Y. (1999) Perlecan is essential for cartilage and cephalic development. Nature Genet **23**: 354-358

Arikawa-Hirasawa E., Wilcox W.R., Le A.H. Silverman N., Govindraj P., Hassell J.R. and Yamada Y. (2001) Dyssegmental dysplasia, Silverman-Handmaker type, is caused by functional null mutations of the perlecan gene. Nature Genet **106**: 431-434

Arikawa-Hirasawa E., Le A.H., Nishino I., Nonaka I., Ho N.C., Francomano C.A., Govindraj P., Hassell J.R., Devaney J.M., Spranger J., Stevenson R.E., Iannaccone S., Dalakas M.C. and Yamada I. (2002) Structural and functional mutations of the perlecan gene cause Schwartz-Jampel syndrome, with myotonic myopathy and chondrodysplasia. Am J Hum Gen **70**: 1368:1375

Aviezer D., Hecht D., Safran M., elsinger M., David G. and Yayon A. (1994) Perlecan, basal lamina proteoglycan, promotes basic fibroblast growth factor-receptor binding, mitogenesis and angiogenesis. Cell **79**: 1005-1013

Bakiri L., Matsuo K., Wisniewska M., wagner E.F. and Yaniv M. (2002) Promoter specificity and biological activity of tethered AP-1 dimers. Mol Cell Biol **22**: 4952-4964

Bi W., Deng J.M., Zhang Z., Behringer R.R. and de Crombrugghe B. (1999) Sox9 is required for cartilage formation. Natur Genet **22**: 85-89

Bi W., Huang W., Whitworth D.J., Deng J.M., Zhang Z., Behringer R.R. and de Crombrugghe B. (2001) Haploinsufficiency of Sox9 results in defective cartilage primordia and premature skeletal mineralization. Proc Natl Acad Soc **98**: 6698-6703

Bock H.C., Michaeli P., Bode C., Schultz W., Kresse H., Herken R. *et al*. (2001) The small proteoglycans decorin and biglycan in human articular cartilage of late-stage osteoarthritis. Osteoarthritis Cartilage **6**: 371-373

Bradford M. M. (1976) Analytical Biochemistry. **72**, 248

Brown J.C., Sasaki T., Gohring W., Yamada Y. and Timpl R. (1997) The C-terminal domain V of perlecan promotes beta1 integrin-mediated cell adhesion, binds heparin, nidogen and fibulin-2 and can be modified by glycosaminoglycans. Eur J Biochem **250**: 39-46

Bühler E.M., Bühler U.K., Stalder G.R., Jani L. and Juril L.P. (1980) Chromosome deletion and multiple cartilaginous exostoses. Eur J Pediatr 133: 163-166

Bühler E.M. and Malik N.J. (1984) The tricho-rhino-phalangeal syndrome(s): chromosome 8 long arm deletion:is there a shortest region of overlap between reported cases? TRP I and II syndromes: are they separate entities? Am J Med Genet **19**: 113-119

Cachon-Gonzalez M.B., Fenner S., Coffin J.M., Moran C., Best S. and Stoye J.P. (1994) Structure and expression of the hairless gene of mice. Proc Natl Acad Sci **91**: 7717-7721

Chang G.T.G., Steenbeek M., Schippers E., Blok L.J., van weerden W.M., van Alewijk D.C.J.G., Eussen B.H.J., van Steenbrugge G.J. and Brinkmann A.O. (2000) Characterization of a zinc-finger protein and its association with apoptosis in prostate cancer cells. J Nat Cancer Inst **92**: 1414-1421

Chang G.T.G, van den Bemd G.J., Jhamai M. and Brinkmann A.O. (2002) Structure and function of GC79/TRPS1, a novel androgen-repressible apoptosis gene. Apoptosis **7**: 13-21

Charité J., DeGraaff W., Shen S. and Deschamps J. (1994) Ectopic expression of Hoxb8 causes duplication of the ZPA in the forelimb and homeotic transformation of axial structures. Cell **78**: 589-601

Chauhan B.K., Reed N.A., Zhang W., Duncan M.K., Kilimann M.W. and Cvekl A. (2002) Identification of genes downstream of Pax6 in the mouse lens using cDNA microarrays. J Biol Chem **277**: 11539-11548

Clausen T., Southan C. and Ehrmann M. (2002) The HtrA family of proteases: implications for proteins and cell fate. Mol Cell **10**: 443-455

Cohen I., Grässel S., Murdoch A.D. and Iozzo R. (1993) Structural characterization of the complete human perlecan gene and its promoter. Proc Natl Acad Sci **90**: 10404-10408

Cope R., Beals R.K. and Bennett R.M. (1986) The trichorhinophalangeal dysplasia syndrome: report of eight kindreds, with emphasis on hip complications, late presentations, and premature osteoarthrosis. J Ped Orthop **6**: 133-138

Costell M., Gustafsson E., Aszodi A., Mörgelin M., Bloch W., Hunziker E., Addicks K., Timpl R. and Fässler R. (1999) Perlecan maintains the integrity of cartilage and some basement membranes. J Cell Biol 5: 1109-1122

Daniel-Vedele F. and Caboche M. (1993) A tobacco cDNA clone encoding a GATA-1 zinc finger protein homologous to regulators of nitrogen metabolism in fungi. Mol. Gen. Genet. **240**: 365-373

Datta S. and Kankel D.R. (1992) 1(1) trol and 1(1) devl, loci affecting the development of the adult central nervous system in *Drosophila melanogaster*. Genetics **130**: 523-537

Dziadek M, Fujiwara S, Paulsson M, Timpl R. (1985) Immunological characterization of basement membrane types of heparan sulfate proteoglycan. EMBO J **4**: 905-912

Elbashir S.M., Harborth J., Lendeckel W., Yalcin A., Weber K. and Tuschl T. (2001) Duplexes of 21-nucleotide RNAs mediate RNA interference in cultured mammalian cells. Nature **411**: 494-498

Erickson A.C. and Couchman J.R. (2000) Still more complexity in mammalian basement membranes. J Hist Cytoch **48** 1291-1306

Felman A.H. and Frias J.L. (1977) The trichorhinophalangeal syndrome: study of 16 patients in one family. Am J Roentgenol **129**: 631-638

Foster J.W., Dominguez-Steglich M.A., Guioli S., Kowk G., Weller P.A., et al. (1994) Campomelic dysplasia and autosomal sex reversal caused by mutations in an SRY-related gene. Nature **372**: 525-530

French M.M., Smith S.E., Akanbi K., Sanford T., Hecht J., Farach-Carson M.C. and Carson D.D. (1999) Expression of the heparan sulfate proteoglycan, perlecan, during mouse embryogenesis and perlecan chondrogenic activity in vitro. J Cell Biol **145**: 1103-1115

Garrick D., Fiering S., Martin D.I. and Whitelaw E. (1998) Repeat-induced gene silencing in mammals. Nature Genet **18**:56-59

Gentile M., Fiorente P., Buonadonna A.L., Macina F. and Cariola F. (2003) A novel mutation in exon 7 in a family with mild tricho-rhino-phalangeal syndrome type I. Clin Genet **63**: 166-167

Giedion A. (1966) Das Tricho-rhino-phalangeale syndrome. Helv Paediat Acta **21**: 475-482

Giedion A. (1968) Zapfenepiphysen. Naturgeschichte und diagnostische Bedeutung einer Störung des enchondralen Wachstums. In: Glaumer R., Rüttiman A., thurn P., Vogler e. (eds) Ergebnisse der medizinischen Radiologie. Georg Thieme Verlag, Stuttgart, pp 59-124

Giedion A. (1998) Phalangeal cone-shaped epiphyses of the hand: their natural history, diagnostic sensitivity, and specificity in cartilage hair hypoplasia and the trichorhinophalangeal syndrome I and III. Pediatr Radiol **28**: 751-758

Gohring W., Sasaki T., Heldin C.H. and Timpl R. (1998) Mapping of the binding of platelet-derived growth factor to distinct domains of the basement membrane proteins BM-40 and perlecan and distinction from the BM-40 collagen-binding epitope. Eur J Biochem 255: 60-66

Gorlin R., Cohen M.M. and Hennekam R.C.M. (2001) Syndromes of the head and neck. Fourth edition. Oxford University Press

Goodman R.M., Trilling R., Hertz M., Horoszowski H., Merlob P. and Reisner S. (1981) New clinical observations in the trichorhinophalangeal syndrome. J Cran Genet and Dev Biol **1**: 15-29

Guo N., Hawkins C. and Nathans J. (2004) Frizzled6 controls hair patterning in mice. Proc Natl Acad Sc **101**:9277-9281

Hammond S.M., Caudy A.A. and Hannon G.J. (2001) Post-transcriptional gene silencing by double-stranded RNA. Nat Rev Gen **2**: 110-119

Harbort J., Elbashir L.M., Bechert K., Tuschl T. and Weber K. (2001) Identification of essential genes in cultured mammalian cells using small interfering RNAs. J Cell Sci 114: 4557-4565

Hatamura I., Kanauchi Y., Takahara M., Fujiwara M., Muragaki Y., Ooshima A. and Ogino T. (2001) A nonsense mutation in TRPS1 in a Japanese family with tricho-rhino-phalangeal syndrome type I. Clin Genet. **59**: 366-367.

He J., Shao G.Z. and Zhou RL (2003) [Effects of the novel gene, LAPTM4B, highly expression in hepatocellular carcinoma on cell proliferation and tumorigenesis of NIH3T3 cells] in chinese Beijing Da Xue Xue Bao **35**: 348-52.

Hilton M.J., Sawyer J.M, Gutierrez L., Hogart A., Kung T.C. and Wells D.E. (2002) Analysis of novel and recurrent mutations responsible for the tricho-rhino-phalangeal syndromes. J Hum Genet **47**: 103-6.

Höög C., Shalling M., Grunder-Brundell E. and Daneholt B. (1991) Analysis of a murine male germ cell-specific transcript that encodes a putative zinc finger protein. Mol. Reprod. Dev. **30**: 173-181

Hopf M., Gohring W., Kohfeldt E., Yamada Y. and Timpl R. (1999) Recombinant domain IV of perlecan binds to nidogens, laminin-nidogen complex, fibronectin, fibulin-2 and heparin. Eur J Biochem **259**: 917-925

Howell C.J. and Wynne-Davies R. (1986) The tricho-rhino-phalangeal syndrome. A report of 14 cases in 7 kindreds. J Bone Joint Surg **68**: 311-314

Iozzo R., Pillarisetti J., Sharma B., Murdoch A.D., Danielson K.G., Uitto J. and Mauviel A. (1997) Structural and functional characterization of the human perlecan gene promoter. J Biol Chem **272**: 5219-5228

Itin P.H., Bohn S., Mathys D., Guggenheim R. and Richard G. (1996) Trichorhinophalangeal syndrome type III. Dermatology **193**: 349-352

Jumlongras D., Bei M., Stimson J. M., Wang W.-F.,DePalma S. R., Seidman C. E., Felbor U., Maas R.,Seidman J. G. and Olsen B. R. (2001) A nonsense mutation in MSX1 cause Witpok syndrome. Am J Hum Gen **69**: 67-74

Kaiser F.J., Tavassoli K., Van den Bemd G.-J., Chang G.T.G., Horsthemke B., Möröy T. and Lüdecke H.-J. (2003a) Nuclear interaction of the dynein light chain LC8a with the TRPS1 transcription factor suppresses the transcriptional repression activity of TRPS1. Hum Mol Gen **12**: 1349-1358

Kaiser F.J., Möröy T., Chang G.T.G., Horsthemke B. and Lüdecke H.-J. (2003b) The RING finger protein RNf4, a co-regulator of transcription, interacts with the TRPS1 transcription factor. J Biol Chem **278**: 38780-38785

Kaiser F.J., Brega P., Raff M.L., Byers P.H., Gallati S., Taylor Kay T., de Almeida S., Horsthemke B. and Lüdecke H.-J. (2004) Novel missense mutations in the TRPS1 transcription factor define the nuclear localization signal. Eur J Hum Gen **12**: 121-126

Knox S., Merry C., Stringer S., Melrose J. and Whitelock J. (2002) Not all perlecan are equal: interactions with fibroblast growth factor 2 (FGF-2) and FGF receptors. J Biol Chem **277**: 14657-14665

Kobayashi H., Hino M., Shimodahira M. *et al*. (2002) Missense mutation of TRPS1 in a family of tricho-rhino-phalangeal syndrome type III. Am J Med Genet **107**:26-29

Kocher M.S. and Shapiro F. (1998) Osteogenesis imperfecta. J. Am Acad Orth Surg **6**: 225-236

Komori T., Yagi H., Nomura S., Yamaguchi A., Sasaki K. et al. (1997) Targeted disruption of Cbfa1 results in a complete lack of bone formation owing to maturational arrest of osteoblasts. Cell **89**: 755-764

Kronenberg H.M. (2003) Developmental regulation of the growth plate. Nature **423**: 332-336.

Kunath M., Lüdecke H.-J. and Vortkamp A. (2002) Expression of Trps1 during mouse embryonic development. Gene Expression Patterns **2**: 119-122

Lallemand D., Spyrou G., Yaniv M. and Pfarr C. M. (1997) Variations in Jun and Fos protein expression and AP-1 activity in cycling, resting and stimulated fibroblasts. Oncogene **14**: 819-830

Langer L.O. (1969) The thoracic-pelvic-phalangeal dystrophy. Clinical delineation of birth defects. Part IV. Skeletal dysplasia.Birth defects IV.55:64

Lanske B., Karaplis A.C., Lee K. Luz A., Vortkamp A., *et al*. (1996) PTH/PTHrP receptor in early development and Indian hedgehog-regulated bone growth. Science **273**: 663-666

Latchman D.S. (1996) Transcription-factor mutations and diseases. N Eng J Med **334**: 28-33

Lebrin F., Goumans M.J., Jonker L., Carvalho R.L., Valdimarsdottir G., Thorikay M., Mummery C., Arthur H.M. and ten Dijke P. (2004) Endoglin promotes endothelial cell proliferation and TGF-beta/ALK1 signal transduction. EMBO J **23**: 4018-4028

Lin X., Wei G., Shi Z., Dryer L., Esko J.D., Wells D.E. and Matzuk M.M. (2000) Disruption of gastrulation and heparan sulfate biosynthesis in EXT1-deficient mice. Dev Biol **2**:299-311

Li D. Y., Sorensen L. K., Brooke B. S., Urness L. D., Davis E. C., Taylor D. G., Boak B. B. and Wendel D. P. (1999) Defective angiogenesis in mice lacking endoglin. Science **284**: 1534-1537

Liu X.-R., Zhou R.-L., Zhang Q.-Y., Zhang Y., Jin Y.-Y., Lin M., Rui J.-A. and Ye D.-X. (2004) Structure analysis and expressions of a novel tetratransmembrane protein, lysosome-associated protein transmembrane 4 B associated with hepatocellular carcinoma. World J Gastroenterol **10**: 1555-1559

Livak K.J. and Schmittgen T.D. (2001) Analysis of relative gene expression data using real-time quantitative PCR and the $2^{-\Delta\Delta CT}$ method. Methods **25**: 402-408

Lüdecke H.-J., Wagner M.J., Nardmann J., La Pillo B., Parrish J.E., Willems P.J., Haan E.A., Frydman M., Hamers G.J.H., Wells D.E., and Horsthemke B. (1995) Molecular dissection of a contiguous gene syndrome: localization of the genes involved in the Langer-Giedion syndrome. Hum Mol Genet **4**: 31-36

Lüdecke H.J., Schaper J., Meinecke P., Momeni P., Gross S., von Holtum D., Hirche H., Abramowicz M.J., Albrecht B., Apacik C., Christen H.J., Claussen U., Devriendt K., Fastnacht E., Forderer A., Friedrich U., Goodship T.H., Greiwe M., Hamm H., Hennekam R.C., Hinkel G.K., Hoeltzenbein M., Kayserili H., Majewski F., Mathieu M., McLeod R., Midro A.T., Moog U., Nagai T., Niikawa N., Ørstavik K.H., Plochl E., Seitz C., Schmidtke J., Tranebjærg L., Tsukahara M., Wittwer B., Zabel B., Gillessen-Kaesbach G. and Horsthemke B. (2001) Genotypic and phenotypic spectrum in the tricho-rhino-phalangeal syndrome type I and III. Am J Hum Genet. **68**: 81-91.

Malik T.H., Shoichet S.A., Latham P., Kroll T.G., Peters L.L. and Shivdasani R. (2001) Transcriptional repression and developmental functions of the atypical vertebrate GATA protein TRPS1. The EMBO J. **20**: 1715-1725

Malik T.H., von Stechow D., Bronson R.T. and Shivdasani R. (2002) Deletion of the GATA domain of TRPS1 causes absence of facial hair and provides new insights into the bone disorder in inherited tricho-rhino-phalangeal syndromes. Mol Cell Biol **22**: 8592-8600

Marchau F., Van Roy B.C., Parizel P.M., Lambert J.R., De Canck I., Leroy J.G., Gevaert C.M., Willems P.J. and Dumon J.E. (1993) Tricho-rhino-phalangeal syndrome type I (TRP I) due to an apparently balanced translocation involving 8q24. Am J Med Gen **45**: 450-455

McCarty A.S., Kleiger G., Eisenberg D. and Smale S.T. (2003) Selective dimerization of a C2H2 zinc finger subfamily. Mol Cell **11**: 459-470

McManus M.T. and Sharp P.A. Gene silencing in mammals by small interfering RNAs. Nat Rev Gen **3**: 737-747

Miner J.H., Li C., Mudd J.L., Go G. and Sutherland A.E. (2004) Compositional and structural requirements for laminin during mouse embryo implantation and gastrulation. Development **131**: 2247-2256

Minina E., Kreschel C., Naski M.C., Ornitz D.M. and Vortkamp A. (2002) Interaction of FGF, Ihh/Pthlh, and BMP signaling integrates chondrocyte proliferation and hypertrophic differentiation. Dev Cell **3**: 439-449

Molkentin J.D. (2000) The zinc finger-containing transcription factors GATA-4, -5, and -6. J Biol Chem **50**: 38949-38952

Momeni P., Glöckner G., Schmidt O., von Holtum D., Albrecht B., Gillessen-Kaesbach G., Hennekam R., Meinecke P., Zabel B., Rosenthal A., Horsthemke B. and Lüdecke H.-J. (2000) Mutations in a new gene, encoding a zinc-finger protein, cause the tricho-rhino-phalangeal syndrome type I. Nature Genet **24**: 71-74

Momeni P. (2001) Identifizierung und charakterisierung des menschlichen *TRPS1*-Gens. PhD Thesis

Mongiat M., Taylor K., Otto J., Aho S., uitto J., Whitelock J.M. and Iozzo R. (2000) The protein core of proteoglycan perlecan binds specifically to fibroblast growth factor-7. J Biol Chem **275**: 7095-7100

Müller-Röver S., Rossiter H., Lindner G., Peters E.M.J., Kupper T.S. and Paus R. (1999) Hair follicle apoptosis and Bcl-2. J Inv Dermatol Symp Proc **4**: 272-277.

Mundlos S., Otto F., Mundlos C., Mulliken J.B., Aylsworth A.S. et al. (1997) Mutations involving the transcription factor CBFA1 cause cleidocranial dysplasia. Cell **89**: 773-779

Nagai T., Nishimura G., Kasai H., Hasegawa T., Kato R., Osashi H. and Fukushima Y. (1994) Another family with tricho-rhino-phalangeal syndrome type III (sugio-Kajii syndrome) Am J Med Genet **49**: 278-280

Nicole S., Davoine C.-S., Topaloglu H., Cattolico L., Barral D., Beighton P., Ben Hamida C., Hammouda H., Cruaud C., White P.S., Samson D., Urtizberea J.A., Lehmann-Horn F., Weissenbach J., Hentati F. and Fontaine B. (2000) Perlecan, the major proteoglycan of basement membranes, is altered in patients with Schwartz-Jampel syndrome (chondrodystrophic myotonia). Nature Genet **26**: 480-483

Niikawa N. and Kamei T. (1986) The Sugio-Kajii syndrome, proposed tricho-rhino-phalangeal syndrome type III. Am J Med Genet **24**: 759-760

Olsen B.R., Reginato A.M. and Wang W. (2000) Bone development. Annu Rev Cell Dev Biol. **16**: 191-220

Ornitz D.M. and Marie P.J. (2002) FGF signaling pathways in endochondral and intramembranous bone development and human genetic disease. Gen & Dev **16**: 1446-1465

Otto F., Thornell A.P. Crompton T., Denzel A. and Gilmour K.C. (1997) CBFA1, a candidate for the cleidocranial dysplasia syndrome, is essential for osteoblast formation and bone development. Cell **89**: 765-771

Paulsson M., Yurchenco P.D., Ruben G.C., Engel J. and Timpl R. (1987) Structure of low density heparan sulfate proteoglycan isolated from a mouse tumor basement membrane. J Mol Biol **197**: 297-313

Perbal B. (1994) Caractérisation et expression du proto-oncogène nov humain dans les tumeurs de Wilms. Bull Cancer (Paris) **81**: 957-961

Perbal B. (2001) NOV (nephroblastoma overexpressed) and the CCN family of genes: structural and functional issues. J Clin Pathol: Mol Pathol **54**: 57-79

Pritchard C.C., Hsu L., Delrow J. and Nelson P.S. (2001) Project normal: defining normal variance in mouse gene expression. Proc Natl Acad Sci **98**:13266-13271

Puthalakath H., Huang D.C., O'Reilly L.A., King S.M. and Strasser A. (1999) The proapoptotic activity of the Bcl-2 family member Bim is regulated by interaction with the dynein motor complex. Mol Cell **3**: 287-296.

Rogalski T.M., Williams B.D., Mullen G.P. and Moerman D.G. (1993) Products of the unc-52 gene in Caenorhabditis elegans are homologous to the core protein of the mammalian basement membrane heparan sulfate proteoglycan. Genes Dev **7**: 1471-1484

Rogalski T.M, Gilchrist E.J., Mullen G.P. and Moerman D.G. (1995) Mutations in the unc-52 gene responsible for the body wall muscle defects in Caenorhabditis elegans are located in alternatively spliced exons. Genetics **139**: 159-169

Rogalski T.M., Mullen G.P., Bush J.A., Gilchrist E.J. and Moerman D.G. (2001) UNC-52/perlecan isoform diversity and function in Caenorhabditis elegans. Biochem Soc Trans **29**: 171-176

Rossi M., Morita H., Sormunen R., Airenne S., Kreivi M., Wang L., Fukai N., Olsen B.R., Tryggvason K. and Soininen R. (2003) Heparan sulfate chains of perlecan are indispensable in the lens capsule but not in the kidney. EMBO J **22**: 236-245

Schipani E., Lanske B., Hunzelman J., Luz A., Kovacs C.S., Lee K., Pirro A., Kronenberg H.M. and Jüppner H. (1997) Targeted expression of constitutively active receptors for parathyroid hormone and parathyroid hormone-related peptide delays endochondral bone formation and rescues mice that lack parathyroid hormone-related peptide. Proc Natl Acad Sci **94**: 13689-13694

Seidman J.G. and Seidman C. (2002) Transcription factor haploinsufficiency: when half a loaf is not enough. J Clin Invest **109**: 451-455

Seitz C.S., Lüdecke H.-J., Wagner N., Brocker E.B. and Hamm H. (2001) Trichorhinophalangeal syndrome type I: clinical and molecular characterization of 3 members of a family and 1 sporadic case. Arch Dermatol **137**: 1437-42.

Semizarov D., Kroeger P. and Fesik S. (2004) siRNA-mediated gene silencing: a global genome view. Nucl Acid Res **32**: 3836-3845

Shao G.-Z., Zhou R.-L., Zhang Q.-Y., Zhang Y., Liu J.-J., Rui J.-A., Wei X. and Ye D.-X. (2003) Molecular cloning and characterization of *LAPTM4B*, a novel gene upregulated in hepatocellular carcinoma. Oncogene. **22**: 5060-5069

Shaulian E. and Karin M. (2001) AP-1 in cell proliferation and survival. Oncogene **20**: 2390-2400

Spranger J., Winterpacht A. and Zabel B. (1994) The type II collagenopathies: a spectrum of chondrodysplasia. Eur J Pediatr **153**: 56-65

Sugio Y. and Kajii T. (1984) Ruvalcaba syndrome: autosomal dominant inheritance. Am J Med Genet **19**: 741-753

Sun L., Liu A. and Georgopoulos K. (1996) Zinc finger-mediated protein interactions modulate Ikaros activity, a molecular control of lymphocyte development. EMBO J **15**: 5358-69

SundarRaj N., Fite D., Ledbetter S., Chakravarti S. and Hassell J.R. (1995) Perlecan is a component of the cartilage matrix and promotes chondrocyte attachment. J Cell Science **108**: 2663-2672

Takekawa M. and Saito H. (1998) A family of stress-inducible GADD45-like proteins mediate activation of the stress-responsive MTK1/MEKK4 MAPKKK. Cell **95**: 521-530

Talts J.F., Andac Z., Gohring W., Brancaccio A. and Timpl R. (1999) Binding of the G domains of laminin alpha1 and alpha2 chains and perlecan to heparin, sulfatides, alpha-dystroglycan and several extracellular matrix proteins. EMBO J **18**: 863-870

Tapanadechopone P., Hassell J.R., Rigatti B. and Couchman J. (1999) Localization of glycosaminoglycan substitution sites on domain V of mouse perlecan. Bioch Biophys Res Commun **265**: 680-690

Taylor V. and Suter U. (1996) Epithelial membrane protein-2 and epithelial membrane protein-3: two novel members of the peripheral myelin protein 22 gene family. Gene **175**: 115-120

Tesche F. and Miosge N. (2004) Perlecan in late stages of osteoarthritis of the human knee joint. Osteoarth and Cart **12**: 852-862

Trainor C.D., Omichinski J.G., Vandergon T.L., Gronenborn A.M., Clore GM. and Felsenfeld G. (1996) A palindromic regulatory site within vertebrate GATA-1 promoters requires both zinc fingers of the GATA-1 DNA-binding domain for high-affinity interaction. Mol. Cell. Biol. **16**: 2238-2247

Trainor C.D., Ghirlando R. and Simpson M.A. (2000) GATA zinc finger interactions modulate DNA binding and transactivation. J Biol Chem **275**: 28157-28166

Ueta C., Iwamoto M., Kanatani N., Yoshida C. et al. (2001) Skeletal malformations caused by overexpression of Cbfa1 or its dominant negative form in chondrocytes. J Cell Biol **153**: 87-99

Vairapandi M., Balliet A.G., Hoffman B. and Liebermann D.A. (2002) GADD45b and GADD45g are cdc2/cyclinB1 kinase inhibitors with a role in S and G2/M cell cycle checkpoints induced by genotoxic stress. J Cell Physiol **3**: 327-338

van der Eerden B.C.J., Karperien M. and Wit J.M. (2003) Systemic and local regulation of the growth plate. Endocr Rev **24**: 782-801

van Leeuwen W., Ruttink T., Borst-Vrenssen A.W., van der Plas L.H., van der Krol A.R. (2001) Characterization of position-induced spatial and temporal regulation of transgene promoter activity in plants**.** J Exp Bot **52**: 949-59.

Vilain C., Sznajer Y., Rypens F., Dèsir D. and Abramowicz M.J. (1999) Sporadic case of trichorhinophalangeal syndrome type III in a European patient. Am J Med Genet **85**: 495-497

Villard J. (2004) Transcription regulation and human diseases. Swiss Med WKLY **134**: 571-579

Vortkamp A., Lee K., Lanske B., Segre G.V., Kronenberg H.M. and Tabin C.J. (1996) Regulation of rate of cartilage differentiation by Indian hedgehog and PTH-related protein. Science **273**: 613-622

Wada T. and Penninger J.M. (2004) Stress kinase MKK7: savior of cell cycle arrest and cellular senescence. Cell cycle **3**: 577-579

Wagner T., Wirth J., Mejer J., Zabel B., Held M., et al. (1994) Autosomal sex reversal and campomelic dysplasia are caused by mutations in and around the SRY-related gene *SOX9*. Cell **79**: 1111-1120

Wallis G.A. (1996) Coordinating chondrocyte differentiation. Curr Biol **6**: 1577-1580.

Warman M.L., Abbott M.H., Apte S.S., Hefferon T., McIntosh I. et al. (1993) A type X collagen mutation causes Schmid metaphyseal chondrodysplasia. Nature Genet **5**: 79-82

Watanabe H., Nakata K., Kimata K., Nakanishi I. and Yamada Y. (1997) Dwarfism and age-associated spinal degeneration of heterozygote cmd mice defective in aggrecan. Proc Natl Acad Sci **94**: 6943-6947

Wilkie A.O.M. and Morriss-Kay G.M. (2001) Genetics of craniofacial development and malformation. Nat Gen Rev **2**: 458-468

Wu Z., Wu J., Jacinto E. and Karin M. (1997) Molecular cloning and characterization of human JNKK2, a novel jun NH(2)-terminal kinase-specific kinase. Molec. Cell. Biol. **17**: 7407-7416

Yang A. and McKeon F. (2000) P63 and P73: P53 mimics, menaces and more. Nat Rev Mol Cell Biol **1**: 199-207

Yu C., Le A.-T., Yeger H., Perbal B. and Alman B.A. (2003) NOV (CCN3) regulation in the growth plate and CCN family member expression in cartilage neoplasia. J of Pathol **201**: 609-615

Zhou G., Garofalo S., Mukhopadhyay K., Lefebvre V., Smith C.N., Eberspaecher H., and de Crombrugghe B. (1995) A 182 bp fragment of the mouse proα1(II) collagen gene is sufficient to direct chondrocyte expression in transgenic mice. J Cell Sci **108**: 3677-3684

Danksagung/Ringraziamenti

Herrn Dr. Hermann-Josef Lüdecke möchte ich danken für seine professionelle Betreuungsarbeit, für die endlose Geduld und für seine ständige Diskussionsbereitschaft.

Herrn Prof. Dr. Bernhard Horsthemke, der mir die Möglichkeit gegeben hat in seinem hervorragenden Institut arbeiten zu dürfen, danke ich für die wissenschaftliche Betreuung.

Herrn Dr. Frank Kaiser möchte ich besonders danken für die freundschaftliche und großartige Zusammenarbeit und für die Unterstützung, vor allem in meiner Anfangszeit in Deutschland.

Herrn Dr. Michael Zeschnigk möchte ich danken für seine zahlreichen Hilfestellungen bei der Auswertung der Expressionsdaten.

Herrn Dr. Christian Kosan, Herrn Dr. Ralph Waldschütz und Herrn Prof. Dr. Tarik Möröy (Institut für Zellbiologie, Universitätsklinikum Essen) möchte ich danken für die sehr gute Zusammenarbeit bei der Herstellung und Charakterisierung der transgenen Mäuse.

Allen Mitarbeiterinnen und Mitarbeitern des Institutes für Humangenetik, mit denen ich während meiner gesamten Doktorarbeit zusammen arbeiten durfte, möchte ich ganz besonders danken für die wunderschöne Atmosphäre im Labor, die großartige Zusammenarbeit und die ständigen Bemühungen mir die deutsche Sprache näher zu bringen.

Mein herzlicher Dank gilt Allen im und außerhalb des Labors, mit denen ich zusammen eine sehr schöne Zeit neben der Arbeit verbracht habe.

Diese Arbeit ist nur möglich gewesen durch die Unterstützung aller derer, denen ich hier meinen Dank ausspreche.

Ringrazio di tutto cuore la mia famiglia e tutte le persone dall'Italia che con il loro continuo incoraggiamento mi hanno dato la forza di vivere questa importante esperienza.

CURRICULUM VITAE

Personal data

Name	Paola
Surname	Brega
Date of birth	15.05.1977
Place of birth	Geneva (CH)
Nationality	Italian

Education

1983-1988	Luigi Mercantini, Primary School
1988-1991	Giulio Cesare, Secondary School
1991-1996	Donatello Serrani, High School
1996-2001	University of Ancona, Faculty of Biological Sciences, Biotecnology Section
2000-2001	Experimental work in the Institute of Microbiology, University of Ancona (Italy), by Prof. Francesca Biavasco
October 2001	Begin of the PhD work in the Institute of Human Genetics, University Duisburg-Essen (Germany), by Prof. Dr. Bernhard Horsthemke